THESIS

COMPATIBLITITY OF HYDROPHOBIC IONIC LIQUIDS WITH HIGH PERFORMANCE CATHODE MATERIALS FOR LITHIUM ION BATTERIES

Submitted by

Ezekial Robert Carnes-Mason

Department of Mechanical Engineering

In partial fulfillment of the requirements

For the Degree of Master of Science

Colorado State University

Fort Collins, Colorado

Summer 2012

Master's Committee:

Advisor: Susan James

John Wilkes
Steven Strauss

ABSTRACT

COMPATIBILITY OF HYDROPHOBIC IONIC LIQUIDS WITH HIGH PERFORMANCE CATHODE MATERIALS FOR LITHIUM ION BATTERIES

Lithium batteries are widely seen as the best choice for the future of energy storage but significant improvements are still required. One important area for improvement is searching for new cathode materials that incorporate lithium at higher capacities and voltages. This increases the energy and power available from an individual electrochemical cell, which reduces the number of cells required thereby reducing the size of a battery pack. While several high voltage cathode materials have been discovered, research has been hindered due to safety concerns with current standard electrolytes at high voltages.

Ionic liquids are a new class of materials that exhibit excellent electrochemical and thermal stability as well as high ionic conductivity. These qualities make them excellent candidates to replace current battery electrolytes but difficulties in purification and the sheer number of possible chemistries have inhibited their study.

In this study four hydrophobic ionic liquids based on pyrrolidinium and piperidinium cations paired with bis(trifluoromethylsulfonyl)imide anions were synthesized using bench top methods. These ionic liquids were successfully incorporated

into working half-cells with $LiNi_{1/3}Mn_{1/3}Co_{1/3}O_2$, a high capacity layered cathode and $LiNi_{0.5}Mn_{1.5}O_4$, a high voltage spinel type cathode. By comparing the behavior of the ionic liquids a clear relationship between cation size and rate capability was shown. The improved performance and safety at elevated temperatures was also demonstrated showing that ionic liquids are excellent candidates for use as battery electrolytes.

ACKNOWLEDGEMENTS

I would like to thank my initial advisor Dr. Manivannan for bringing me into his group and introducing me to this project. I am also grateful to Dr. Susan James and Dr. John Wilkes for helping me continue once Dr. Manivannan left to enter industry. Additionally I would like to thank Dr. Steven Strauss for reviewing this work and agreeing to serve on my committee.

Cynthia Corley, Hannah Miller, Peg Williams and everyone else at the United States Air Force Academy provided invaluable assistance with the synthesis and characterization of the ionic liquids. Brandon Kelly provided endless help with the theory and design of my batteries. Dr. Amy Prieto and Dr. Derek Johnson were also extremely helpful with interpreting results and fine tuning my battery test procedures.

Finally I would like to thank my parents for their unwavering support through this entire process.

TABLE OF CONTENTS

LIST OF TABLES

LIST OF FIGURES

Chapter 1: Introduction

1.1 Aim of Research

As modern society becomes more dependent on technology and more concerned with minimizing our impact on the environment, the need for reliable energy storage is becoming increasingly important. Batteries have long been the dominant device for energy storage but the increasing demand for advanced portable electronics such as personal computers and smartphones has placed new constraints on battery size and rates of charge. Development of electrically powered cars in particular, which require very high power and energy densities, is significantly limited by current battery technology.

Lithium ion batteries are currently the most widely studied system for portable electronics. The majority of research has focused on the development of novel anode and cathode materials with ever increasing lithium storage capacities. By contrast there have been very few advances in electrolyte chemistry beyond the move from aqueous to organic solvents due to incompatibility of lithium metal with water. The electrolyte has a large effect on the maximum rate at which a battery can be charged or discharged as well as constraining the maximum potential difference between the anode and cathode. Both of these factors heavily affect the maximum power a battery can deliver. Battery safety is also an issue that has become significant in recent years, with the reactivity of organic electrolytes being a main factor in thermal runaway and explosive failure.

Ionic liquids are a recently discovered class of materials characterized by good ionic conductivity, low volatility and wide electrochemical windows. There has been an

increasing amount of study into using ionic liquids as battery electrolytes, but an ever expanding number of possible chemistries and wide range of properties makes selecting the "perfect" ionic liquid impossible. Instead any attempt to select an ionic liquid must focus on its compatibility with a specific battery architecture. Additionally, due to their exceptional solvating properties it is difficult to completely purify ionic liquids. Several recently discovered ionic liquids based on the bis(trifluoromethylsulfonyl)imide anion show significant hydrophobicity which makes them easier to synthesize in an open environment without extensive precautions against contamination. Simplification of synthesis is essential if ionic liquid production is to be scaled up for use as a battery electrolyte. The focus of this thesis is to synthesize several hydrophobic ionic liquids using simple bench-top methods that can be used as battery electrolytes without further purification. The compatibility of these ionic liquids with promising high voltage cathode materials will then be investigated in an effort to show how ionic liquids can play a critical role in future lithium ion batteries.

1.2 Structure of an Electrochemical Cell

A battery operates by converting chemical energy into electrical energy, by means of an electrochemical oxidation-reduction (redox) reaction. The driving principle is the exchange of electrons from one material to another in an electrochemical cell such as the one shown in figure 1. A commercial battery may contain one or more of these individual cells connected in series or parallel in order to achieve the desired voltage and capacity.

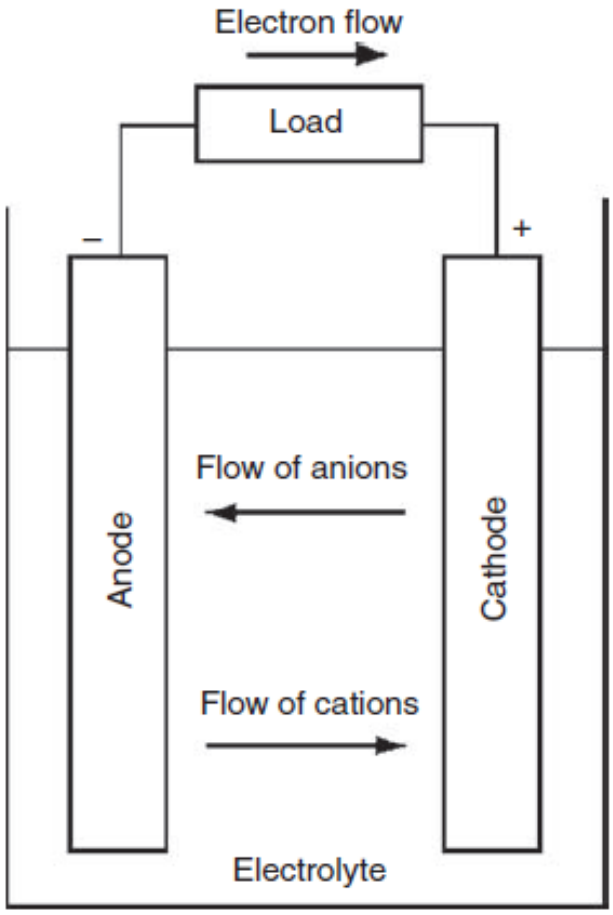

Figure 1: Basic electrochemical cell [1]

All batteries consist of three basic components; a cathode, an anode, and an electrolyte. During discharge an oxidation reaction occurs at the anode which produces electrons and positively charged ions. The electrons pass through an external circuit and produce power while the ions pass through the electrolyte. The electrons and positive ions then recombine via a reduction reaction that occurs at the cathode. In a primary battery this process is irreversible and the battery is discarded once it has completely discharged. In a secondary battery the cycle can be reversed by using an outside power source to pass a current through the cell in the opposite direction.

1.3 Battery Parameters

1.3.1 Specific Energy

Perhaps the most important metric for determining the effectiveness of a battery is the specific energy, also known as energy density. This value, measured in watt-hours per kilogram, is basically a measurement of how long an external load can be powered by a single discharge of the battery. Since the amount of energy available depends on how large the battery is, reported values are normalized by the mass of active material. It is clear from figure 2 that lithium batteries greatly exceed all other major battery chemistries. This is due to the unique electrochemical properties of the lithium atom which will be described later.

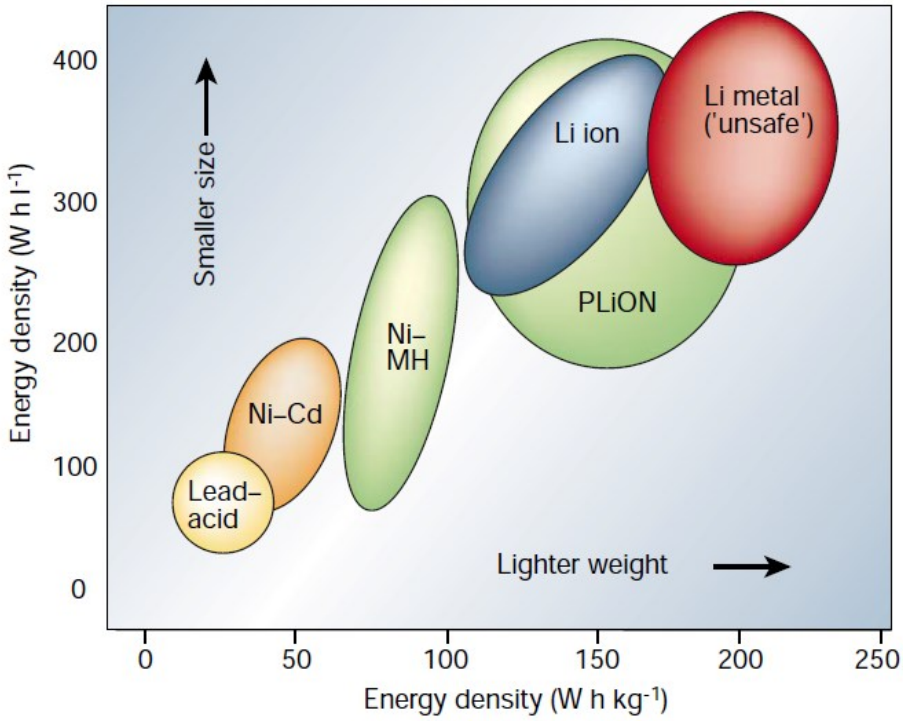

Figure 2: Energy density of common battery chemistries [2]

1.3.2 Specific Capacity

The specific energy of a battery is closely related to the specific capacity of the electrode materials. This value is usually reported in milliamp-hours per gram and is a measurement of how many electrons can be extracted from an electrode during each charge or discharge cycle. This quantity is again normalized by mass so that it is unaffected by the size of the battery. The overall specific capacity of a cell is determined by the electrode with the smaller capacity. In lithium ion cells which are the focus of this thesis the cathode is almost always the limiting factor. Current cathode materials have specific capacities in the range of 100-200 mAh/g compared to graphitic carbon (the most common anode material for li-ion batteries) which has a specific capacity of around 300 mAh/g. The first lithium batteries were made with a pure lithium metal anode which has a specific capacity of approximately 3,860 mAh/g. However, they failed to achieve widespread commercial success due to safety concerns that will be explained later.

1.3.3 Specific Power

Another important parameter for battery operation is how much power can be provided per unit mass. This value, measured in watts per kilogram, is particularly important for high power applications such as acceleration of electric vehicles where a large amount of energy must be provided in short amount of time. Specific power is heavily influenced by the voltage difference between the anode and cathode and the speed of ion transfer between the electrodes. These two factors depend greatly on the properties of the electrolyte.

1.3.4 Cell Voltage

A key parameter to maximizing the specific power of a battery is increasing the voltage difference between the anode and cathode. This difference is determined by the relative voltages at which the redox reactions take place but is limited by electrochemical stability of the electrolyte as shown in Figure 3.

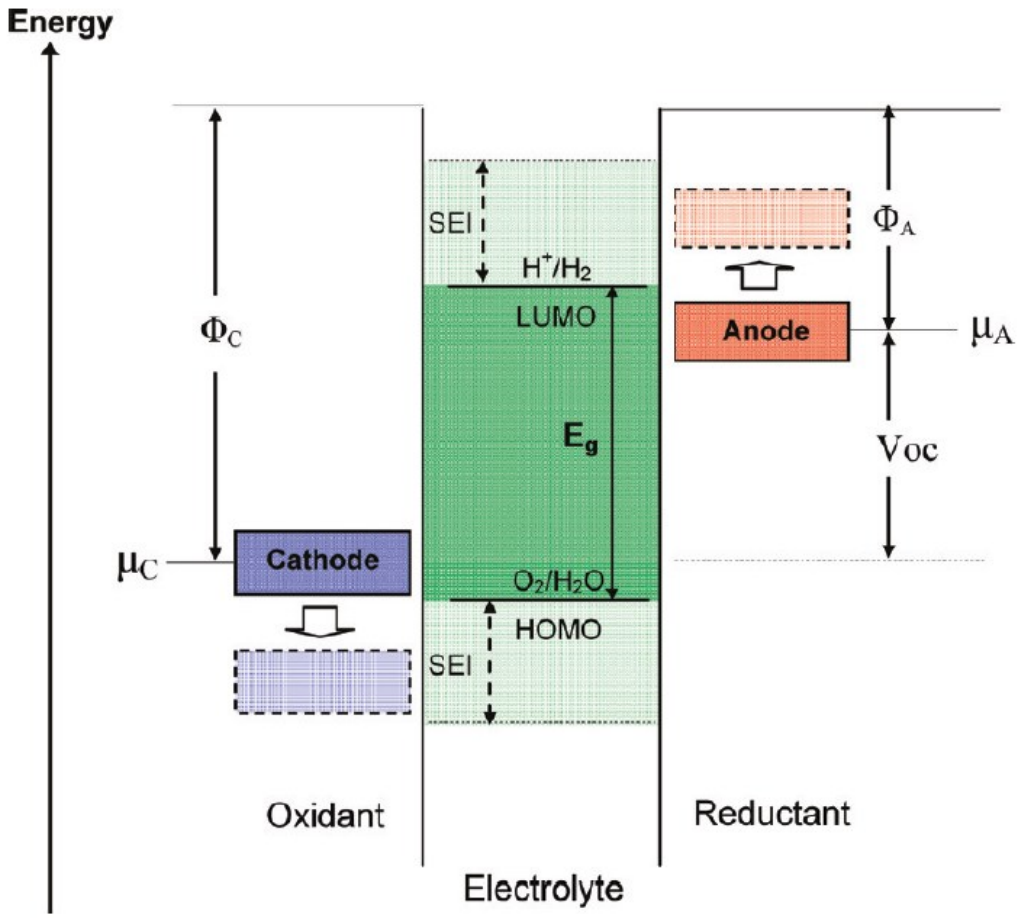

Figure 3: Energy diagram of a battery [3]

. The oxidation at the anode should take place at an energy below the lowest unoccupied molecular orbital (LUMO) of the electrolyte and the reduction should take

place at an energy above the highest occupied molecular orbital (HOMO) of the electrolyte. Attempting to operate the cell outside of this window can result in a breakdown of the electrolyte which will degrade the performance of the cell over time and can cause significant safety concerns due to the release of heat and flammable gases. Electrode combinations with wider and wider voltage differences are continuing to be developed but cannot be implemented into commercial batteries until electrolytes with better stability are discovered.

1.3.5 Rate Capability

Closely related to the specific power of a cell is the rate capability. This is a direct measurement of how quickly a battery is charged or discharged. Rate capability is reported as a C-rate with 1C corresponding to a battery being completely charged or discharged in one hour. The maximum C-rate is a measurement of how large of a current the battery can support, which is determined by the rate of the redox reactions occurring at the electrodes and the ionic conductivity of the electrolyte. High rate capability is essential for quick charging batteries and high power applications.

1.3.6 Cycleability

Another important measurement of battery quality is how many times it can be successfully cycled (i.e. discharged and recharged) without serious loss of capacity. Repeatedly inserting and removing lithium into and out of an intercalation material creates a strain on the lattice that can eventually lead to breakdowns in the structure and lower its capacity. Breakdown of the electrolyte will also affect the cycleability of a

battery. In order to be commercially viable a battery should be able to operate for several thousand cycles without a serious loss of capacity.

1.3.7 Safety

Battery safety has recently become a major issue with reports of laptop batteries overheating and bursting into flames [4] as well as more recent reports of fires in electric vehicles such as the Chevy Volt [5]. Such fires occur due to reactions between the electrolyte and electrodes and must be controlled before large scale implementation of electric vehicles or large grid installations.

1.4 Lithium Batteries

1.4.1 Primary Lithium Batteries

The energy available from a battery is determined by how many charge carriers can be transferred between the electrodes at a reasonable rate and the voltage at which this transfer occurs. Since the movement of electrons through a wire is virtually instantaneous when compared to the rest of the system, the transfer of positive ions is the rate limiting process. The low weight (6.94 g/mol) [1] and highly negative reduction potential (-3.01 V vs NHE) [1] of lithium make it an ideal anode material. The first batteries to take advantage of this superior energy density were lithium-iodine batteries developed for implantable medical devices [6]. These batteries achieved an energy density of about 250 Wh/kg [6] a significant increase over other chemistries in use at the time. The success of these lithium-iodide batteries led to the development of a variety of primary battery designs using lithium anodes and a wide array of cathode materials. A

major breakthrough came in 1978 with the discovery of intercalation compounds into which lithium can be reversibly inserted and extracted [7]. This allowed for the first re-chargeable lithium batteries.

1.4.2 Secondary Lithium Batteries

The intercalation cathode materials used in secondary lithium batteries rely on the ability of transition metals to exist in several oxidation states and form stable crystal structures with space for the lithium ions to move in and out. The first commercial secondary lithium batteries developed by the Exxon Company in the early 1980s used a titanium disulfide structure shown in figure 4.

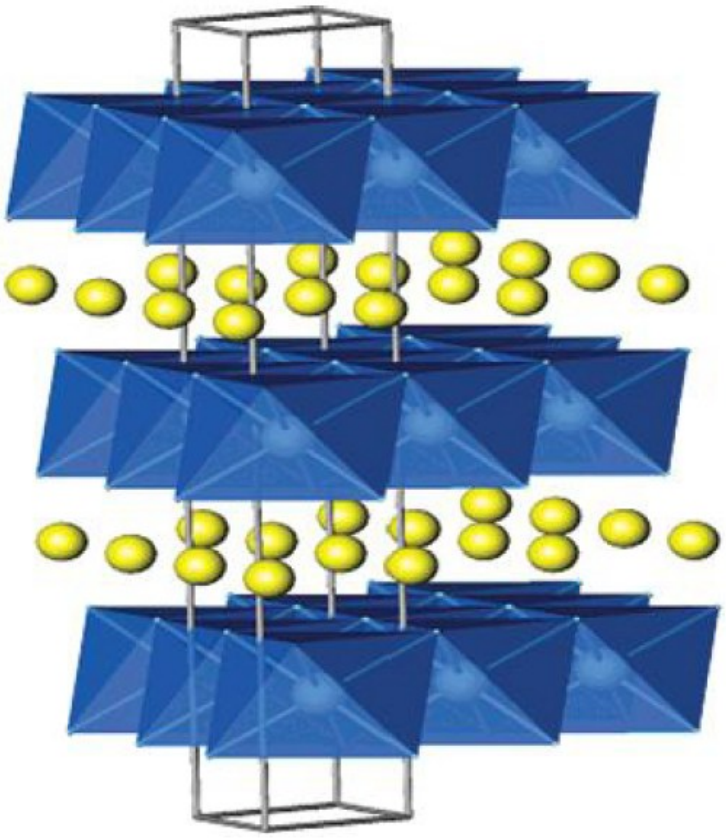

Figure 4: Layered structure of $LiTiS_2$ [8]

Although the cathode performed superbly, safety concerns arose due to the high reactivity of the lithium anode. It was known that lithium metal reacted with the electrolyte to form a passivation layer called a solid electrolyte interface (SEI). This layer is permeable to lithium ions but prevents further breakdown of the electrolyte. It was discovered, however, that poorly formed SEI layers could cause uneven lithium deposition which could lead to dendritic growth and eventual shorting of the cell. These safety concerns ultimately limited the success of secondary batteries with pure lithium metal anodes and led to a search for alternative anode materials. This search culminated in the development of a system first known as the "rocking chair battery" which later came to be called a lithium ion battery and is the dominant battery system used to this day.

1.4.3 Lithium Ion Batteries

The first commercial lithium ion battery was produced by the SONY Corporation in 1991. It featured a lithium cobalt oxide ($LiCoO_2$) cathode first developed by John Goodenough *et al* in 1980 [9]. This high density intercalation compound was paired with a petroleum coke anode [1] that was also able to reversibly intercalate lithium. The combination of these two compounds and a lithium salt dissolved in an organic solvent produced a cell that could be reliably cycled with a capacity of around 130 mAh/g and allowed for subsequent surge in consumer electronics. Figure 5 shows a schematic of a lithium ion cell with a lithium metal oxide cathode and carbon based anode. Although significant research is ongoing into developing improved cathodes, $LiCoO_2$ is still

featured in the vast majority of commercial batteries. Petroleum coke has been replaced by spherical graphite anodes which provide higher specific capacities and better safety.

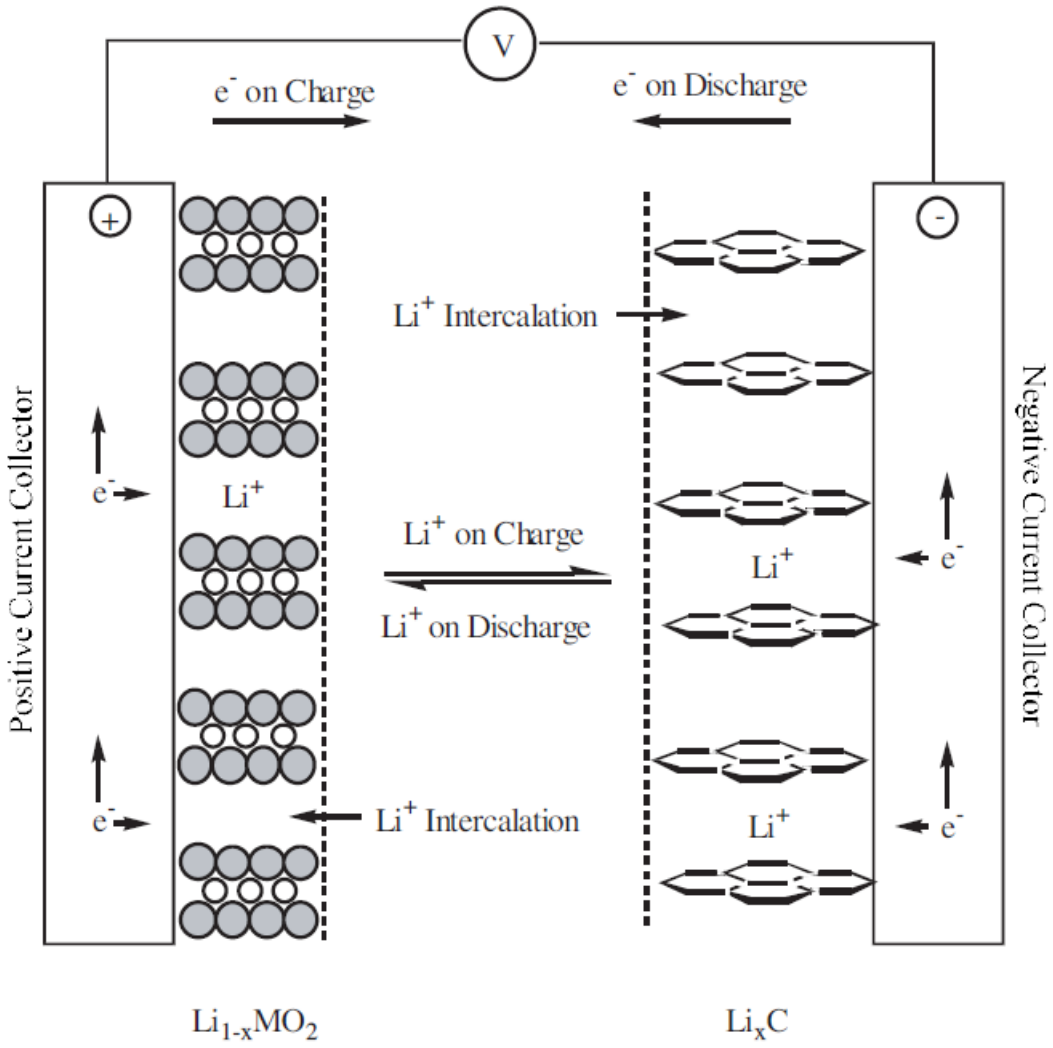

Figure 5: Electrochemical processes of a Li-ion cell [1]

1.5 Current Progress

Although commercial lithium ion batteries have not changed significantly since the introduction of the first working cell, there is a wide range of research currently ongoing to improve the energy density, rate capabilities, and safety of these systems. This research is primarily focused on developing new electrode materials with higher specific capacities and wider voltage differences between cathode and anode. Electrolytes have received much less attention because the electrodes were seen as the limiting factors and basic lithium salts in organic solvents seemed to be effective enough. The recent development of electrode materials near (and in many cases beyond) the electrochemical stability of organic solvents has led to a significant increase in research of these materials. This section aims to provide a brief overview of recent research into each component of a lithium ion battery and the challenges remaining for each.

1.5.1 Anode

The current standard for anode materials remains carbon based intercalation materials. Recent advances in processing have produced carbon based anodes with specific capacities in the range of 450 mAh/g [2]. This is well above the capacity for most cathode material and therefore satisfactory for most new battery systems, though the search for higher capacity anodes continues. The main issue with anode materials is the low intercalation voltages, which are very close to the plating potential of metallic lithium and below the thermodynamic stability of most electrolyte materials. It is therefore essential that the anode encourages the formation of a good SEI layer, which

prevents the formation of dendritic lithium as well as further decomposition of the electrolyte.

Currently, the most promising materials to replace carbon as an anode are lithium alloys with silicon or tin which have much higher capacities (around 4000 mAh/g for Li-Si and 990 mAh/g for Li-Sn [10]) compared to carbon as well as slightly more positive intercalation voltages. These materials suffer from significant volumetric changes during intercalation, which leads to breakdown during extended cycling. This problem is being addressed by the development of nanostructure morphologies, but there is still work to be done to reach commercial viability.

Titanium oxide structures are also being studied as novel anode materials. The intercalation of these materials is between 1.2V and 2.0V versus lithium which is within the stability window of common electrolyte materials. This increased voltage is not ideal though because it reduces the overall voltage of the battery. These materials also have lower capacities than graphite. The increased stability is a key advantage, however, which helps maintain the interest in these materials.

The ideal anode material is still solid metallic lithium. Efforts to develop such batteries focus on the development of new electrolytes that are thermodynamically stable down to the required voltage. There are also investigations being conducted in to additives that enhance SEI formation to provide more stable interfaces.

1.5.2 Cathode

Recent developments for cathode materials will be explored in depth in the next chapter. Briefly, the two main goals in cathode research are to find materials with higher

specific capacities and higher intercalation voltages relative to lithium. The former increases the specific energy of the battery while the latter improves the specific power. Another important driving force for new cathode development is the desire to replace expensive and toxic cobalt with more environmentally friendly materials such as nickel and manganese.

1.5.3 Electrolyte

Very little progress has been made into improving electrolyte materials since the switch from aqueous to organic solvents required by the move to lithium as the active material. Many researchers consider the electrolyte chemistry trivial as long as the ionic conductivity is high enough to ensure that the electrochemical reactions at the electrodes are the rate determining steps. In reality, however, the interaction between the electrolyte and the electrodes is a critical factor in the behavior of a battery. Ideally the electrolyte should not undergo any oxidation or reduction within the voltage window set by the redox behavior of the electrodes. However, due to the extremely negative reduction potential of lithium, no currently used electrolyte is entirely resistant to reduction at the required potentials. Organic electrolytes are able to function due to the formation of a SEI layer. This occurs when a small portion of the electrolyte is reduced on the anode to form a layer that is permeable to lithium ions but prevents further reduction of the electrolyte. Ethylene carbonate is particularly good at forming this passivation layer on graphite anodes and is therefore used in the vast majority of electrolyte solutions.

The current standard electrolyte in commercial batteries is a lithium salt dissolved in a mix of organic solvents. $LiPF_6$ is the most used lithium salt because it has the best

compromise of all the necessary qualities including solubility in organic solvents, conductivity, and stability towards the solvents as well as the other parts of the battery. Ethylene carbonate is the most common organic solvent used in battery electrolytes due to its ability to form a good SEI layer on common anode materials. It is often mixed with one or more linear carbonates such as dimethyl carbonate in order to lower its melting point and viscosity [11].

The most common electrolyte solution, and the one used as a benchmark in this thesis, is 1M $LiPF_6$ dissolved in an equal mixture of ethylene carbonate and dimethyl carbonate. This combination performs well enough in current battery systems but growing safety concerns and incompatibility with newer cathode materials have necessitated the search for alternative materials.

Ionic liquids are one possible alternative. Their excellent electrochemical stability and good ionic conductivity make them attractive as electrolyte materials but they are plagued by high viscosity and cost. There is a wide range of possible ionic liquid chemistries so it is difficult to determine which ones will work best with each cathode or anode material. This thesis aims to investigate the potential of several ionic liquids that have favorable qualities for high voltage cathode materials and metallic lithium anodes. In particular determining if they can be used without extensive purification, which would lower the cost of manufacture and is essential if they are to be scaled up for mass production.

Chapter 2: Cathode Materials

2.1 Introduction

The majority of research into improving Li-ion batteries is focused on developing suitable cathode materials. A successful cathode should be able to incorporate a large amount of lithium into its structure with little or no change to its lattice. The intercalation of lithium into the structure should also occur at a high voltage in relation to the anode material in order to maximize the power of the system. The most successful cathode materials are based on transition metal oxides where the intercalation of lithium into the structure occurs as a result of the reduction of the transition metal. The voltage of the cell is determined by the difference in electrochemical potential between the reduction of the metal and the oxidation of lithium. Energy diagrams of several important transition metals are shown in Figure 6.

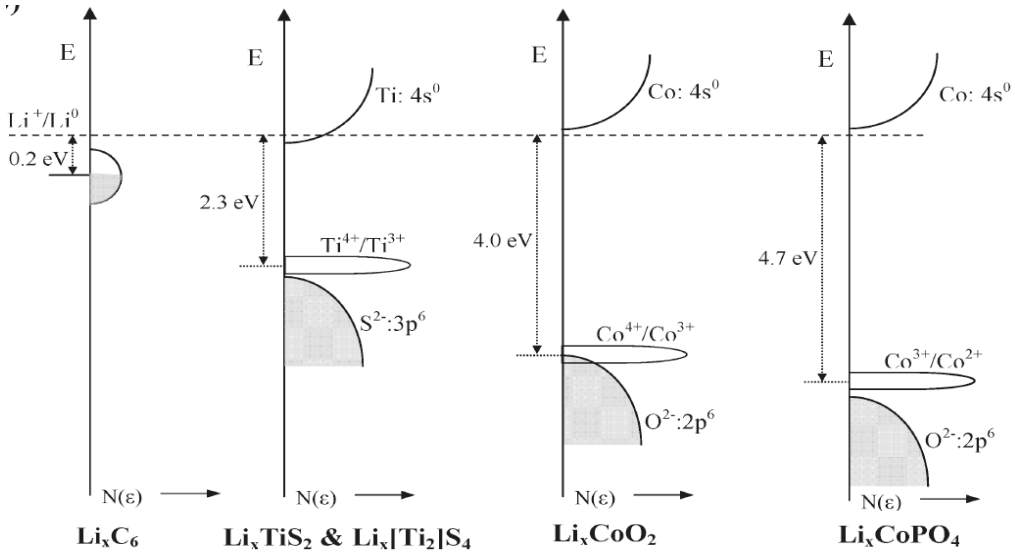

Figure 6: Density of states for various Li-ion cathode materials [3]

The two most common structures used as battery cathodes are the layered structure of $LiMO_2$ (M=Co, Ni, or Mn) and the spinel structure of $LiMn_2O_4$. Understanding the advantages and difficulties of each of these structures is essential to understanding how to design the next generation of batteries and will be the focus of the rest of this chapter.

2.2 $LiMO_2$

The $LiMO_2$ structure consists of a close packed cubic lattice of oxygen atoms in which the octahedral sites are filled with alternating layers of Li and transition metal atoms as diagramed in figure 7.

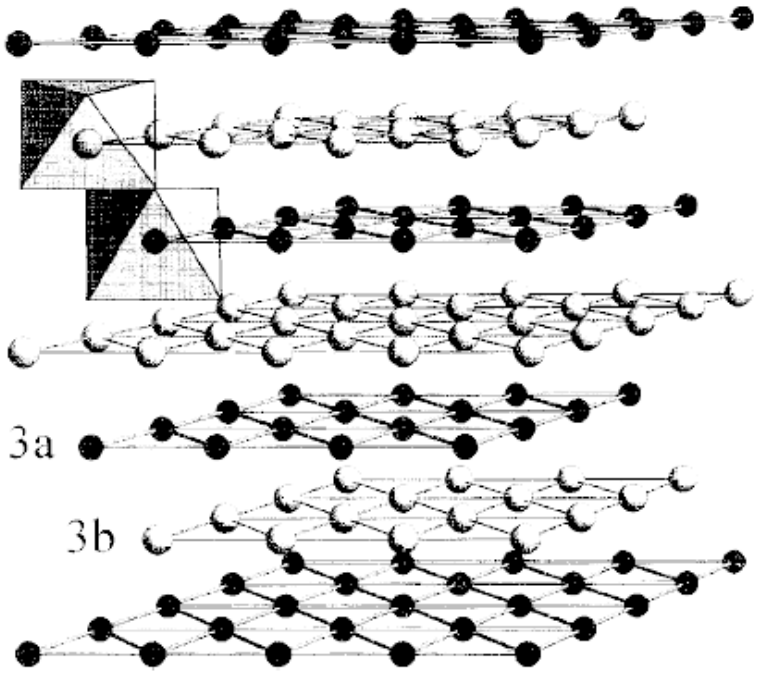

Figure 7: Representation of layered $LiMO_2$ structure [12]

Black spheres=transition metal ions

White spheres=Lithium ions

Lithium atoms are removed from the lattice by increasing the oxidation state of the M^+ ions. As the lithium content decreases there are several phase changes which differ depending on the chemical makeup of the lattice. Stabilizing these changes is important to improving the capacity and cycling behavior of these layered cathodes. The first systems that were characterized consisted of a single metal oxide species but more recent studies have shown significant improvement when a combination of several different transition metals are used.

2.2.1 Lithium Nickel Oxide ($LiNiO_2$)

The first $LiMO_2$ system discovered was lithium nickel oxide ($LiNiO_2$). Nickel was an attractive material due to its low cost and good oxidation voltage, but commercialization proved difficult. This was mainly due to low ordering of the structure, which caused significant migration of nickel into the lithium layer. At small concentrations this helped stabilize the structure as the lithium was removed, but it was often high enough to inhibit the passage of lithium into and out of the material, which had detrimental effects on the rate and cycling abilities of the material. Phase changes at low concentrations of lithium have also been shown to cause a release of oxygen from the material which can create significant safety concerns when a flammable electrolyte is present.

2.2.2 Lithium Manganese Oxide ($LiMnO_2$)

Lithium manganese oxide has also been studied as a layered cathode material but has not achieved much success on its own. This is largely due to the fact that $LiMnO_2$ readily

converts to the more thermodynamically stable spinel structure ($LiMn_2O_4$) upon cycling. The spinel structure has been extensively studied as a cathode material in its own right but its appearance in the layered structure causes problems and is undesirable.

2.2.3 Lithium Cobalt Oxide ($LiCoO_2$)

The first commercially successful Li-ion batteries featured lithium cobalt oxide ($LiCoO_2$) as the cathode. Lithium is removed from the material by oxidizing the cobalt from Co^{+3} to Co^{+4} which occurs at roughly 4.0 V versus Li^+/Li^0 as shown in figure 6. The behavior of $LiCoO_2$ can differ somewhat based on the synthesis procedure but the capacity is generally accepted as around 155 mAh/g at a voltage of 3.88 V [1]. This was a significant increase in energy density (roughly 3x) over NiCd batteries and it paved the way for a revolution in portable electronics. The main drawback of cobalt is high cost and slight toxicity which prevents the possibility of large scale applications based solely on cobalt chemistry. Recent research on layered cathodes has therefore focused on reducing the amount of cobalt in the structure while maintaining the good capacity and voltage required for commercial batteries.

2.2.4 Lattice Substitutions

The first attempt at combining multiple transition metals into the same lattice focused on the combination of nickel and cobalt in a $LiNi_{1-y}Co_yO_2$ system. It was discovered that the addition of cobalt inhibited the migration of nickel into the lithium layer. This combination also demonstrates less of a tendency to release oxygen at low concentrations of lithium which reduces safety concerns. Substitution of cobalt into the

$LiMn_{1-y}Co_yO_2$ system was also attempted. The addition of cobalt was shown to delay the conversion to the spinel form, but it did not completely prevent it. Although there is an increase in conductivity, the unavoidable spinel formation limited the study of this system.

The combination of manganese and nickel in the $LiNi_{1-y}Mn_yO_2$ system was the first to show a dramatic improvement over the single atom phases. Specifically, the $LiNi_{0.5}Mn_{0.5}O_2$ system was shown by Ohzuku et al [13] to have comparable electrochemical behavior to that of the $LiCoO_2$ system as shown in figure 8.

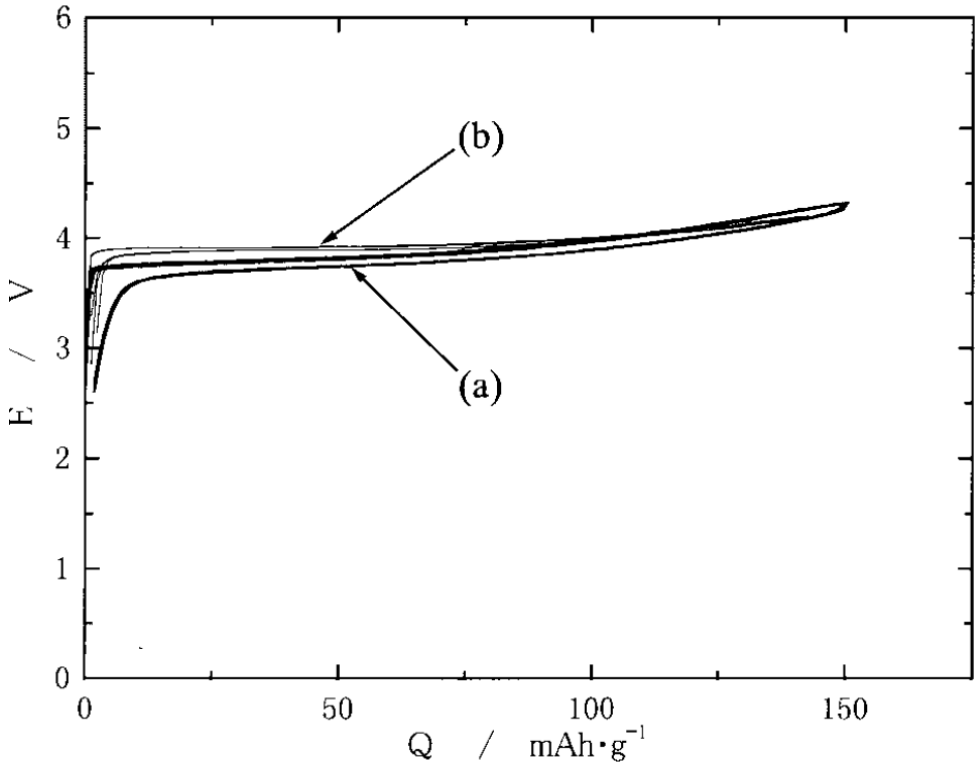

Figure 8: Charge and discharge curves of (a) $LiNi_{0.5}Mn_{0.5}O_2$ and (b) $LiCoO_2$ cells [13]

Simply matching the performance of the $LiCoO_2$ material with lower cost, more environmentally benign nickel and manganese was a significant accomplishment but further research showed improved performance with capacities up to 190 mAh/g at 4.6 V

[8]. Studies have shown that lithium deintercalation occurs as a result of Ni^{+2}/Ni^{+3} and Ni^{+3}/Ni^{+4} redox couples while the manganese remains as Mn^{+4} and simply maintains the structure. The lack of a Mn^{+3}/Mn^{+4} eliminates the possibility of Jahn-Teller distortion which has been known to cause structural degradation over multiple cycles in other manganese cathodes. One negative aspect of this material is that it, like $LiNiO_2$, exhibits migration of Ni into the Li layer which decreases the rate capability. Attempts to prevent this migration led to the inclusion of Co into the structure and the discovery of one of the most promising new cathode materials $LiMn_{1/3}Ni_{1/3}Co_{1/3}O_2$.

2.2.5 $LiMn_{1/3}Ni_{1/3}Co_{1/3}O_2$

There has been extensive research into the $LiMn_{1/3}Ni_{1/3}Co_{1/3}O_2$ cathode as it shows an excellent combination of the positive aspects of each element while minimizing the possible drawbacks of each. The addition of Co does indeed limit the migration of nickel to the lithium layer which increases rate capabilities and stability. The manganese is also kept in the Mn^{+4} state as a spectator ion while the electrochemical reactions causing intercalation of lithium are performed by nickel and cobalt. Capacities of over 200 mAh/g at voltages near 5V have been reported in literature [14] but charging to such high voltages is usually accompanied by significant capacity fade. One of the remaining difficulties with $LiMn_{1/3}Ni_{1/3}Co_{1/3}O_2$, as with all of the layered structures, is instability of the lattice as lithium is removed from the structure. This is an unavoidable consequence of attempting to remove entire layers of an extended solid and it is for this reason that significant research has also been performed on the spinel structure of $LiMn_2O_4$.

2.3 $LiMn_2O_4$ Spinel

The spinel structure is similar to the layered structure in that it is based on a close packed cubic lattice of oxygen anions with manganese cations occupying the octahedral sites and lithium cations on the tetrahedral sites. The difference is that instead of the manganese and lithium ions separated into different layers, the manganese ions create a 3D lattice with tunnels for lithium insertion and removal as shown in figure 9.

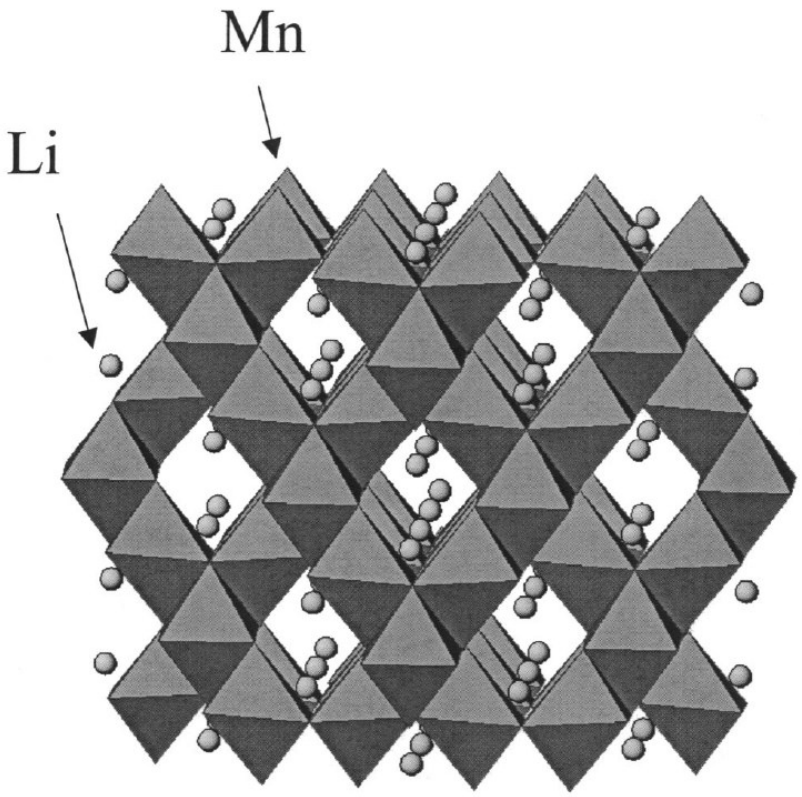

Figure 9: Spinel structure showing MnO_6 octahedra and Li pathways [15]

When compared to $LiCoO_2$ the spinel has a lower capacity (120 mAh/g) but can sustain a slightly higher voltage (4 V) [1]. While the stabilizing effect of the 3D manganese lattice helps to increase rate capacity and allows for easy removal of a large

percentage of the lithium ions, the material suffers from significant capacity fade when cycled or stored at elevated temperatures. There are several suggested causes for this capacity fading; two suspected causes are dissolution of Mn^{+2} into the electrolyte and Jahn-Teller distortion. Both of these result from the Mn^{+3}/Mn^{+4} redox couple that governs the lithium intercalation. In the presence of an acid such as hydrofluoric acid, which can arise from reactions between $LiPF_6$ (used in most electrolyte solutions) and water, two Mn^{+3} ions can form a Mn^{+2} ion and an Mn^{+4} ion. The Mn^{+2} ion then dissolves into the electrolyte causing a loss of active material in the electrode. Jahn-Teller distortion is a phase change phenomenon unique to Mn^{+3} which can create strain on the lattice and degrade its stability. Since both of these phenomena are caused by the presence of Mn^{+3} it was thought that substitution of cobalt or nickel into the lattice as the redox agent could eliminate this capacity fade problem. This led to the discovery of the $LiNi_{0.5}Mn_{1.5}O_4$ spinel that is currently one of the most promising new cathode materials.

2.4 $LiNi_{0.5}Mn_{1.5}O_4$ Spinel

$LiNi_{0.5}Mn_{1.5}O_4$ seems to have all of the desirable characteristics of a Li-ion cathode material. The spinel framework provides an ordered pathway for fast diffusion of lithium into and out of nearly all of the available tetrahedral sites. While there are fewer sites available compared to the layered materials, the complete removal of Li allows for capacities of up to 147 mAh/g [16]. The availability of the Ni^{+2}/Ni^{+4} redox pathway also significantly limits the presence of Mn^{+3} which dramatically reduces the capacity fade. Furthermore, the combination of manganese and nickel orbitals lowers the energy of the Ni^{+2}/Ni^{+3} and Ni^{+3}/Ni^{+4} couples creating a significant increase in the voltage

of the cell as shown in figures 10 and 11. The single voltage plateau is also desirable over the two plateaus observed in the pure spinel as it allows for a constant voltage over the entire charge discharge cycle, which is important for real world applications.

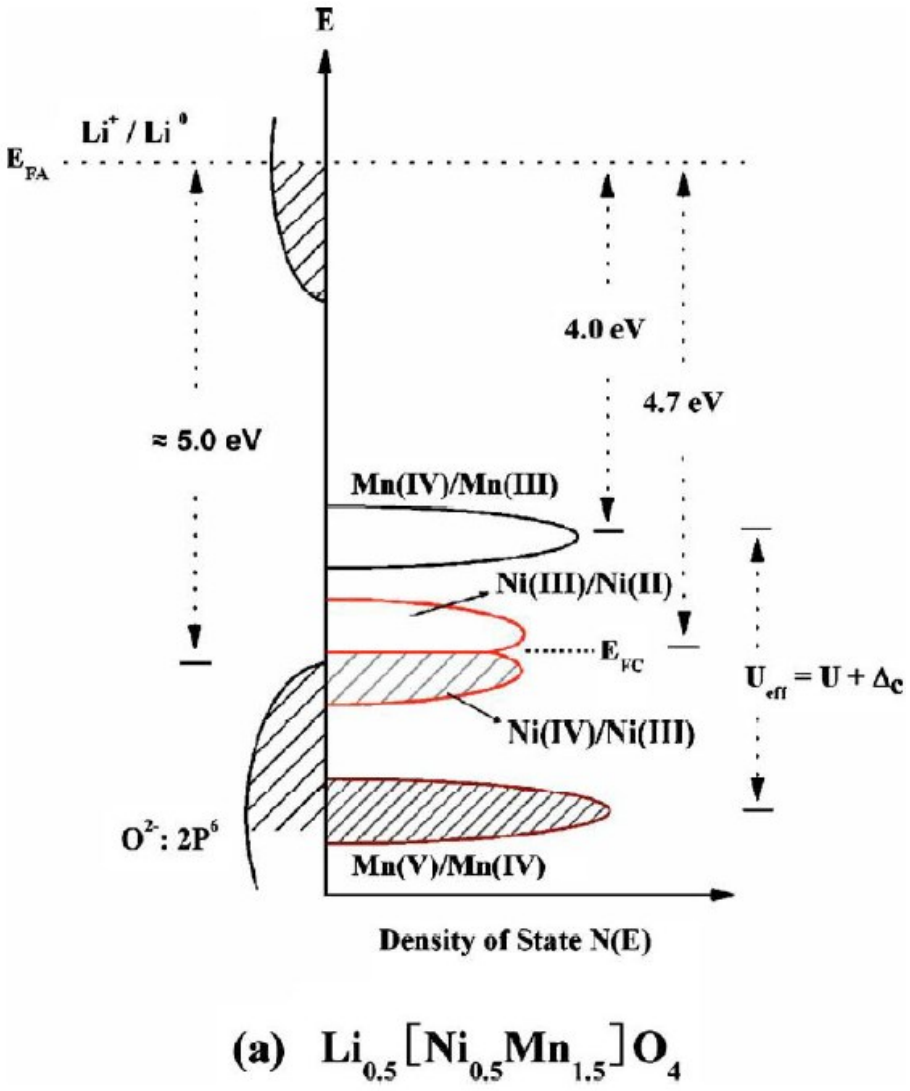

Figure 10: Density of states in $LiNi_{0.5}Mn_{1.5}O_4$ [17]

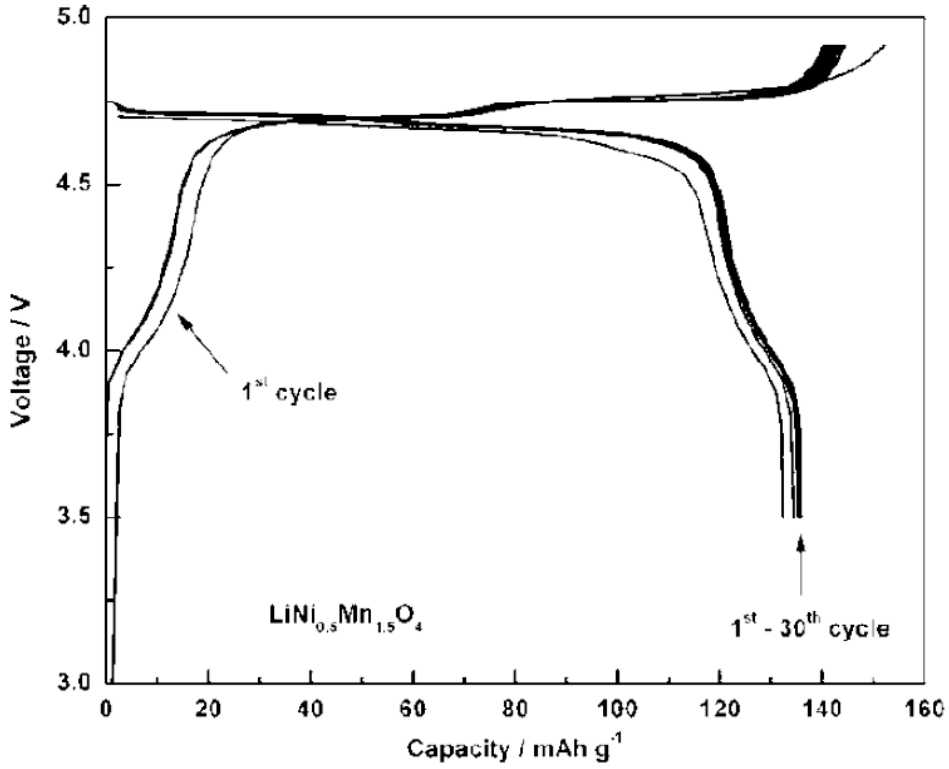

Figure 11: Charge/discharge curves of $LiNi_{0.5}Mn_{1.5}O_4$ [17]

The two main difficulties with $LiNi_{0.5}Mn_{1.5}O_4$ are control of synthesis and decomposition of the electrolyte. There are reports in literature of a tendency to form a separate $Li_xNi_{1-x}O$ phase which is thought to be related to the migration of Ni into Li sites as observed in the layered materials. There are reports that adding a small amount of Co to the structure can have a stabilizing effect much like that seen in the layered cathodes [16]. Studies are ongoing to find the best synthesis procedure with the sol-gel and co-precipitation methods being the most common. The decomposition of electrolytes at the operating voltages of $LiNi_{0.5}Mn_{1.5}O_4$ is due to limitations of the electrolytes themselves, not the cathode material, but it is a limiting factor in the study of these materials and the design of more stable electrolytes is imperative to future studies of these materials.

2.5 Summary

Since being introduced into the market by Sony in the early 1990s, lithium ion batteries have quickly become the dominant power source for a wide variety of applications, most notably portable electronics. There is also significant interest in lithium ion batteries as storage devices for new technologies such as electric vehicles and renewable energy systems. There is still work to be done to raise the power and energy density to levels required for these applications, and significant cost reduction is necessary. Cobalt was the first metal to achieve commercial success but concerns about limited availability and toxicity have led researchers to look for alternative materials with similar electrochemical behavior. Nickel and manganese have been shown to combine effectively with each other and cobalt to produce excellent energy densities. Manganese and nickel are both earth abundant and safe and so are excellent candidates for minimizing cost and safety issues that currently inhibit the continued expansion of Li-ion battery applications. The high voltages versus lithium are of particular interest because a significant increase in power is necessary for electric vehicle applications. Unfortunately, complete studies of high voltage behavior are currently impossible due to the need for new electrolyte systems that are more resistant to oxidation at these voltage levels. Attempts to increase the capacity and rate capabilities of these high voltage materials is ongoing, but it is clear that cathode design is no longer the primary limiting factor in battery performance.

Chapter 3: Ionic Liquids

3.1 *Introduction*

The term ionic liquid is difficult to define with great certainty because it is used to refer to a broad class of materials, which can have a wide variety of characteristics. In the most basic sense ionic liquids are molten salts, which consist solely of the cations and anions that make up the salt given enough energy to prevent crystallization. Molten salts should not be confused with salt solutions, which consist of ions dissolved in some other molecular solvent such as water. The pure ionic nature of molten salts contributes to an array of unique and interesting characteristics such as resistance to oxidation and reduction, low vapor pressure, and high ionic conductivity. Unfortunately, the strength of ionic bonds present in salts generally contributes to high melting points (e.g. 800^{o}C for NaCl) making their unique liquid properties useless for room temperature applications. Ionic liquids, however, are a class of salts that have significantly depressed melting points. Most literature uses 100°C as a divider with anything having a lower melting point being called an ionic liquid and anything higher being called a molten salt.

3.2 *History of Ionic Liquids*

It is difficult to determine the beginning of ionic liquid research because many compounds that are now know to be ionic liquids were thought to be useless side products of other synthesis reactions. The most widely cited example is the “red oil”

formed during Friedel-Crafts alkylation reactions first described in the 19th century [18]. These reactions used alkyl halides in the presence of a Lewis acid catalyst such as $AlCl_3$ to alkylate an aromatic compound. A separate phase was often observed that is now thought to be a chloroaluminate ionic liquid. The first material to be reported as a low melting salt was ethylammonium nitrate, discovered in 1914 by Paul Walden and having a melting point of 12°C [19]. Throughout the early and mid-20th century a variety of other low melting salts were discovered and reported without any serious investigation into possible uses of these materials. The recent history of ionic liquid research extends from work done at the U.S. Air Force Academy by Lowell King, John Wilkes, and Richard Carlin [18]. Their work began as an investigation of molten salts for use in thermal batteries and led to several breakthroughs that greatly increased the overall interest in ionic liquids as a valuable tool in synthesis and electrochemistry.

Thermal batteries are mainly used in systems that require a long shelf life and high power output over a short time such as missiles and spacecraft. They are primary batteries featuring a molten salt electrolyte that is solid during storage and melted by a pyrotechnic when activated. The standard electrolyte when King *et al* began their research was a eutectic composition of 58.5 mol % LiCl with KCl [18]. This system had a lower melting point (355°C) than many inorganic salts known at the time, but the operating temperature was still high enough to cause problems for electronics near the batteries and so a search for lower melting electrolytes was necessary. King *et al* began their research with an investigation into the alkali chloride-aluminum chloride system which ultimately led to the discovery of a NaCl-$AlCl_3$ mixture with a 107°C eutectic melting temperature and an operating temperature of 175°C. This was a significant

improvement over previous inorganic salt electrolytes but still impractical. A major breakthrough occurred when the Air Force Academy researchers rediscovered the work done in 1948 by Frank Hurley and Thomas Wier on mixtures of $AlCl_3$ and 1-ethylpyridinium bromides. Through collaboration with Professor Robert A. Oysteryoung at Colorado State University a system consisting of 1-butylpyridinium chloride and aluminum chloride was developed which had a melting point of 40°C at an equimolar concentration [20]. The discovery of this mixture can be considered the beginning of the modern era of ionic liquids.

While the 1-butylpyridiniumCl-$AlCl_3$ ionic liquid was a significant achievement it also had several drawbacks that led to the continuing search for better systems. The first was that the butylpyridinium cation is easily reduced making it incompatible with aluminum electrodes. This led the Air Force Academy group to perform a series of molecular orbital calculations to identify other potential cations that would be harder to reduce based on their lowest unoccupied molecular orbital (LUMO) energy. This ultimately led to the investigation of dialkylimidazolium cations, which remain the dominant class of cations used in ionic liquids to this day.

The other main difficulty with this first modern ionic liquid is that it is highly reactive with water, including the generation of highly corrosive hydrochloric acid. This reactivity was determined to be caused by the anion so a new phase of research was begun to create low melting salts with dialkylimidizolium cations and various water stable anions. A wide variety of suitable anions were quickly discovered including tetrafluoroborate, hexafluorophosphate, and bis(trifluoromethylsulfonyl)imide. Furthermore, these water-stable ionic liquids could be easily prepared via a simple

metathesis reaction with the appropriate silver salt. From the publication of the first paper on air and water stable ionic liquids by Wilkes and Zaworotko in 1992 [21] there has been an exponential increase in the number of ionic liquids reported. There seems to be an unlimited number of cation/anion combinations that yield salts with melting points at or even below room temperature. A large number of them are based on heterocyclic organic cations paired with organic or inorganic anions that have a diffuse charge but new classes of cations and anions continue to be discovered. The wide array of possible chemistries leads to a wide variety of physical properties that can be tailored to an ever increasing number of possible applications. The next section of this thesis will be an investigation of the various properties important for battery electrolytes and how they are affected by the selection of cation and anion.

3.3 Ionic Liquids as Battery Electrolytes

While the number of possible ionic liquid chemistries continues to grow with each passing year, research into ionic liquids as battery electrolytes has focused mainly on combinations of heterocyclic amine cations with inorganic anions. These chemistries are favored for their relative ease of preparation and tendency to exhibit those properties most favorable for battery electrolytes: wide electrochemical windows and high conductivities.

3.3.1 Cations

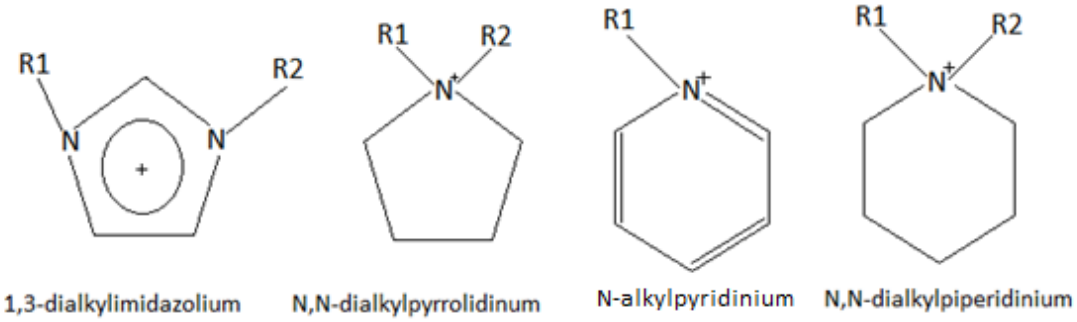

Figure 12: Common cations for ionic liquids used as battery electrolytes

Figure 12 shows several of the most common ionic liquid cations. As stated above, pyridinium was key to the initial discovery of room temperature ionic liquids, but it was too easily reduced to be of use in most electrochemical applications. Research into similar structures led to the discovery of imidazolium as an excellent candidate for electrochemical applications due to its higher resistance to reduction. Imidazolium based ionic liquids also tend to have the higher conductivities than other families. This is why imidazolium based ionic liquids continue to be the most widely studied family for most applications. The R groups attached to the nitrogen atoms are generally straight chain alkyl groups. The length of the alkyl chains can have significant effects on the physical properties of the ionic liquids such as melting point and viscosity.

Pyrrolidinium and piperidinium have gained increased interest in recent years because their reduction potentials are very close to the reduction potential of lithium [22]. This has renewed hope in the possibility of using metallic lithium as an anode material because an electrolyte that is thermodynamically stable against lithium would not need to rely on the development of an SEI layer which can breakdown and lead to dendritic growth.

3.3.2 Anions

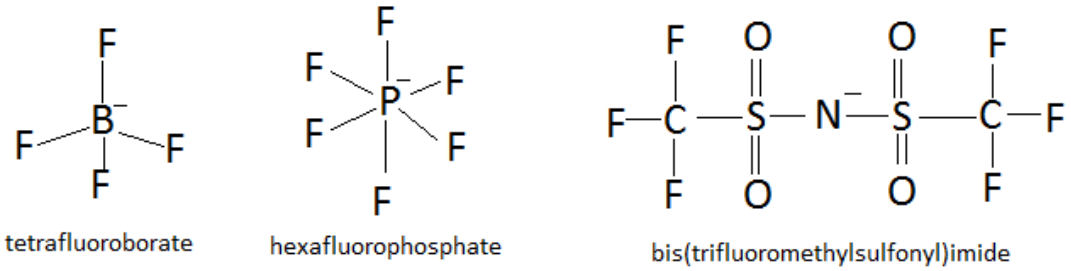

Figure 13: Common anions for ionic liquids used as battery electrolytes

Figure 13 shows some of the most common anions currently used for ionic liquids. The chloroaluminate systems that dominated early ionic liquids research have largely been replaced by these water-stable anions. Tetrafluoroborate was one of the first anions successfully paired with the imidazolium cation [21]. Although they are described as water-stable, ionic liquids with the tetrafluorobrate anion are generally hydrophilic which makes them difficult to purify. Lithium hexafluorophosphate is a common component in organic battery electrolytes so it would seem like a good candidate for ionic liquid electrolytes. However, the melting points of ionic liquids with the hexafluorophosphate anion generally have higher melting points than ionic liquids with other anions. Furthermore, the possible formation of HF gas is one of the problems with the use of lithium hexafluorophosphate in carbonate electrolytes and still remains a problem with its use in ionic liquids.

One of most promising anions studied for use in battery electrolytes is bis(trifluoromethylsulfonyl)imide (TFSI). Its large size results in low melting points when mixed with a wide variety of cations [23]. In addition to its large size, the TFSI

anion exhibits significant charge delocalization along its S-N-S backbone. This delocalization decreases the ability to form hydrogen bonds, which lowers the viscosity and increases the hydrophobicity, both of which are highly desirable characteristics for electrolytes. This charge delocalization also causes the TFSI anion to have a strong resistance to oxidation, which contributes to a high anodic stability and therefore increases the maximum voltage to which a battery can be charged. This increased anodic stability is essential for the use of high voltage cathode materials. The next section of this thesis will be a review of the key physical properties of ionic liquids for use as battery electrolytes and how that led to the choice of cations and anions used in this study.

3.4 Physical Properties of Ionic Liquids

3.4.1 Conductivity and Viscosity

Ionic conductivity is perhaps the most important property to consider when determining the suitability of a material as an electrolyte. Ionic liquids are composed entirely of charge carrying species, which would seem ideal for high conductivities. In reality, however, the large size and strong interactions of individual ions in ionic liquids significantly lowers their mobility limiting the overall ionic conductivity. The conductivity of most ionic liquids falls within the range of 0.1-18 mS/cm [24]. This falls well below the conductivities for most aqueous electrolytes, which are on the order of 400-500 mS/cm [23], but is on par with the organic solvents currently used as battery electrolytes.

The identity of the cation has a profound effect on the conductivity of an ionic liquid. Ionic liquids based on the imidazolium cation generally have higher conductivities (closer to 10 mS/cm) while use of piperidinium or pyrrolidinium generally yields conductivities around 2 mS/cm [23].

The conductivity of an ionic liquid is strongly linked with its viscosity because of the correlation between viscosity and ion mobility. The identity of the anion has a profound effect on the viscosity with the delocalized charge of the TFSI anion leading to some of the least viscous ionic liquids.

3.4.2 Lithium Transference

In order to properly function as an electrolyte for a lithium ion battery, an ionic liquid must be able to transfer lithium ions at a high enough rate so as not to limit the reaction rate at the electrodes. The diffusion rates of individual ions are difficult to measure directly in ionic liquids. The lithium transference is generally increased by dissolving a lithium salt into the ionic liquid thereby increasing the lithium concentration. It is best to use a lithium salt with the same anion that is already present in the ionic liquid to minimize the number of species present. Unfortunately, the addition of lithium salt increases the viscosity of the solution, which lowers the overall conductivity. Therefore the concentration is kept relatively low at around 0.3 mol/kg [25].

3.4.3 Melting Point

In order to be useful as electrolytes it is necessary that the ionic liquids used are liquid over the range of temperatures experienced by the electrochemical device. The melting point of an ionic liquid is most heavily influenced by the size of the cation and anion, with larger sizes leading to lower melting points. The symmetry of the ions also has an effect with more asymmetric cations generally having lower melting points. Extending the alkyl chain length can decrease melting points but it also increases the viscosity, which negatively affects electrolyte performance. Therefore a balance must be struck between lower melting points and higher viscosities.

3.4.4 Electrochemical Stability

Along with conductivity, electrochemical stability is the most important property for assessing the potential of ionic liquids as battery electrolytes. The electrochemical stability of an ionic liquid is defined as the difference in the voltages that cause reduction of the cation (the cathodic limit) and oxidation of the anion (anodic limit). Ideally, an electrolyte will be stable above and below the intercalation voltages for the anode and cathode materials. It is well documented, however, that carbonate electrolytes are not entirely stable down to the voltages associated with graphite intercalation [11]. Instead, a small amount of the electrolyte breaks down forming the kinetically stable SEI layer. Similarly, although some carbonate electrolytes are deemed stable up to 5 volts versus lithium, there is evidence of breakdown reactions that have detrimental effects on the cycle life and can lead to the release of hazardous gasses.

It is difficult to reliably compare the electrochemical windows of various ionic liquids due to the large number of possible combinations and testing conditions. Ionic liquids have been shown to behave differently on glassy carbon and platinum electrodes [22] and the widespread use of different reference electrodes make comparisons between different studies very difficult. However, general trends can be deduced which show why certain families of ionic liquids have come to dominate the field of lithium ion batteries.

The anodic potentials are very similar for most of the common anions currently used in ionic liquids, though the delocalization of the negative charge on the TFSI ion gives it a slightly higher oxidation potential.

The cathodic side is much more variable with imidazolium cations reducing around 1 V versus lithium while pyrrolidinium and piperidinium have reduction potentials near or negative to the lithium redox potential. The first lithium ion batteries were made with imidazolium based ionic liquids due to their higher conductivity. However, most recent research focuses on the increased stability provided by the lower reduction potentials of pyrrolidinium and piperidinium. It has been suggested that the more positive reduction potential of imidazolium is due to the acidic nature of the carbon between the two alkylated nitrogen atoms, but few studies have been done on ionic liquids in which the carbon has also been alkylated.

3.5 Summary

The high ionic conductivity, low volatility, and excellent electrochemical stability of ionic liquids make them ideal candidates for use as the next generation of battery electrolytes. Out of the wide variety of possible combinations of cations and anions that

qualify as ionic liquids the most promising chemistries incorporate cyclic amine cations and large inorganic anions. Piperidinium and pyrrolidinium based cations have the highest resistance to reduction and the bis(trifluoromethylsulfonyl)imide anion provides the most hydrophobic and least viscous liquids as well as having an excellent resistance to oxidation. Ionic liquids made from these materials were therefore selected for this study. Ionic liquids of this type have been shown to function well with $LiCoO_2$ cathodes [26] but few studies have been done with other cathodes. There is also only a limited amount of research into the effects of increasing the length of the alkyl chains attached to the base rings. The compatibility with novel cathode materials and effects of longer alkyl chain are therefore the key parameters investigated in this thesis.

Chapter 4: Experimental Methods

4.1 Specific Aims

4.1.1 Specific Aim 1: Ionic Liquid Synthesis

4.1.1.1 Objective

The primary objective of this thesis is to synthesize a series of ionic liquids using simple bench top techniques and achieve low levels of impurities so they can be used as battery electrolytes without further purification. Simplifying the synthesis methods and minimizing the amount of purification that must be done are important ways to minimize cost. Lowering cost is essential if production is to be scaled up to levels required for mass production of ionic liquid based batteries.

4.1.1.2 Hypothesis

The use of hydrophobic ionic liquids should help minimize impurities because they can easily be washed with water and dried by simply heating under vacuum.

4.1.2 Specific Aim 2: Determination of Effects of Cation Size

4.1.2.1 Objective

A variety of techniques will be used to characterize the ionic liquids to make sure the desired liquids were synthesized and to determine if extending the alkyl chain length has any effect on the properties. The most important test is cyclic voltammetry to

determine the oxidation and reduction potentials of the ionic liquids, which is important for their potential use as battery electrolytes. Cyclic voltammetry will also show any electrochemically active impurities that could have significant influence on battery performance.

4.1.2.2 Hypothesis

Extending the length of the alkyl chains attached to the cations should decrease the melting points of the liquid by making it more difficult for the liquids to crystallize. It will likely increase the viscosity which will have a negative impact on the ionic conductivity and rate capability.

4.1.3 Specific Aim 3: Assessment of Battery Performance

4.1.3.1 Objective

Electrochemical cells will be constructed with the ionic liquids and two cathode materials that show promise for use in commercial batteries. The cells will be repeatedly charged and discharged at a constant voltage to determine what effects the ionic liquids have on the rate capability, specific capacity, and cycleability of the cathode materials.

4.1.3.2 Hypothesis

The large electrochemical windows of all of the selected ionic liquids should allow for good compatibility with high voltage cathodes and minimize side reactions that can negatively affect cycleability. The lower ionic conductivities may limit the rate capabilities but the theoretical specific capacity should be achievable at low rates.

4.1.4 Specific Aim 4: Demonstration of Enhanced Safety

4.1.4.1 Objective

The biggest concern over currently used electrolyte materials is the possibility of reactions with cathode materials at high voltages and temperatures. These reactions can create oxygen gas evolution that may combust causing fires. The low-volatility, non-flammability, and high thermal stability of ionic liquids makes them ideal for preventing these undesired reactions. Tests will be done to examine the reactivity of delithiated cathode materials with a standard electrolyte as well as several of the ionic liquids.

4.1.4.2 Hypothesis

The carbonate electrolytes should show a variety of reactions at increased temperatures while the ionic liquids should show little or no activity.

4.2 Ionic Liquid Synthesis

The procedure for making heterocyclic ionic liquids is generally divided into two steps. First, a neutral heterocyclic molecule is alkylated to form a positively charged cation which forms a halogen salt. This salt is then dissolved in deionized water and mixed with a salt made from the desired anion that has also been dissolved in deionized water. This metathesis reaction results in the desired ionic liquid forming as a hydrophobic phase. The undesired waste salts are soluble in water and can be removed by washing repeatedly.

4.2.1 Materials

1-methylpyrrolidine, 1-methylpiperidine, iodobutane, and iodohexane were purchased from Aldrich and used as received in the initial quaternization reactions. Anhydrous acetonitrile and ethyl acetate obtained from the supplies at the United States Air Force Academy were used in the purification of the quaternized salts. Lithium bis(trifluoromethylsulfonyl)imide was purchased from Aldrich and used along with deionized water for the metathesis reaction.

4.2.2 Quaternization Reactions

4.2.2.1 Butylmethylpyrrolidinium Iodide

1-Methylpyrrolidine was mixed with a slight molar excess of iodobutane in a 250 ml 3-neck, round bottom flask and diluted with acetonitrile to mitigate the exothermic nature of the reaction. The solution was stirred at room temperature for 48 hours. The solution began clear but soon turned yellow. Increase in temperature occurred for the first few minutes indicating an exothermic reaction. Boiling was observed, but this stopped as the temperature decreased.

After 48 hours the solution was placed in an ice bath and an addition funnel was used to add anhydrous ethyl acetate to the flask. The butylmethylpyrrolidinium iodide (BMPyrr-I) is much less soluble in ethyl acetate compared to acetonitrile, so as the makeup of the solution changes to mostly ethyl acetate, the BMPyrr-I is forced out of solution and precipitates as fine white crystals. The ethyl acetate was first added quickly 2-3 ml at a time allowing a significant portion of the salt to form. The solution was then mixed to allow the salt to dissolve and another 2-3 ml was quickly added. This process

continued until the precipitate formed into large clumps that did not dissolve. The ethyl acetate was then added drop wise until no further precipitation was observed.

Once the salt was completely precipitated a gas dispersion tube was then placed into the flask and the excess liquid consisting of acetonitrile, ethyl acetate, and a small amount of BMPyrr-I still in solution was removed by vacuum. A small amount of acetonitrile was added to re-dissolve the crystals and crystallization process was then repeated two more times to remove impurities and leave a fine white powder which was stored in a nitrogen dry box for future use.

4.2.2.2 Hexylmethylpyrrolidinium Iodide

1-Methylpyrrolidine was mixed with a slight molar excess of iodohexane in a 250 ml 3-neck round bottom flask. In order to mitigate the exothermic behavior of the reaction the 1-methylpyrrolidine was diluted with 10 mg of acetonitrile and the iodohexane was added drop wise. The solution started clear but soon turned yellow while increasing in temperature and boiling. After approximately ten minutes the solution cooled and the boiling subsided. The solution was left stirring overnight.

Once the reaction had completed the solution was placed in an ice bath and an addition funnel was used to add ethyl acetate to force the hexylmethylpyrrolidinium Iodide (HMPyrr-I) to precipitate. A steady stream of ethyl acetate was added to the solution while it was slowly stirred. When the ethyl acetate was first added a fine white precipitate developed that floated on top of the solution. The stir and flow rates were varied to ensure that the precipitate did not separate into an oil or crash out into a solid clump. When the concentration of ethyl acetate in the solution reached a critical point the

precipitate condensed into larger crystals that sank to the bottom of the flask. At this point the flow of ethyl acetate was reduced to 1-2 drops per second and addition continued until no further precipitation was observed. The excess liquid was then removed by vacuum and the salt was re-dissolved in a small amount of acetonitrile. The crystallization process was repeated two more times to remove impurities and produce a clean white salt that was stored in a nitrogen dry box for future use.

4.2.2.3 Butylmethylpiperidinium Iodide

1-Methylpiperidinium was combined with a slight molar excess of iodobutane in a 3 neck round bottom flask. A white precipitate began to form immediately upon mixing. Acetonitrile was added which dissolved the precipitate, though after a few minutes of stirring a precipitate reformed indicating that it was semi-soluble in acetonitrile. A total of 10 ml of acetonitrile was added and the solution was left to stir for 48 hours. After 48 hours a precipitate had reformed. The flask was placed in an oil bath and heated to 70° C. Not all of the precipitate dissolved so another 10 mL of acetonitrile was added and the solution was mixed for 1 hr to encourage further reaction. After 1 hr the solution was allowed to cool to room temperature and an increased amount of precipitation was observed. Another 20 mL of acetonitrile was added and the solution was heated to 60° C for another hour.

The solution was cooled to room temperature with no observed precipitation, but precipitation occurred quickly when placed in an ice bath. Ethyl acetate was added until no further precipitation was observed. The liquid was then removed via vacuum filtration leaving a white precipitate with green areas against the glassware. The precipitate was

re-dissolved using 10 ml of acetonitrile and heating to 60° C. Precipitation again occurred quickly in an ice bath and was completed with ethyl acetate. The liquid was again filtered off and the process was repeated a third time to leave a white precipitate which was dried under vacuum for two hours and then transferred to a glass jar and stored in a nitrogen dry-box for future use.

4.2.2.4 Hexylmethylpiperidinium Iodide

1-Methylpiperidinium was mixed with a slight molar excess of iodohexane in a round bottom, 3-neck flask. 10 mL of acetonitrile was added to prevent the product from precipitating and the solution was left to mix for 48 hours. After 48 hours the solution was tinted yellow and a small amount of precipitate was observed. The solution was heated to 60° C in an oil bath and bubbling was observed indicating further reaction. The bubbles stopped after 30 minutes and did not resume when the temperature was increased to 70° C. The solution was left stirring at 60° C overnight. When the solution was cooled to room temperature no precipitation was observed but a precipitate formed quickly when ethyl acetate was added to the solution while the flask was submerged in an ice bath.

The precipitate was less dense then the acetonitrile and ethyl acetate mixture so it collected on the top of the solution. The mixing speed was slowly increased as more precipitate formed. Once a critical amount of ethyl acetate was added the precipitate quickly filled the liquid and further precipitation was impossible. The liquid was then filtered out via vacuum and the precipitate was re-dissolved by adding 10 mL of acetonitrile and mixing at 60^{o}C. The salt was purified a total of three times and dried

under vacuum overnight. It was then transferred to a glass jar and stored in a nitrogen dry-box for future use.

4.2.3 Metathesis Reaction

The procedure for the metathesis reaction was identical for all of the ionic liquids synthesized. The iodide salt created in the previous step and lithium bis(trifluoromethylsulfonyl)imide (LiTFSI) were each dissolved in 100 mL of de-ionized water and combined in a 250 mL flat bottom flask. A slight molar excess of the lithium salt was used to ensure that all of the iodide salt reacted. The solution was stirred for two hours at 80° C until it had separated into two phases. The ionic liquid settled below the lighter aqueous phase containing lithium iodide salt and other impurities. A syringe was used to remove the majority of the aqueous phase that was then replaced with 100 ml of fresh deionized water. The solution was then mixed for another 2 hours to allow completion of the reaction.

After the reaction had completed the aqueous phase was again removed and the solution was washed several times with 100 ml of de-ionized water until the aqueous phase remained clear at room temperature indicating a lack of dissolved impurities. The ionic liquid was then dried in a vacuum oven at 90° C overnight.

4.3 Cathode Synthesis

The active materials for the two selected cathodes were synthesized using the sol-gel technique. For the spinel material $LiNi_{0.5}Mn_{1.5}O_4$ stoichiometric amounts of lithium acetate dihydrate, nickel acetate tetrahydrate, and manganese acetate tetrahydrate were

dissolved in 75 ml of deionized water and heated to 70^{o}C on a hotplate while being mixed using a magnetic stir bar. Citric acid was dissolved in 25 ml of deionized water and also heated to 70^{o}C. Once the two solutions had reached 70^{o} C they were mixed together, and left stirring overnight at 90^{o} C. The layered material $LiMn_{1/3}Ni_{1/3}Co_{1/3}O_2$ was prepared in a similar fashion using lithium acetate dehydrate, manganese acetate tetrahydrate, nickel acetate tetrahydrate, and cobalt acetate tetrahydrate.

After 12 hours the water in both samples had evaporated leaving a gel at the bottom of each beaker. The stir bars were removed and the beakers were placed in a furnace. The furnace was heated to 450^{o}C at a rate of 2^{o}C/min and held for 4 hours to burn off organic byproducts. Once the organic products were removed a black powder remained in the beakers. This powder was broken up and transferred to high temperature crucibles. The samples were then calcined in a high temperature furnace at 800^{o}C for 12 hours. Each crucible produced a fine black powder that was homogenized with a mortar and pestle and placed into a sample vial for future use.

4.4 Materials Characterization

4.4.1 Nuclear Magnetic Resonance (NMR)

The structures of the prepared ionic liquids were first characterized by ^{1}H NMR. Several drops of each ionic liquid were placed into an NMR sample tube that was then filled with duterated acetonitrile. Scans were performed with a Varian Mercury 300 NMR Spectrometer. ^{1}H NMR is useful in determining the structure of organic molecules by distinguishing the bonding behavior of the various protons in the structure. It can therefore be used to distinguish between the four different organic cations used in this study.

4.4.2 Differential Scanning Calorimetry (DSC)

The melting point of the liquids was determined by differential scanning calorimetry. Milligram samples of each ionic liquid were placed in hermetically sealed aluminum pans. The pan was then placed in a 2920 modulated DSC made by TA Instruments with an empty pan as a reference. The samples were each cooled to -80° C and the heat flow was measured against that of the empty pan. DSC is useful in determining phase change points of materials which show up as a peak or valley where a large change in heat flow occurs over a short temperature range.

4.4.3 Ionic Conductivity

The conductivity of the prepared ionic liquids was tested using a model 31A conductance bridge and model 3403 conductivity cell made by Yellow Springs Instruments (figures 14 and 15). The analyte was placed in the conductivity cell as

shown in figure 15 and an estimated range was selected on the bridge device. The appropriate dial was adjusted until only the two farthest LEDs on the meter were illuminated. The sensitivity was then slowly increased while the dial was adjusted to maintain the widest possible gap between the LEDs. Through this method a value for the conductance of the material was determined in microsiemens . The cell was first calibrated using a sample of 0.75M solution of KCl for which the conductivity at different temperatures was previously calculated. The calculated conductivity divided by the measured conductance gave a cell constant which was then used to calculate the conductivity of each ionic liquid from the measured conductance values.

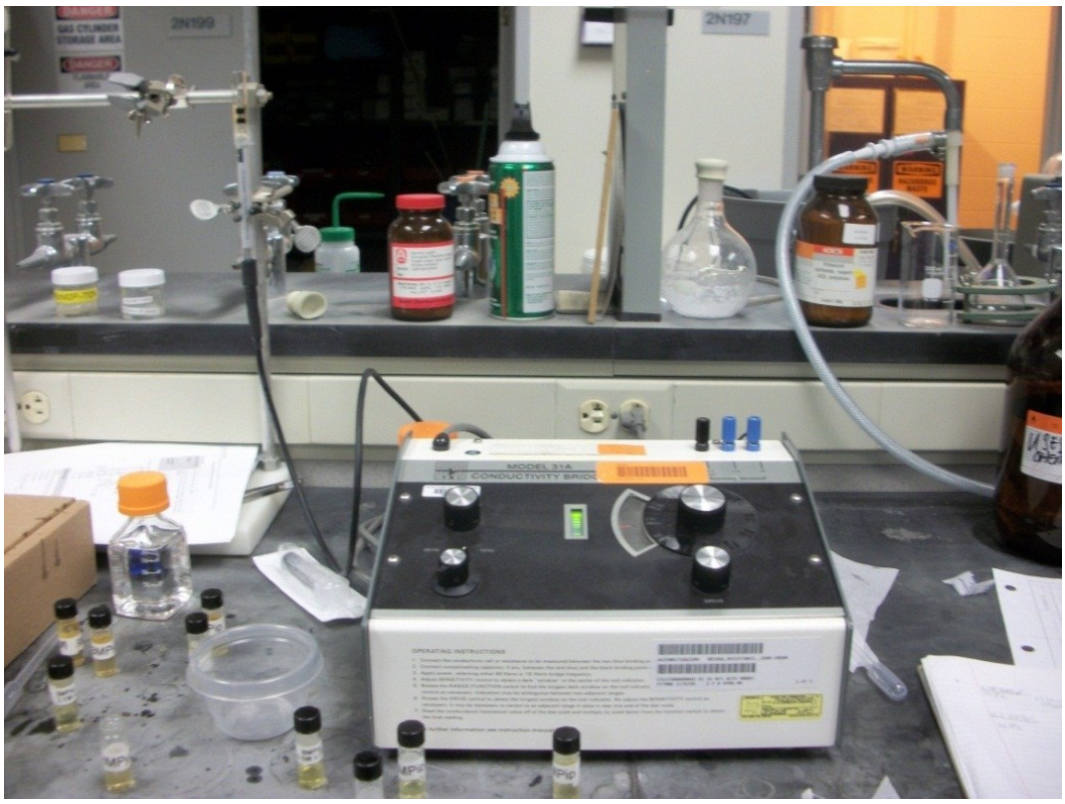

Figure 14: Conductance bridge on lab bench top

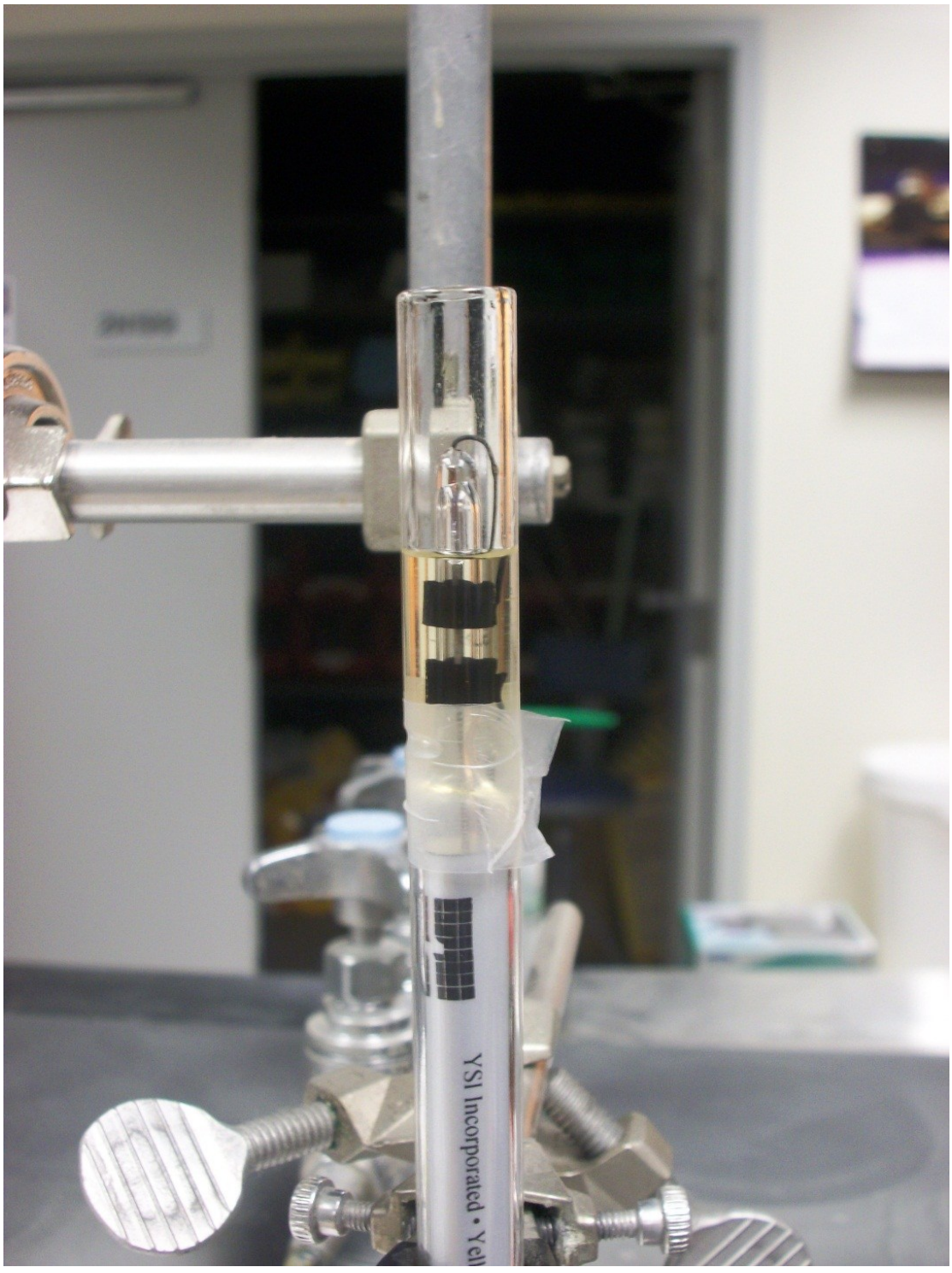

Figure 15: Conductivity cell filled with ionic liquid

4.4.4 Cyclic Voltammetry

Two rounds of cyclic voltammetry studies were performed on each ionic liquid using two different potentiostats. The wide electrochemical windows anticipated for the ionic liquids exceed those of the most common solvents used for electrochemical measurements. Therefore the window was determined by performing scans on the ionic liquids themselves without dissolving them in any solvent. This gave clear values for the electrochemical window but showed several strange electrochemical reactions that could be impurities in the ionic liquids or a function of performing the experiments in an open atmosphere. Another round of scans was done in a nitrogen environment with the ionic liquids dissolved in a solution of 0.1M $TBABF_4$ in acetonitrile. While this setup was not able to reach the anodic and cathodic limits of the ionic liquids it gave a better view of possible electrochemically active species within the solvent window.

For the neat ionic liquid study a three electrode cell was built consisting of a glassy carbon working electrode, a nickel foil counter electrode, and an Ag/Ag^+ reference electrode (figure 16). The reference electrode was constructed by placing a silver wire in a fritted tube along with a 0.1 M solution of silver trifluoromethane sulfonate dissolved in the ionic liquid that was being studied. The nickel foil counter electrode was placed in a separate fritted tube with a small amount of pure ionic liquid. These tubes and the glassy carbon electrode were placed in a 10 mL beaker so that they were submerged in a sample of the pure ionic liquid. The electrodes were held in place by drilling holes in a rubber stopper and securing the stopper in the beaker. The constructed cell was connected to an EG&G model 273A Potentiostat/Galvanostat from Princeton Applied Research. A series of single vertex sweeps were performed at 50 mV/s. For each test cell the voltage of the

cell was increased to a specified value then returned to the rest potential. The voltage was increased by 0.2 V for each cycle until the current began to drastically increase indicating oxidation or reduction of the electrolyte.

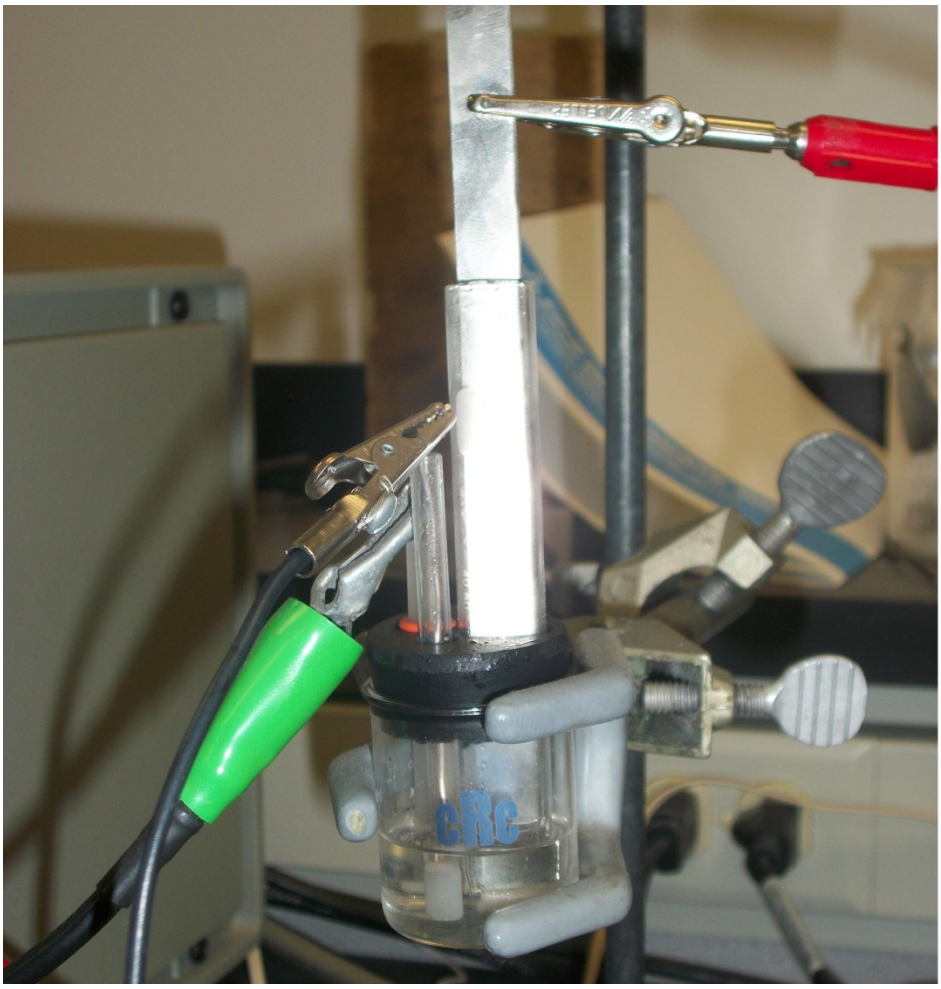

Figure 16: Electrochemical cell constructed for pure ionic liquid scans

For the tests in acetonitrile a three-electrode cell was set up using a platinum disc as the working electrode, a platinum wire as the counter electrode, and a silver wire as the reference electrode (figure 17). The cell was filled with approximately 5 ml of a 0.1M $TBABF_4$ solution in dried acetonitrile. Scans were performed with a CHI 1232 electrochemical analyzer at 60 mV/s. A voltage window of -1.8V to 2V was used in

order to avoid oxidation or reduction of the acetonitrile solution. Before each ionic liquid was tested, a blank scan was taken of just the acetonitrile solution. Enough ionic liquid was then added to create a 0.2M concentration and the resulting scan was compared to the blank to determine the electrochemistry of the ionic liquid. A scan was also taken with a 1 mM concentration of ferrocene in order to calibrate the voltages to the standard hydrogen electrode (SHE).

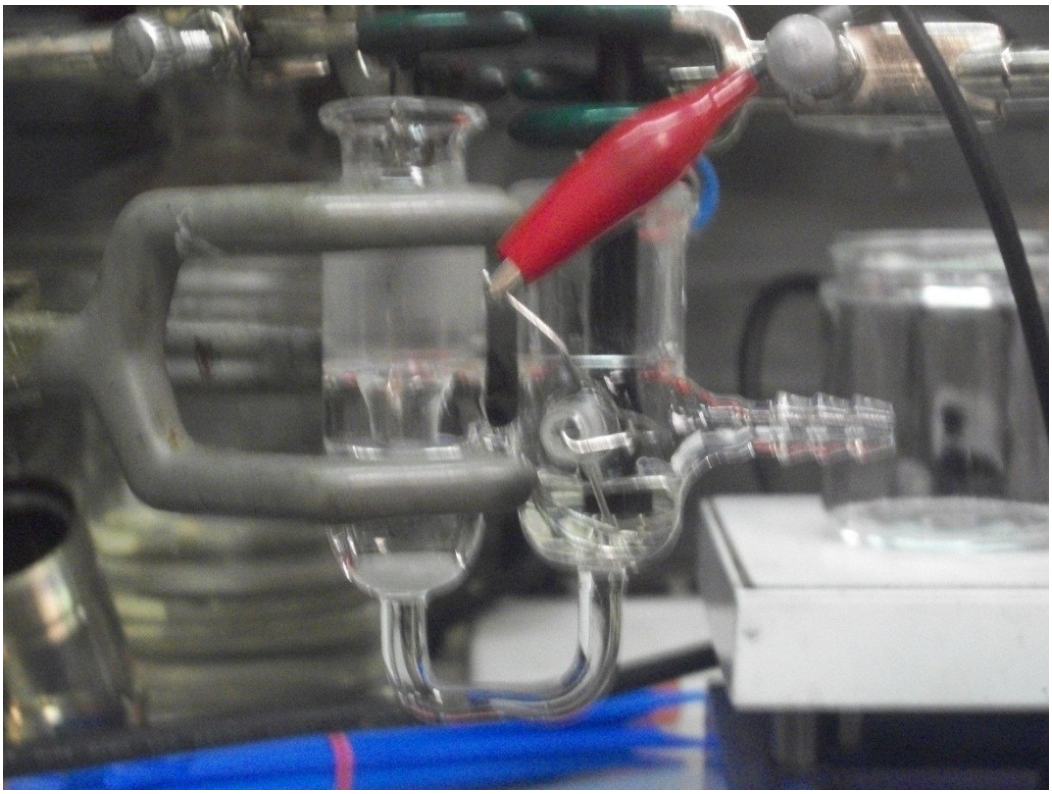

Figure 17: Electrochemical cell used for solvated ionic liquid tests

4.4.5 Water Content

Figure 18: Karl-Fischer Volumetric Titrator

The water content of each ionic liquid was determined using a Karl-Fischer volumetric titrator produced by Mettler Toledo (figure 18). In Karl-Fischer titration approximately 0.2g of sample is placed into the test cell and iodine is added until it no longer reacts with the sample. The titrator then reports the water content on a mass and percentage basis.

4.4.6 X-Ray Diffraction (XRD)

X-Ray diffraction was performed on the prepared cathode materials to ensure that the desired phase was achieved. XRD measures the distance between the planes of a crystal by directing X-rays at varying angles and measuring the intensity of the diffracted rays. The samples were analyzed with a Scintag X_2 powder X-ray diffraction system that used CuK_α radiation with a wavelength of 1.5406 Å. The data was viewed with EVA software and compared with lattice parameter data provided by the joint committee on powder diffraction standards (JCPDS)

4.5 Assessment of Battery Performance

Electrochemical cells were constructed to test the performance of the synthesized ionic liquids as battery electrolytes. The cells consisted of a cathode produced from the synthesized oxide materials, a lithium foil anode, a glass fiber separator and a lithium salt dissolved in the various ionic liquids as electrolytes. Benchmark tests were also performed by constructing cells with a standard 1M $LiPF_6$ in a 1:1 ethylene carbonate, dimethyl carbonate electrolyte.

4.5.1 Slurry Coatings

In order to function in an electrochemical cell the active cathode materials must be incorporated into a conductive coating spread onto an aluminum backing. This slurry consisted of the active material, carbon black, polyvinylidene fluoride (PVdF), and N-methyl-2-pyrrolidone (NMP). These materials were combined in a sample vial and homogenized, then placed in a vacuum chamber for degassing. Once the solutions were

degassed a draw-down machine was used to spread the slurry across a sheet of aluminum foil. The coatings were then heated to 70° C in a vacuum furnace for three hours to dry.

4.5.2 Electrolyte Preparation

To properly function as an electrolyte for lithium ion batteries, lithium must be added to the prepared ionic liquids so that it becomes the dominant charge carrier. This is done by dissolving a lithium salt in the ionic liquid. It is best to use a lithium salt consisting of the same anion that is in the ionic liquid in order to minimize the species present. One would like for the lithium concentration to be as high as possible so that it becomes the dominant charge carrier. In reality however the ionic conductivity of the solution decreases as more of the lithium salt is added due to increasing viscosity, which is likely due to the lithium forming various complexes with the anion. There is likely an optimal salt concentration with the highest possible lithium transference while maintaining good ionic conductivity. This concentration is likely different for each ionic liquid and difficult to determine without testing a wide range of concentrations. For this study an initial round of battery testing was done with lithium concentrations of approximately 1 mol/kg of LiTFSI in each ionic liquid. This was determined to be much too high as the capacities achieved were much lower than the theoretical capacities for the electrode materials as well as the control cells constructed with a standard carbonate electrolyte. A second round of tests was then performed with a concentration of 0.2 mol/kg of LiTFSI in each ionic liquid, which was closer to optimal values for similar ionic liquids reported in literature [25].

4.5.3 Half-Cell Construction

The cells were assembled in a T-cell configuration as shown in figure 19.

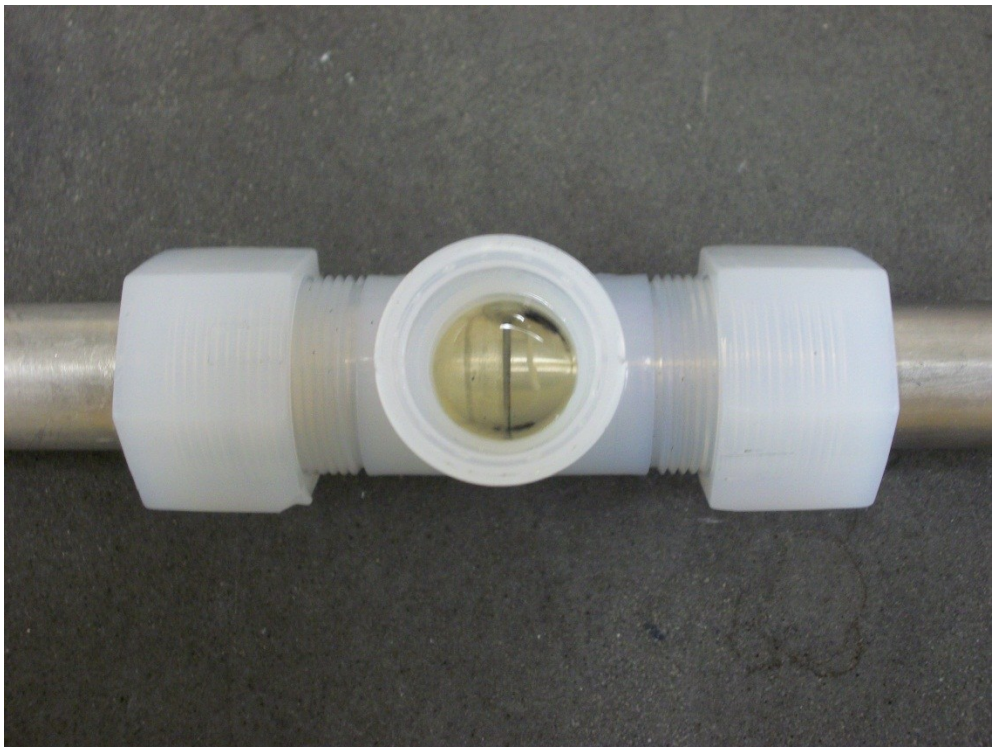

Figure 19: T-Cell used for Battery Cycling Tests

The cathode was prepared by punching a ¾ inch diameter disc out of the prepared slurry coatings then placing it on an aluminum cylinder and covering it with the separator. The aluminum cylinder was then placed in one side of a plastic "T" and a plastic nut was used to create an airtight seal. The assembly was then placed into an argon dry box. The anode of the T-cell was constructed by placing a disc of lithium foil on a stainless steel current collector consisting of two cylinders separated by a spring. This assembly was placed in the other side of the plastic "T" with the spring ensuring good contact with the separator. Another plastic screw was used to create an air-tight

seal. A small amount of electrolyte was added by pipette through the top of the plastic "T". Enough electrolyte was used to completely wet the separator and provide a small excess on top for future absorption. The ionic liquids were heated in an oven to 90° C before adding them to the cell to decrease viscosity to ensure complete wetting of the separator. A cap was screwed onto the top of the cell to keep the inside air free and the cells were left overnight to equilibrate.

4.5.4 Galvanic Cycling

The cells were cycled on an Arbin BT2000 Galvanostat. In galvanostatic cycling the current is held constant and the voltage at the working electrode is varied within a specified range. In the T-cell configuration the cathode functions as the working electrode and the lithium functions as both the counter and reference electrodes. For this study the cells were cycled at several different currents to determine how the charging rate affected the performance of cells with ionic liquid electrolytes. The cells with the $LiNi_{1/3}Mn_{1/3}Co_{1/3}O_2$ cathode were cycled between 2.5V and 4.5V versus lithium. The cells with the $LiMn_{1.5}Ni_{0.5}O_4$ cathode were cycled between 3V and 5V versus lithium.

4.6 Demonstration of Enhanced Safety

After galvanic cycling, several of the cells were charged back to their maximum voltage and held there to remove as much lithium from the lattice as possible. This puts the cathode into a highly reactive state. A small amount of this delithiated material was then placed in a DSC pan with a small amount of either the carbonate electrolyte or an ionic liquid and heated to 400°C to detect any possibly hazardous reactions.

Chapter 5: Results and Discussion

5.1 Visual Comparison of Ionic Liquids

The synthesized ionic liquids are named butylmethylpyrrolidinium bis(trifluoromethylsulfonyl)imide (BMPyrrTFSI), hexylmethylpyrrolidinium bis(trifluoromethylsulfonyl)imide (HMPyrrTFSI), butylmethylpiperidinium bis(trifluoromethylsulfonyl)imide (BMPipTFSI), and hexylmethylpiperidinium bis(trifluoromethylsulfonyl)imide (HMPipTFSI). Figure 20 shows samples of the liquids with varying degrees of yellow tint.

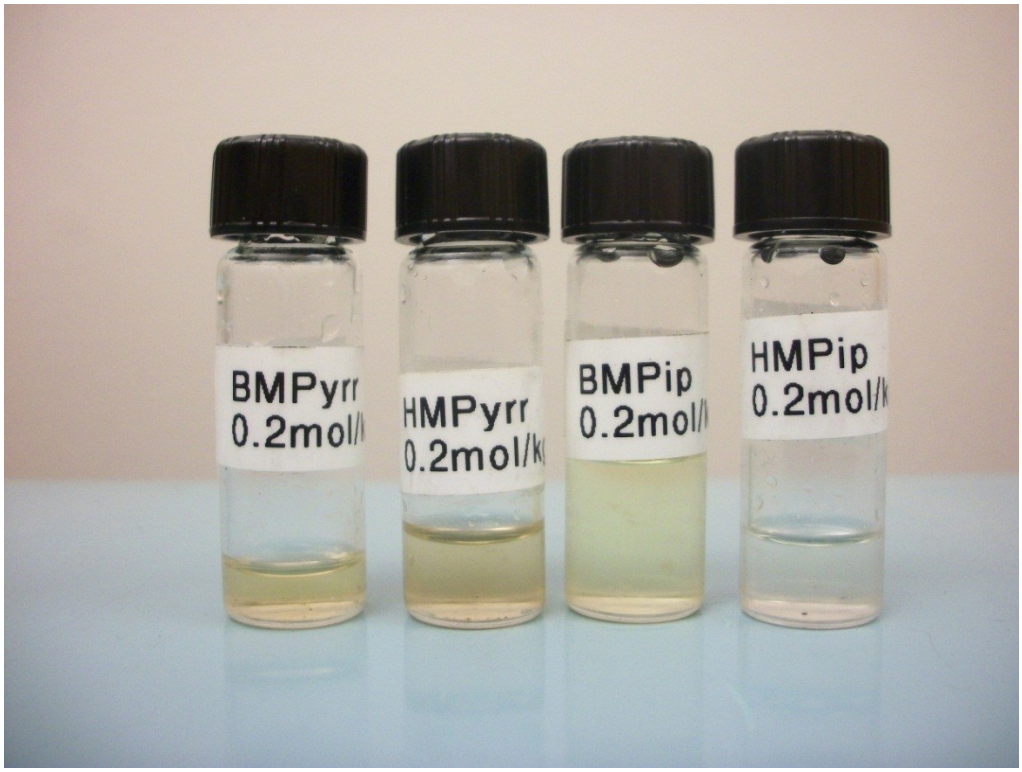

Figure 20: Samples of the four synthesized ionic liquids

The color was consistent for each liquid across several rounds of metathesis reactions. This suggests that the coloration is due to the conditions during the alkylation process. It is likely that the color is related to the iodine used as the alkylating agent. The HMPipTFSI sample was the clearest, suggesting that it has the lowest amount of impurities and the optimal synthesis conditions

5.2 Nuclear Magnetic Resonance

Figures 21-24 show the ^{1}H NMR spectra for the four different ionic liquids synthesized in this study. The peaks can easily be correlated to the appropriate structural features. The peaks at 1.9 ppm in each spectra are due to the dueterated acetonitrile that the ionic liquids were dissolved in for the scans. The peaks at 2.1 ppm in the piperidinium samples may be a small amount of water present in the samples. It is clear from these spectra that the desired ionic liquids were synthesized with minimal impurities.

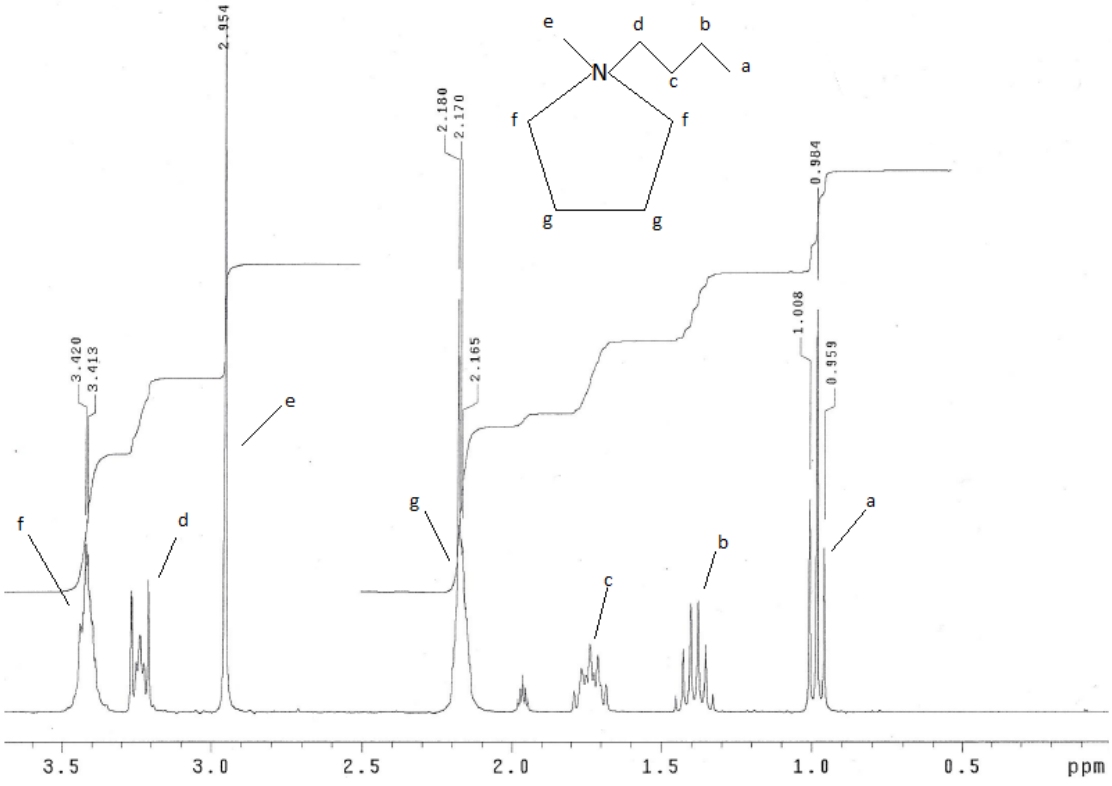

Figure 21: ^{1}H NMR of Butylmethylpyrrolidinium

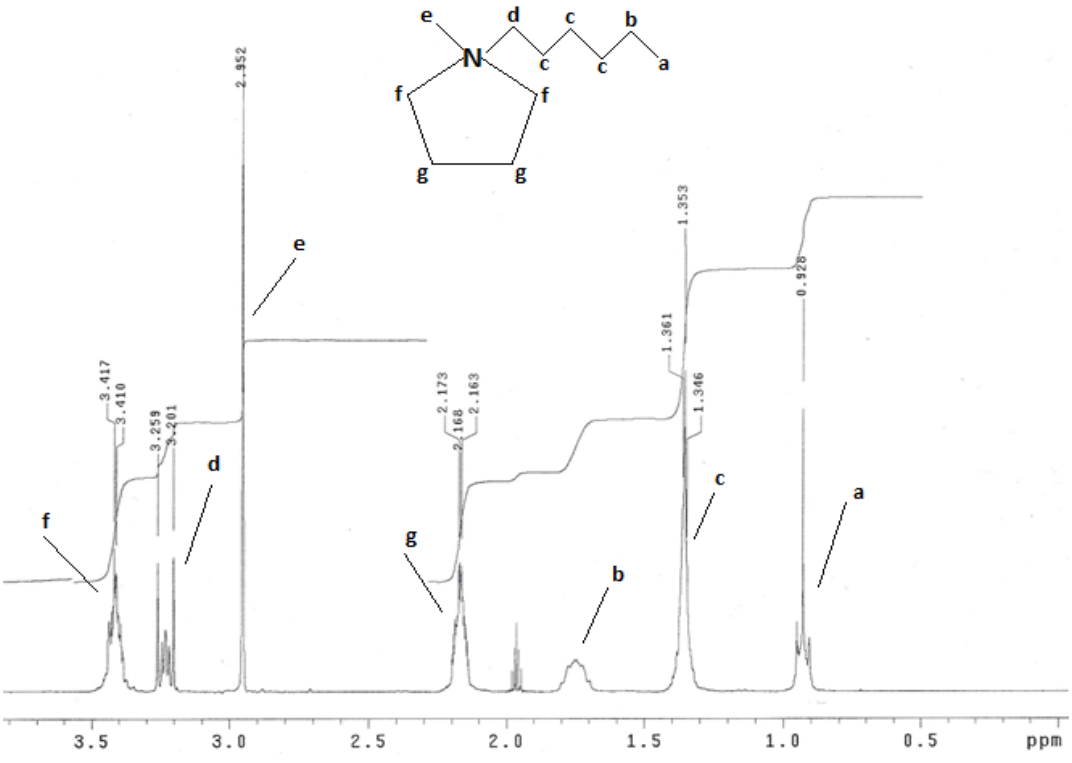

Figure 22: [1]H NMR of Hexylmethylpyrrolidinium

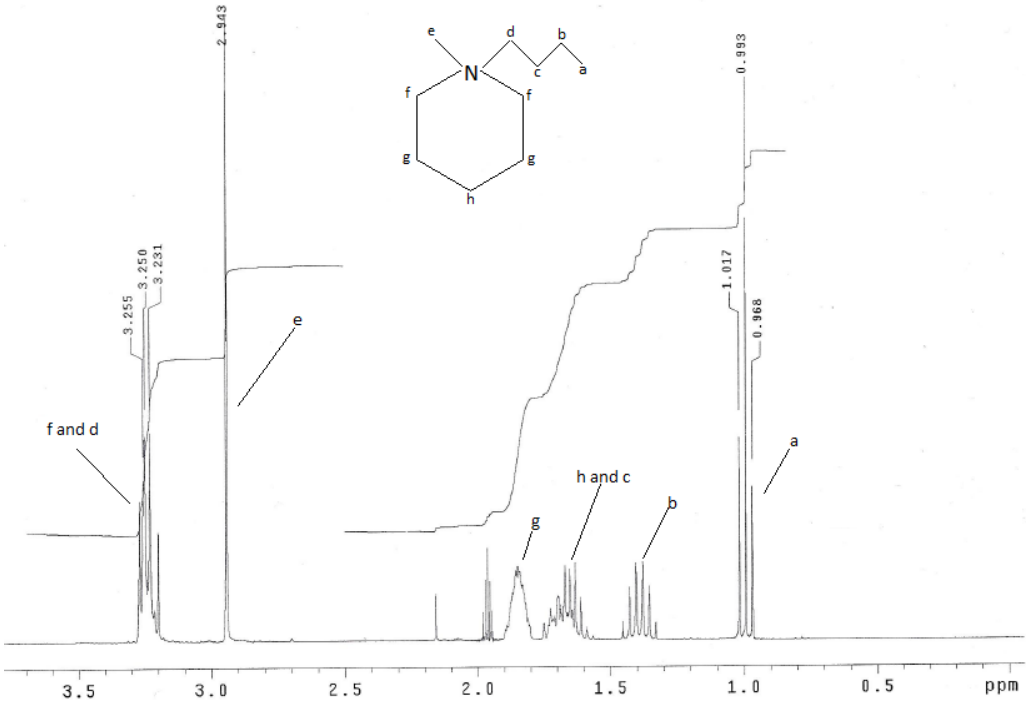

Figure 23: [1]H NMR of Butylmethylpiperidinium

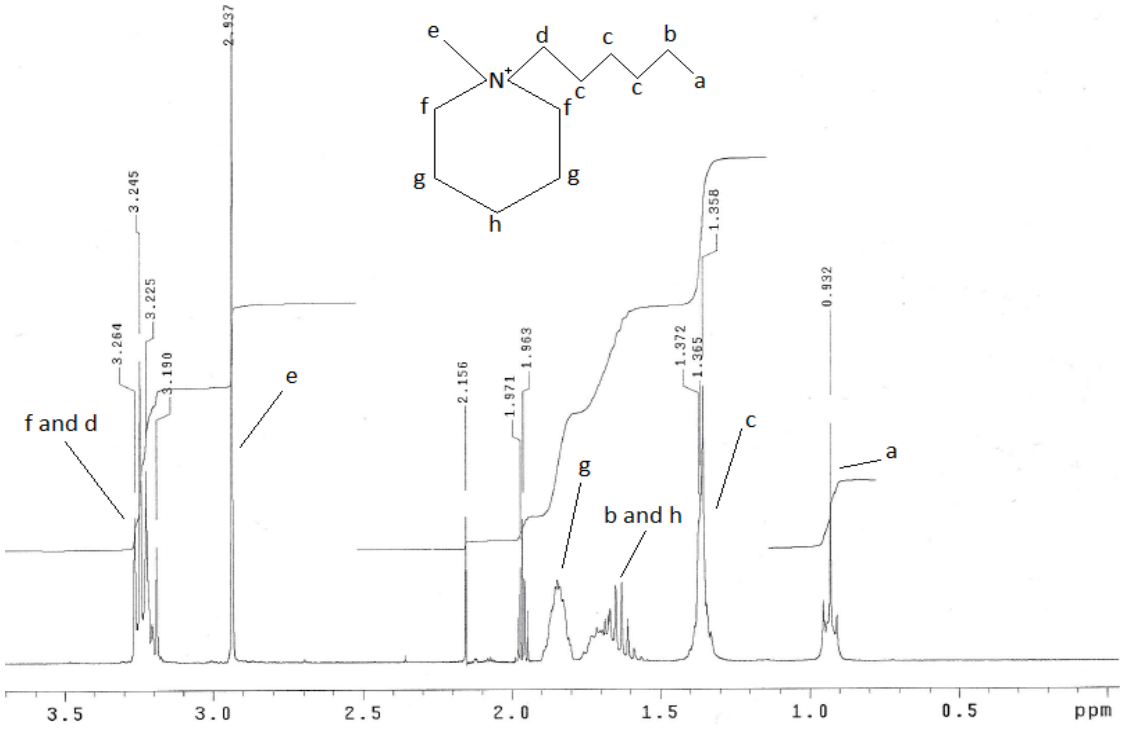

Figure 24: ^{1}H NMR of Hexylmethylpiperidinium

5.3 Differential Scanning Calorimetry

Figures 25-28 show the DSC thermograms for the synthesized ionic liquids with arrows indicating the scan direction.

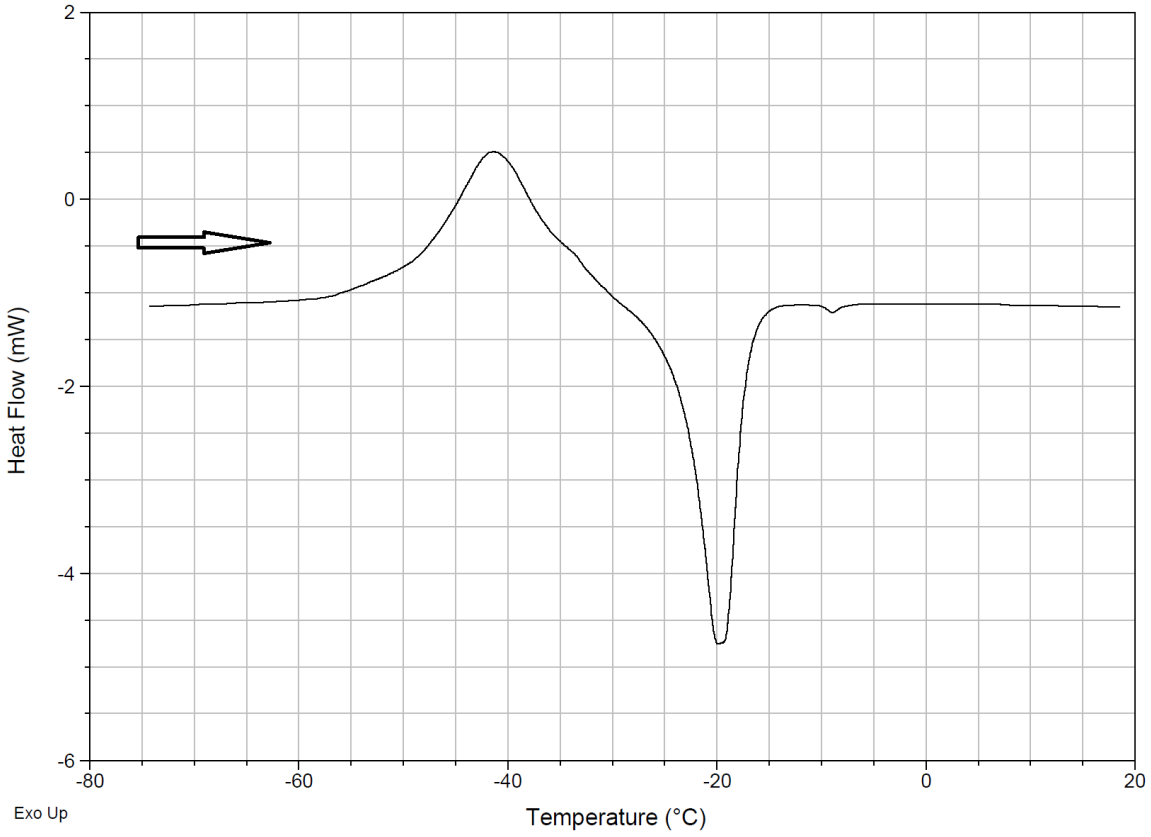

Figure 25: DSC thermogram of BMPyrrTFSI

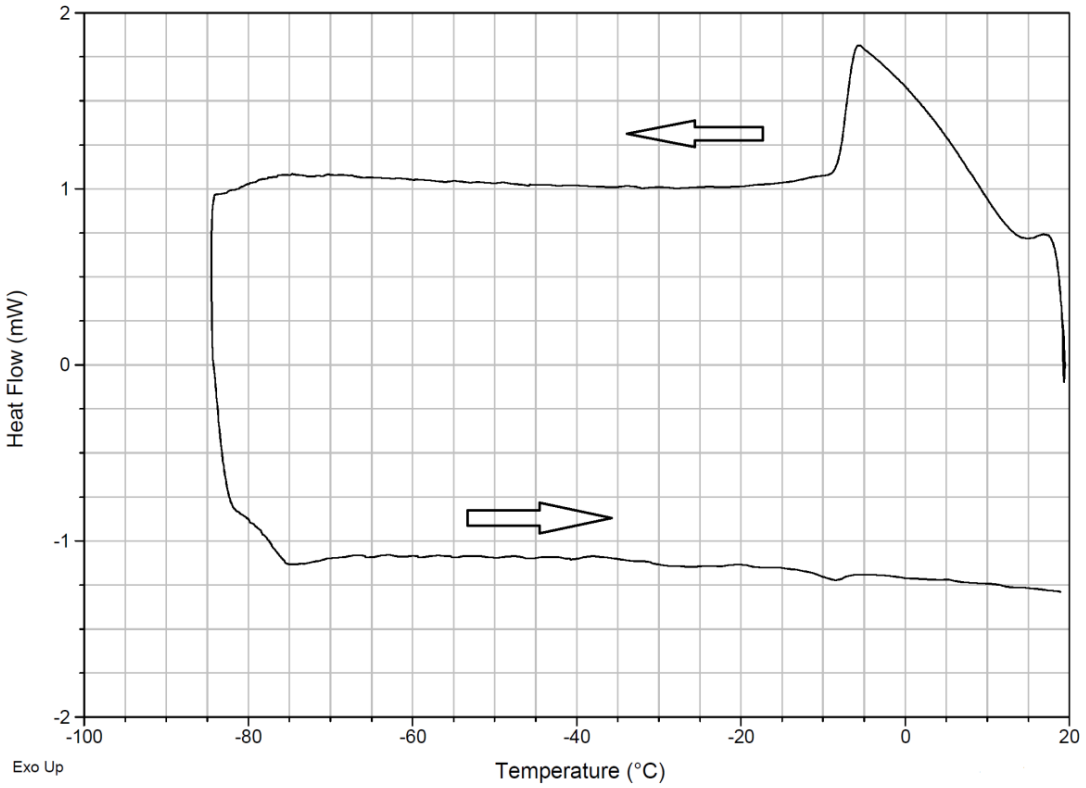

Figure 26: DSC thermogram of BMPipTFSI

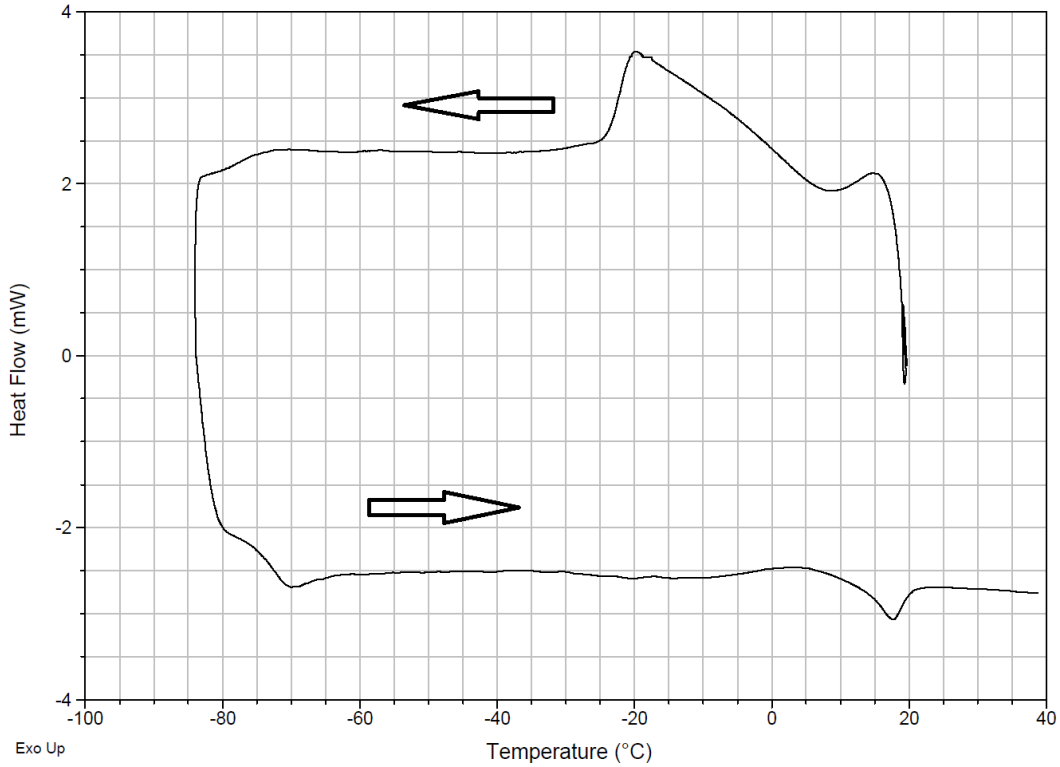

Figure 27: DSC thermogram of HMPipTFSI

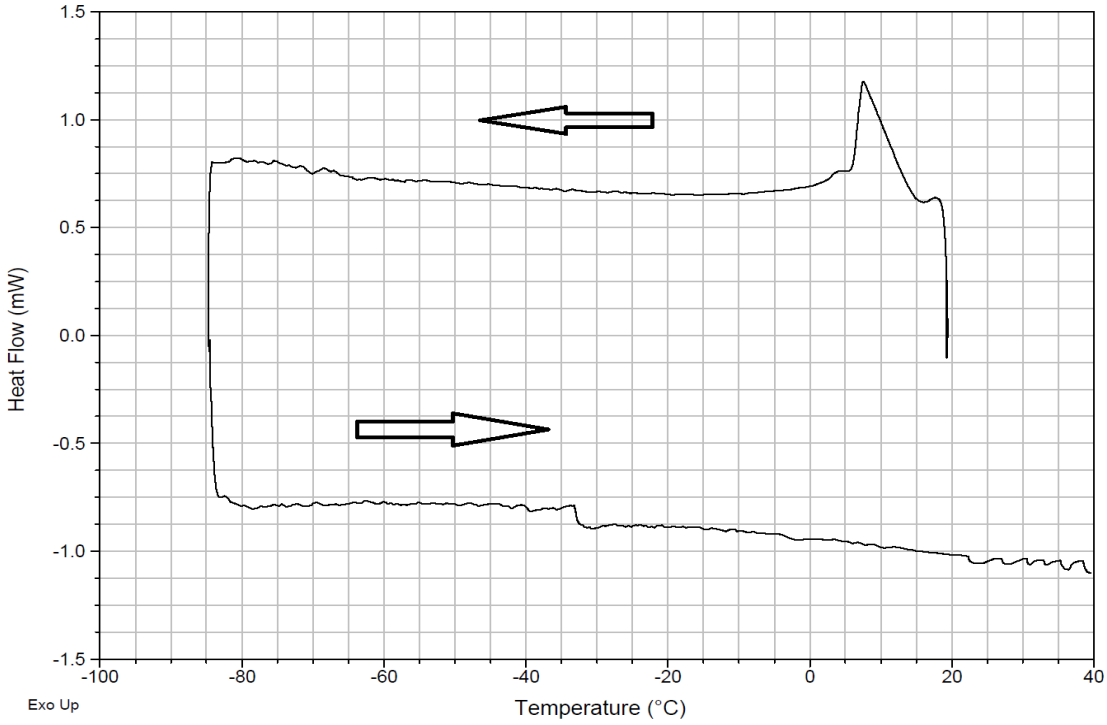

Figure 28: DSC thermogram of HMPyrrTFSI

Exact melting points are difficult to determine because ionic liquids tend to exhibit super cooling behavior and do not readily freeze when cooled at the rates required for DSC measurements. BMPyrrTFSI for example showed no phase change behavior when cooled from room temperature to -80°C at 5°C/min but showed the exothermic and endothermic peaks in figure 22 upon reheating. This freezing and melting behavior upon reheating matches reports from literature for this material [27] . The thermogram for BMPipTFSI, shows an exothermic peak around -6° C followed by a glass transition around -75° C. There is little change in the heat flow upon reheating, only a very small endothermic bump around -8° C which again displays the erratic melting behavior of ionic liquids. Like the BMPyrrTFSI date, -6° C matches reports for the BMPipTFSI melting point [28]. HMPipTFSI shows similar behavior to BMPipTFSI with an

exothermic peak around -20° C. The only endothermic peak is a small one around 17° C during reheating. This discrepancy is likely due to supercooling and the 17° C melting point matches reports from literature [28]. HMPyrrTFSI did not show any clear crystallization or melting behavior unless it was cooled at 2° C/min as shown in figure 25. The slow scan shows an exothermic peak around 10° C.

The difficulty in obtaining clear pictures of the low temperature behavior of ionic liquids makes it difficult to draw conclusions about the effect of alkyl chain length on melting point. The slower cooling rates required to produce observable phase change behavior demonstrates a suppression of crystallization, but when phase change does occur it occurs at similar or even slightly higher temperature. Furthermore, the high viscosity of these materials (which is heavily temperature dependent) significantly lowers the conductivity as temperature decreases which negatively affects battery performance. These results indicate no conclusive improvement in low temperature behavior due to extending the alkyl chain length.

5.4 Ionic Conductivity

Table 1 shows the conductivities of the ionic liquids as synthesized and doped with 0.2 mol/kg LiTFSI. Although the overall ionic conductivity decreases, doping is necessary to achieve appropriate lithium transference. The ionic liquids show the predicted trend of decreasing conductivity with increasing cation size. This should correlate to the maximum rate capability of the electrolytes

Table 1: Conductivities of neat and doped ionic liquids (mS/cm^2)

Cation	As Synthesized	0.2 mol/kg LiTFSI
Butylmethylpyrrolidinium	2.782	1.947
Hexylmethylpyrrolidinium	1.357	1.052
Butylmethylpiperidinium	1.135	0.625
Hexylmethylpiperidinium	0.607	0.451

5.5 *Cyclic Voltammetry*

5.5.1 *Scans of Pure Ionic Liquids*

Figures 29 and 30 show the results of the CV scans in the pure ionic liquids. The estimated voltage windows of each are summarized in Table 2. The anodic limit was taken at the point where the current reached 4 µA. The cathodic sweeps showed a much clearer limit where the current began to quickly increase over a narrow voltage range. The limit was taken at the point where the current reached 40 µA which is above the current due to impurities.

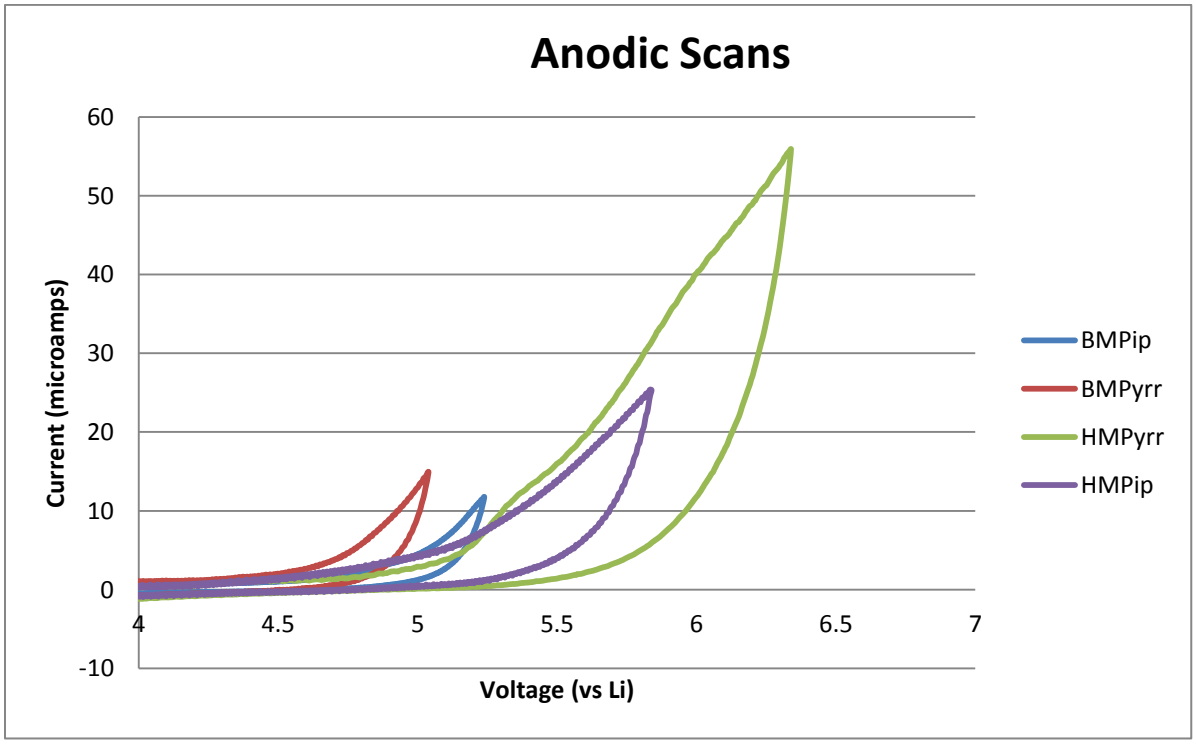

Figure 29: Anodic limits of ionic liquids

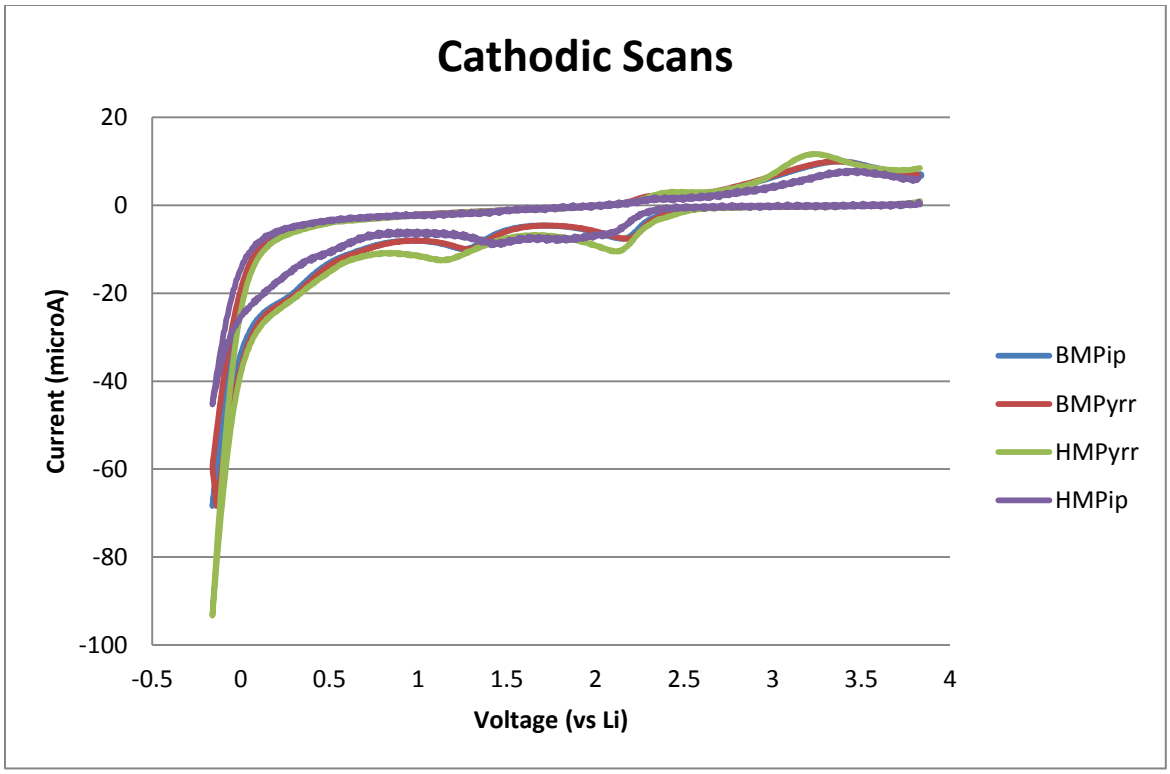

Figure 30: Cathodic limits of ionic liquids

Table 2: Estimations of the electrochemical windows of each ionic liquid

Cation	Anodic Limit (vs Li)	Cathodic Limit (vs Li)	Window
Butylmethylpyrrolidinium	4.7 V	-0.09 V	4.79 V
Hexylmethylpyrrolidinium	5.1 V	-0.01 V	5.11 V
Butylmethylpiperidinium	4.9 V	-0.04 V	4.94 V
Hexylmethylpiperidinium	5.0 V	-0.13 V	5.13 V

The anodic scans of each liquid showed no electrochemical activity until the continuous increase in current indicating the oxidation of the anion. It is interesting that the ionic liquids show a variable oxidation behavior despite each having the same anion.

The effect seems to be more connected to the alkyl chain length then the ring structure. It may be due to the longer chains helping to shield the anion from the oxidation activities of the electrode, perhaps due to the formation of a passivation layer. Conversely, the lower ionic conductivity resulting from the longer chains could be causing a delay between when the electrolyte begins to breakdown and when the current begins to increase. Reports in literature give anodic limits of around 5.5 versus lithium for a wide variety of TFSI based ionic liquids so the observed values seem low, but the values in literature use much higher current limits (around 1 mA) which is possibly responsible for the discrepancy. Although the measured windows are smaller than those predicted by literature, all four ionic liquids show wide enough windows to indicate that they will be compatible with the layered cathode material. The ionic liquids featuring hexyl chains should also be compatible with the higher voltage redox couple of the spinel material.

The cathodic scans show several undesirable electrochemical reactions before the large scale reduction of the cations. It has been shown that trace impurities such as water and oxygen can cause oxidation peaks around 1.5V and 2V versus lithium so they are likely responsible for these peaks. The current effect is very small relative to the electrolyte breakdown so the impurity levels are likely very low. Furthermore, aside from the reduction wave between 3.0 and 3.5 V all of the impurity electrochemistry occurs below the voltages that will be used to test the compatibility of these ionic liquids with cathode materials. The 3.0V reduction wave is a concern however, which is why additional scans were done in a dry box to determine if it is due to contamination from performing the first scans in open air.

5.5.2 Scans of Ionic Liquids in Acetonitrile

Figures 31 through 34 show the results of scans performed in a nitrogen dry box. Each scan shows a quasi-reversible redox reaction centered around 2.25 volts. The reduction peak matches the first peak seen in the pure ionic liquid scans which is likely attributed to oxygen dissolved in the ionic liquid. The coupled oxidation peak at 2.5V could in fact correspond to the waves seen at 3 V in the pure ionic liquids. It is possible that the viscosity of the pure ionic liquids reduces the conductivity enough to cause the separation of peaks.

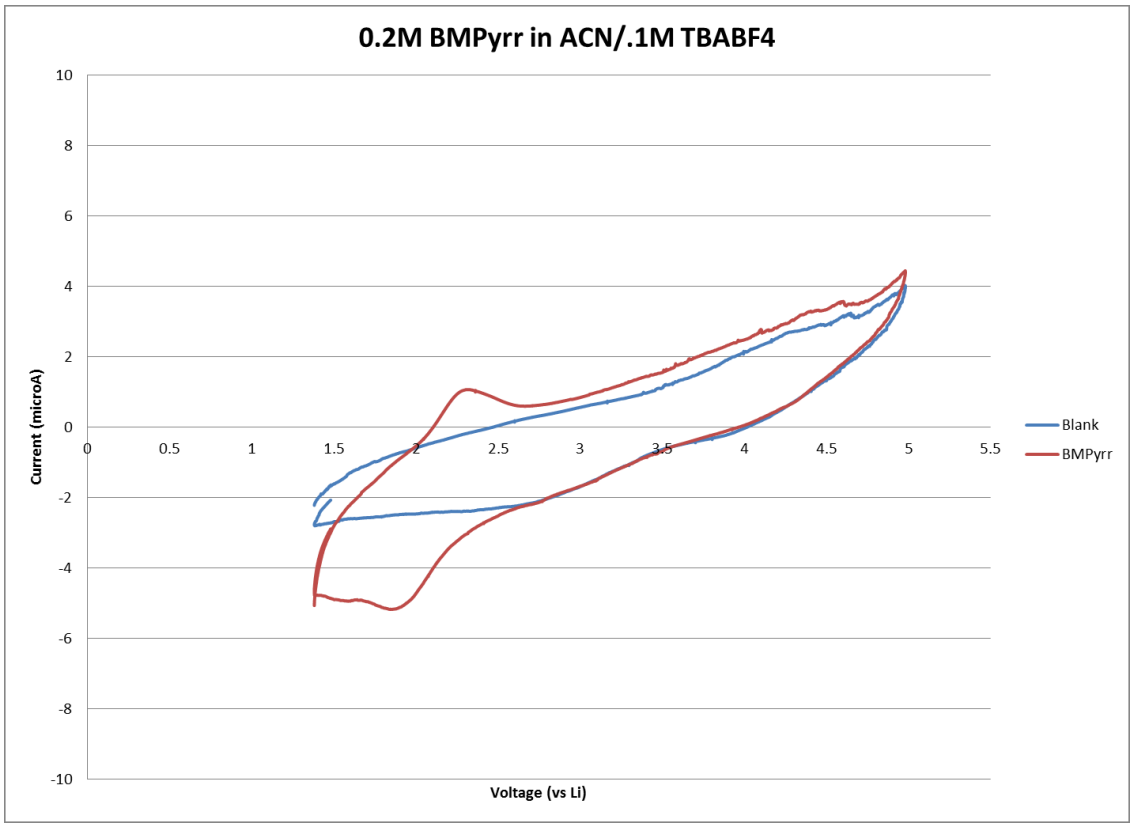

Figure 31: CV Scan of 0.2M BMPyrrTFSI in acetonitrile

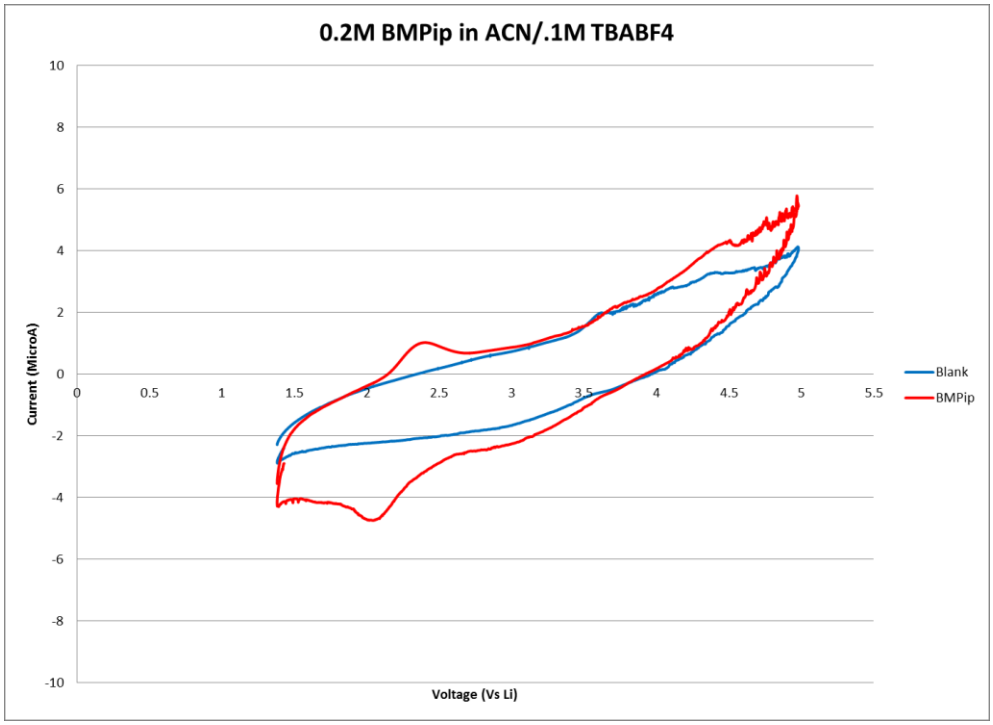

Figure 32: CV scan of 0.2M BMPipTFSI in acetonitrile

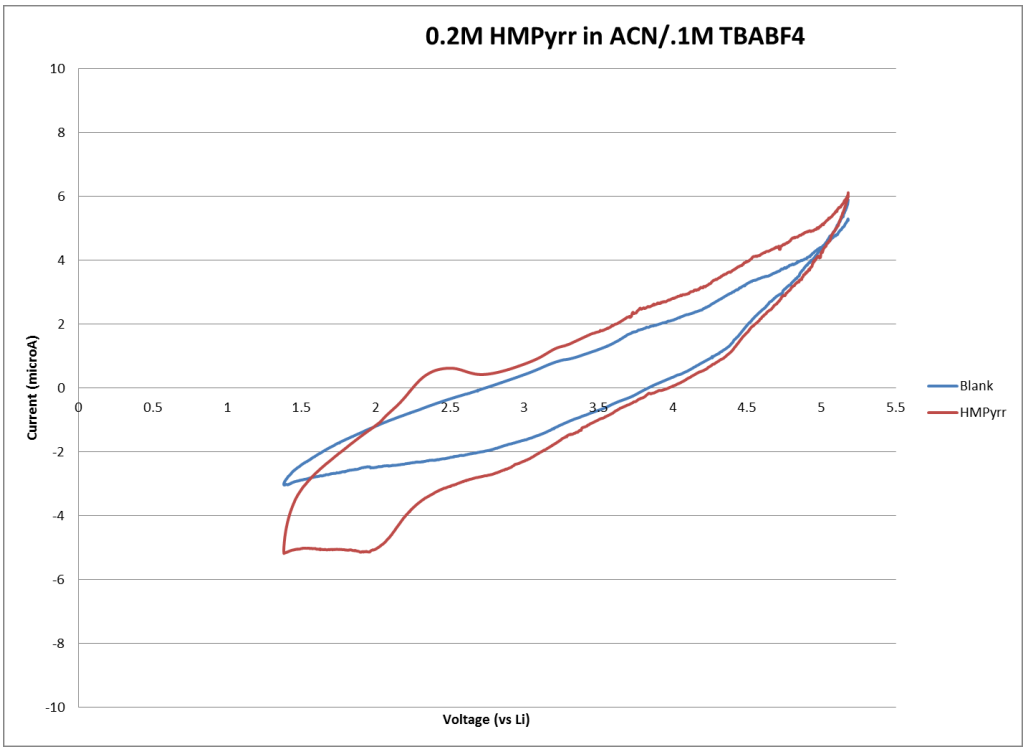

Figure 33: CV scan of 0.2M HMPyrrTFSI in acetonitrile

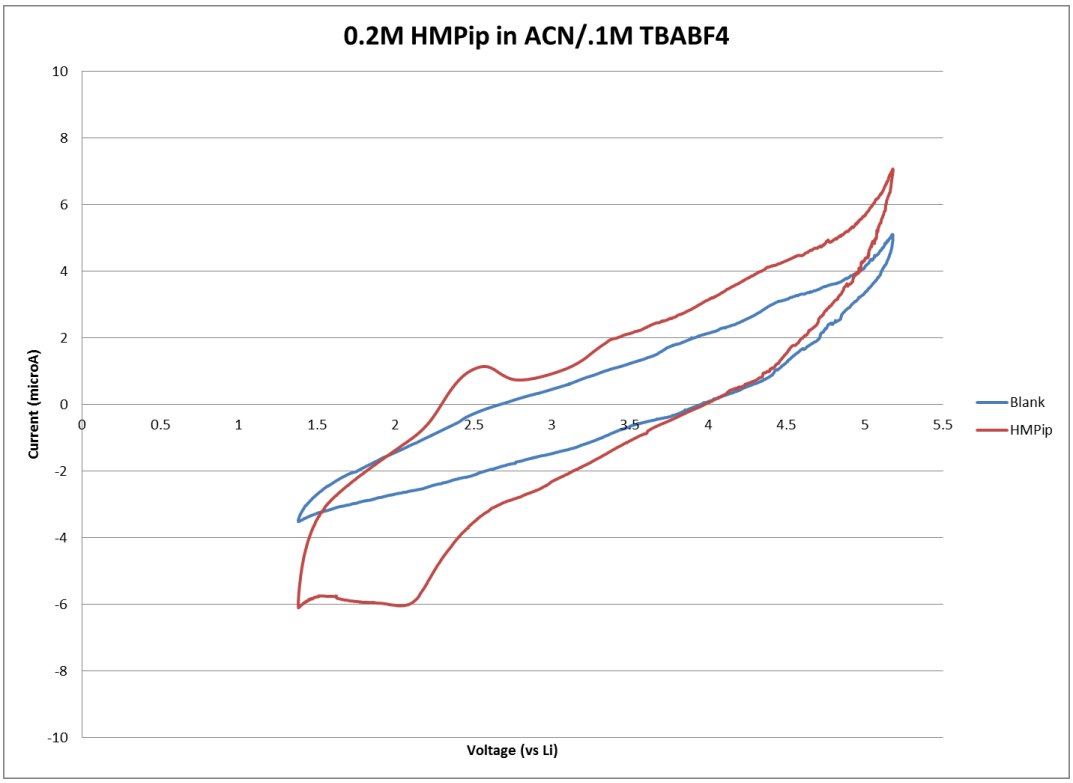

Figure 34: CV scan of 0.2M HMPipTFSI in acetonitrile

Figure 35 shows the scan of a 1mM concentration of ferrocene in the BMPyrrTFSI sample. The purpose of this scan is to show that the concentrations of impurities in the ionic liquids must be very low based on the relative current densities produced by such a small concentration of ferrocene. This scan also serves to calibrate the voltages since the redox potential of ferrocene is known to be 0.64 V versus the standard hydrogen electrode.

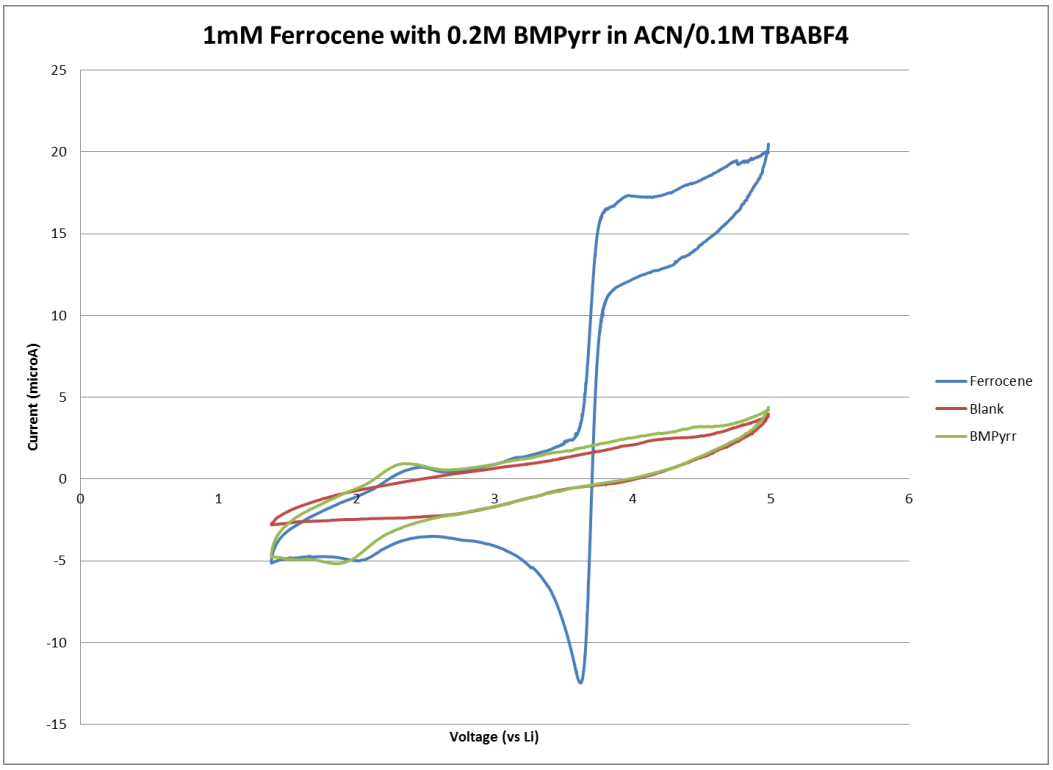

Figure 35: CV scan of 1mM ferrocene and 0.2M BMPyrrTFSI in acetonitrile

5.6 Water Content

Table 3 shows the water concentrations in parts per million (ppm) for each ionic liquid. The water levels are substantially higher than those reported in literature. This is likely due to the fact that the ionic liquids were dried in a vacuum oven while in 3 ml sample vials, which created a very small surface area for the water to evaporate from. Water is known to shrink the electrochemical window of ionic liquids, which may explain why the measured windows are smaller than those reported in literature.

Table 3: Water content in ionic liquids

Cation	Water Content (ppm)
Butylmethylpyrrolidinium	1350
Hexylmethylpyrrolidinium	1540
Butylmethylpiperidinium	740
Hexylmethylpiperidinium	1100

5.7 X-Ray Diffraction

Figures 36 and 37 show the peaks obtained from the x-ray diffraction scans performed on each cathode material. The black trace shows the results of the tested sample while the red lines show the expected peaks for each material. The peaks show good matching indicating that the desired oxide materials were synthesized.

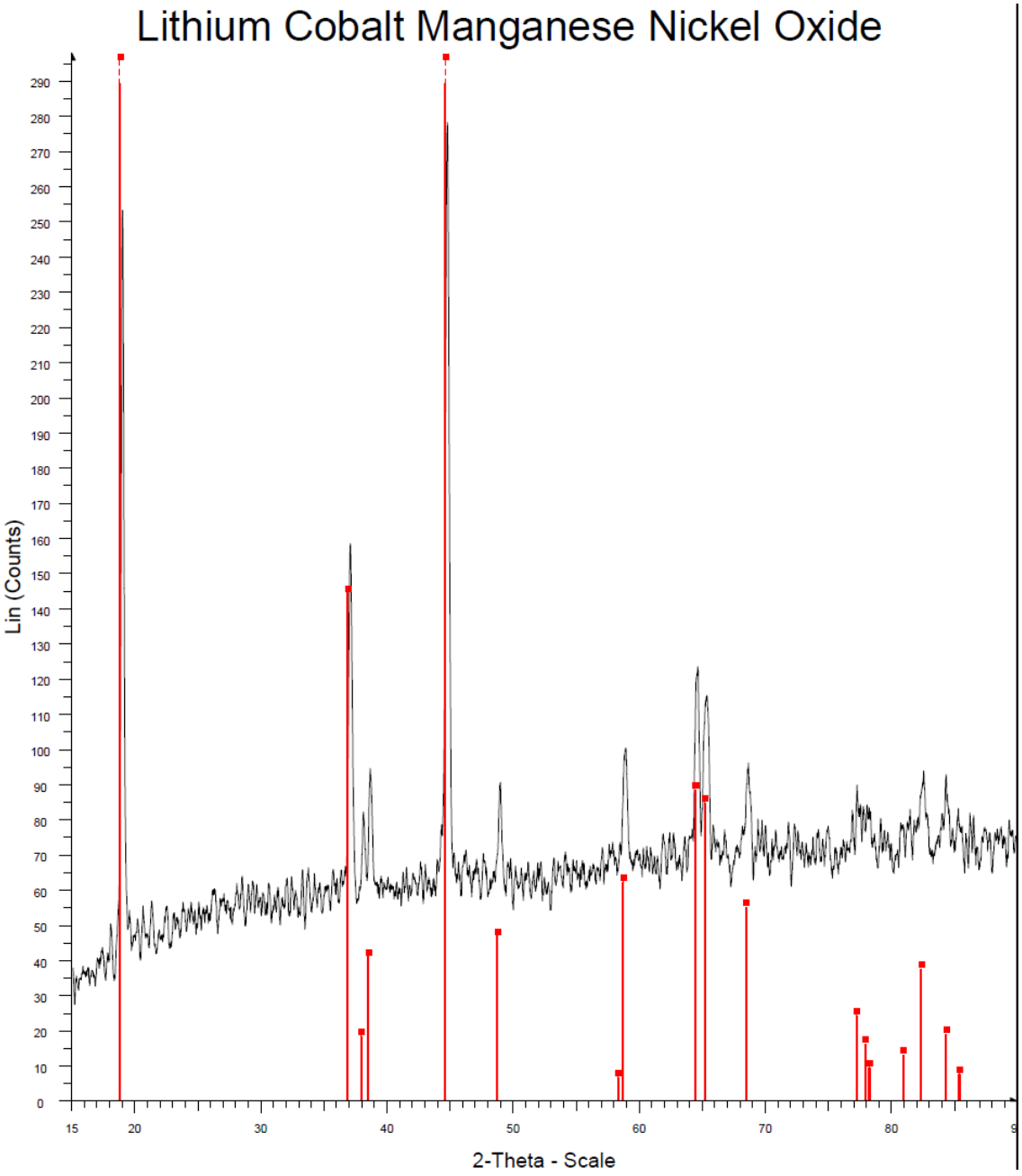

Figure 36: XRD scan of $LiCo_{1/3}Mn_{1/3}Ni_{1/3}O_2$

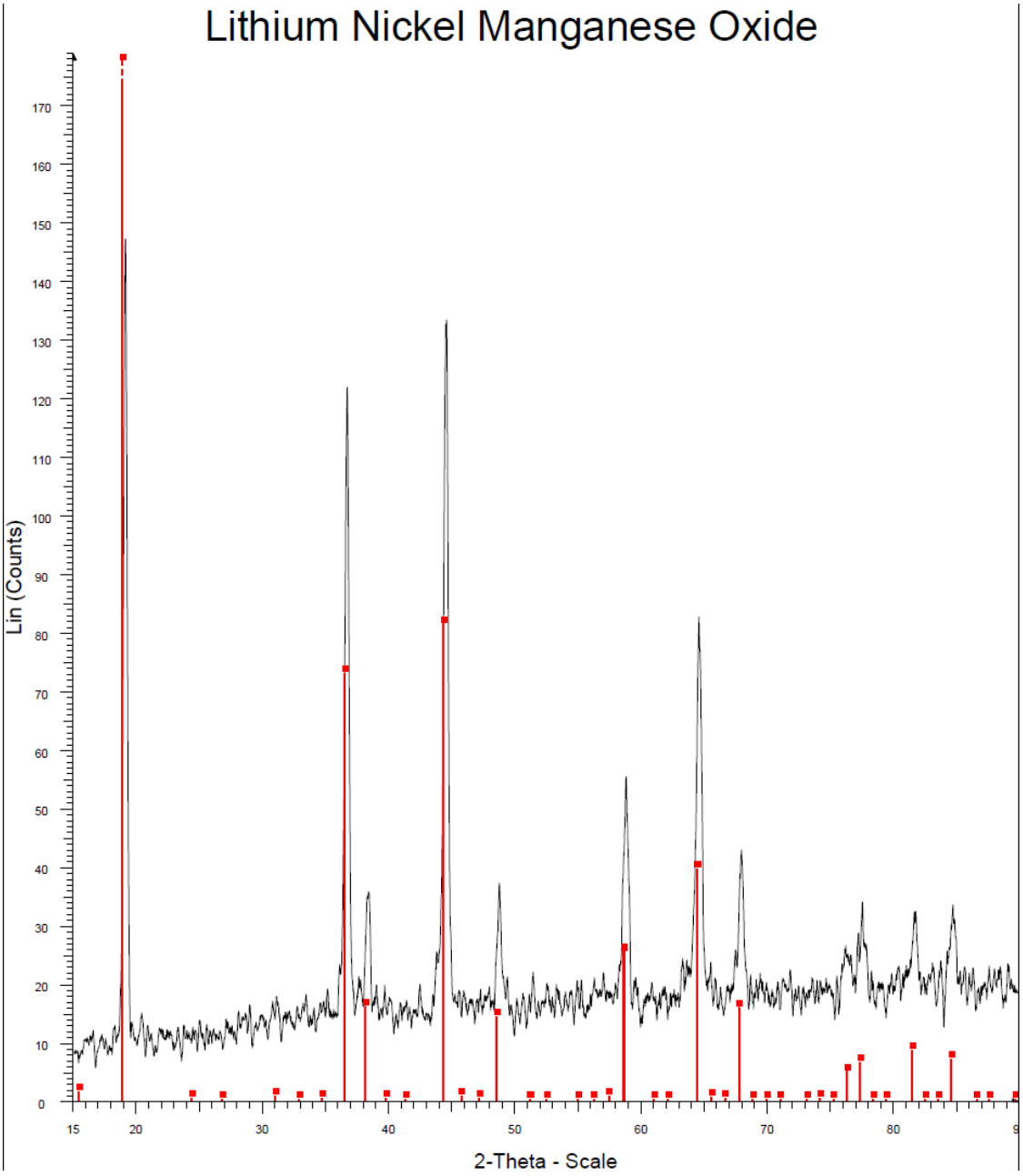

Figure 37: XRD scan of $LiNi_{0.5}Mn_{1.5}O_4$

5.8 *Battery Performance*

5.8.1 *$LiNi_{1/3}Mn_{1/3}Co_{1/3}O_2$ with Carbonate Electrolyte*

Figure 38 shows the specific capacity for the first, third, and fifth cycles of a $LiNi_{.33}Mn_{.33}Co_{.33}O_2$ cathode with a standard carbonate electrolyte at a rate of C/5. The first cycle had a specific charge capacity of 204 mAh/g and then showed a slight but steady decrease in capacity over 5 cycles. The discharge capacity was 197 mAh/g for the first cycle and showed a similar steady decrease.

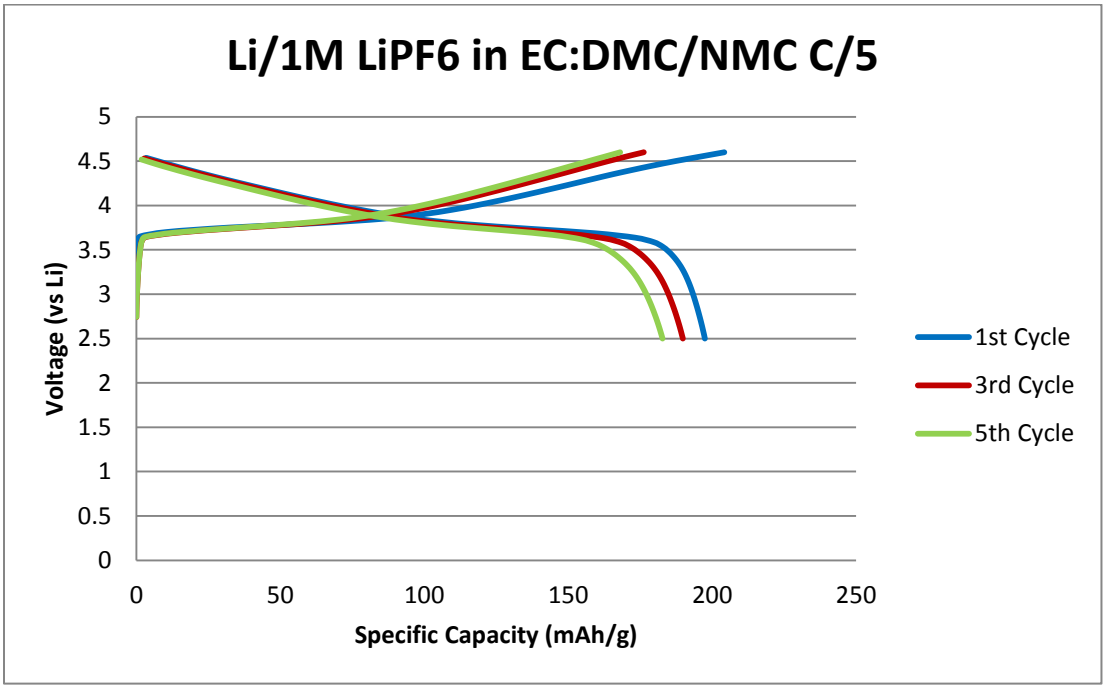

Figure 38: Specific capacity of layered cathode with carbonate electrolyte

Figure 39 shows the differential capacity for the same cycles. The differential capacity plot shows that the battery is reversibly intercalating lithium with an average voltage of 3.8V as reported in literature [10]. The capacities obtained also match well to

reports in literature. There are reports that the capacity can be increased by charging to higher voltages, but this leads to a breakdown of the cathode material due to dissolution of the active species into the electrolyte. This shows that the desired electrode material was indeed made and performs as expected with the standard electrolyte. The compatibility of the synthesized ionic liquids with this cathode will be determined by their relative performance in terms of specific capacity and rate capabilities.

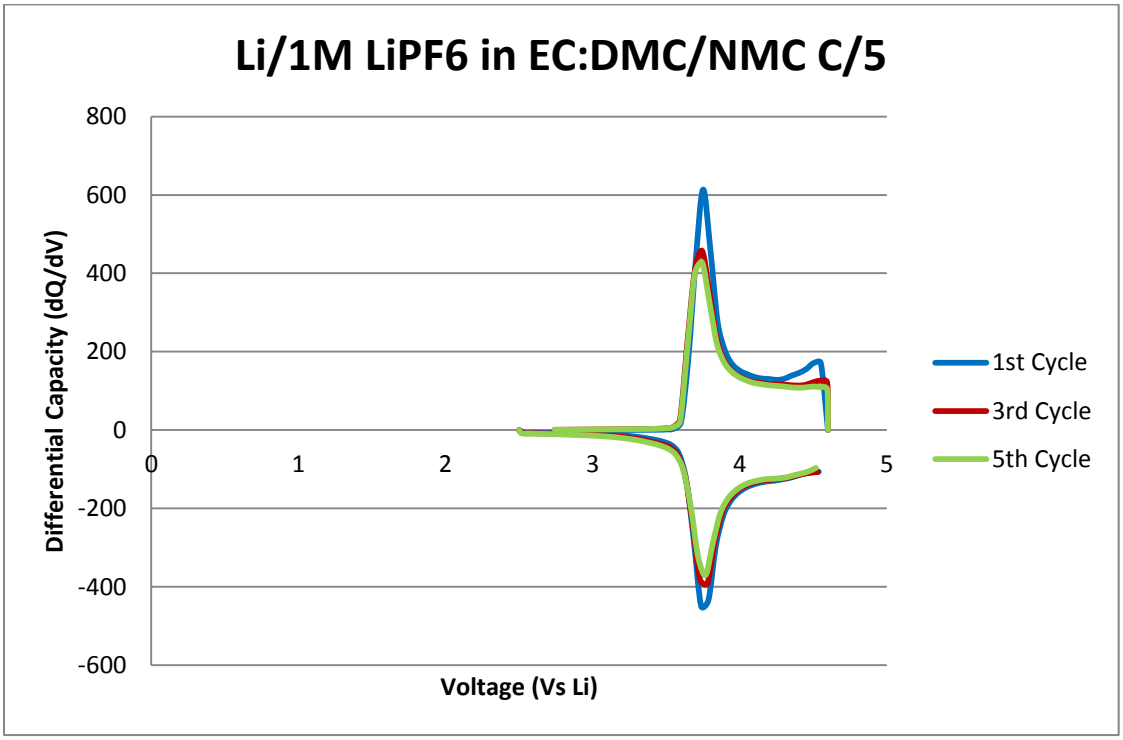

Figure 39: Differential capacity of layered cathode with carbonate electrolyte

5.8.2 $LiNi_{1/3}Mn_{1/3}Co_{1/3}O_2$ with Ionic Liquid Electrolyte

5.8.2.1 1 mol/kg LiTFSI in Ionic Liquid Electrolyte

For the first round of battery tests, 1 mol/kg of LiTFSI was dissolved into each ionic liquid. This was done to increase the lithium concentration in order to increase the lithium transference numbers. Some literature reports that the only limiting factor in the amount of lithium that could be added was the point at which the liquid crystalized at room temperature [29]. The 1 mol/kg samples remained liquid for several days and were put into test cells. Figure 40 shows the specific capacities for the first charge/discharge cycle of each ionic liquid.

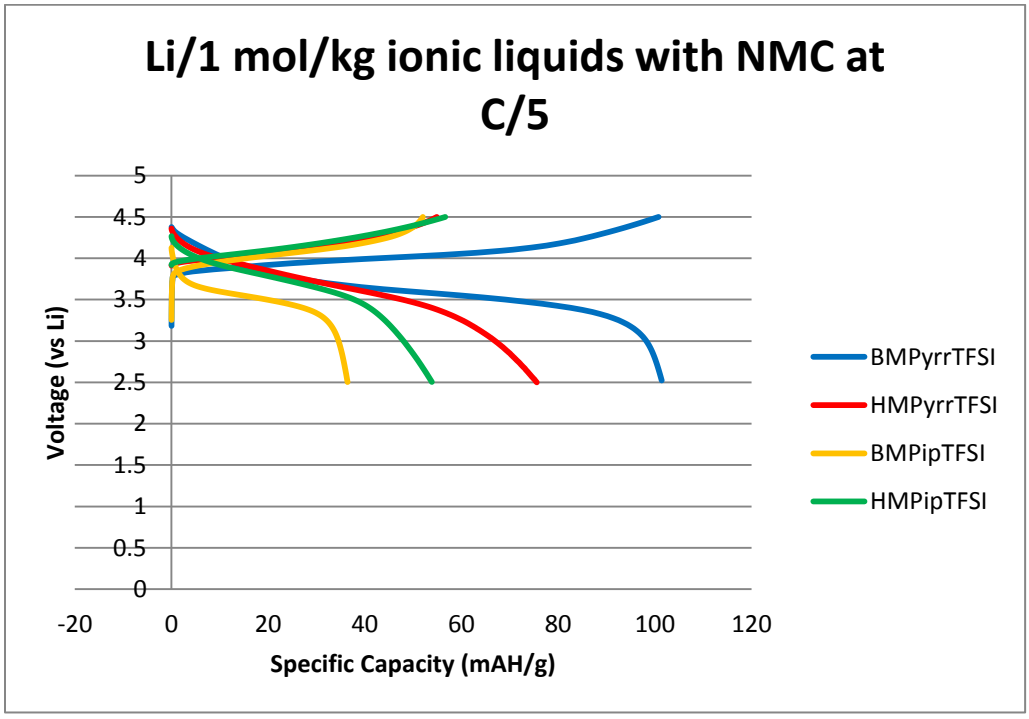

Figure 40: Specific capacities of each ionic liquid with 1 mol/kg LiTFSI

The ionic liquids generally follow the expected trend of decreasing capacity with decreasing ionic conductivity. BMPyrrTFSI performed the best as expected due to its significantly higher ionic conductivity. All of the capacities were significantly below that of the carbonate. Furthermore, the BMPipTFSI electrolyte showed a tendency to solidify after several cycles effectively killing the test cells. A further review of literature led to the conclusion that increasing the LiTFSI concentration drastically reduces the ionic conductivity and therefore only increases the lithium transference up to a certain point [25]. A new set of batteries was therefore constructed with a much lower concentration of LiTFSI.

5.8.2.2 0.2 mol/kg LiTFSI in Ionic Liquid Electrolyte

After the poor performance of the 1 mol/kg LiTFSI batteries a new round was constructed with a concentration of 0.2 mol/kg LiTFSI. This concentration should increase the lithium concentration enough to have a beneficial effect on the lithium transference numbers without being too detrimental to the overall ionic conductivity.

Initial attempts to cycle batteries at a rate of C/5 with the ionic liquids as electrolytes again failed to reach capacities similar to those of the carbonate electrolytes. The rate of charge had to be reduced to C/20 to see similar behavior. Figures 41 through 48 show the specific and differential capacities of representative cells for each ionic liquid at a rate of C/20.

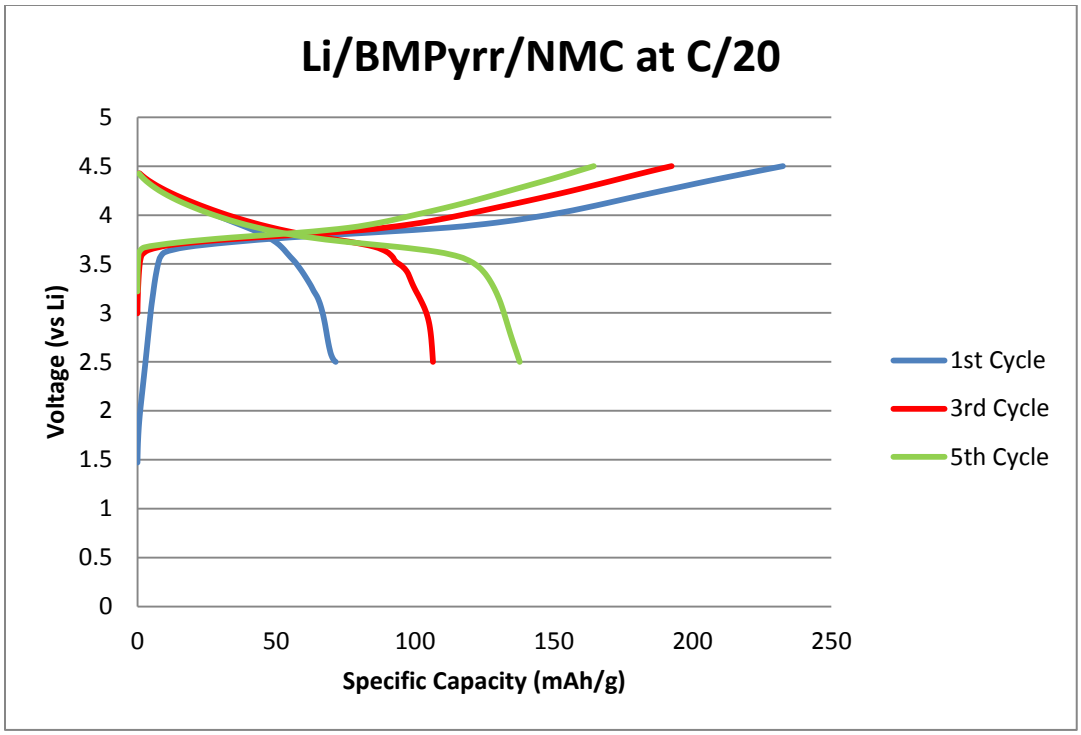

Figure 41: Specific capacity of layered cathode with BMPyrr electrolyte

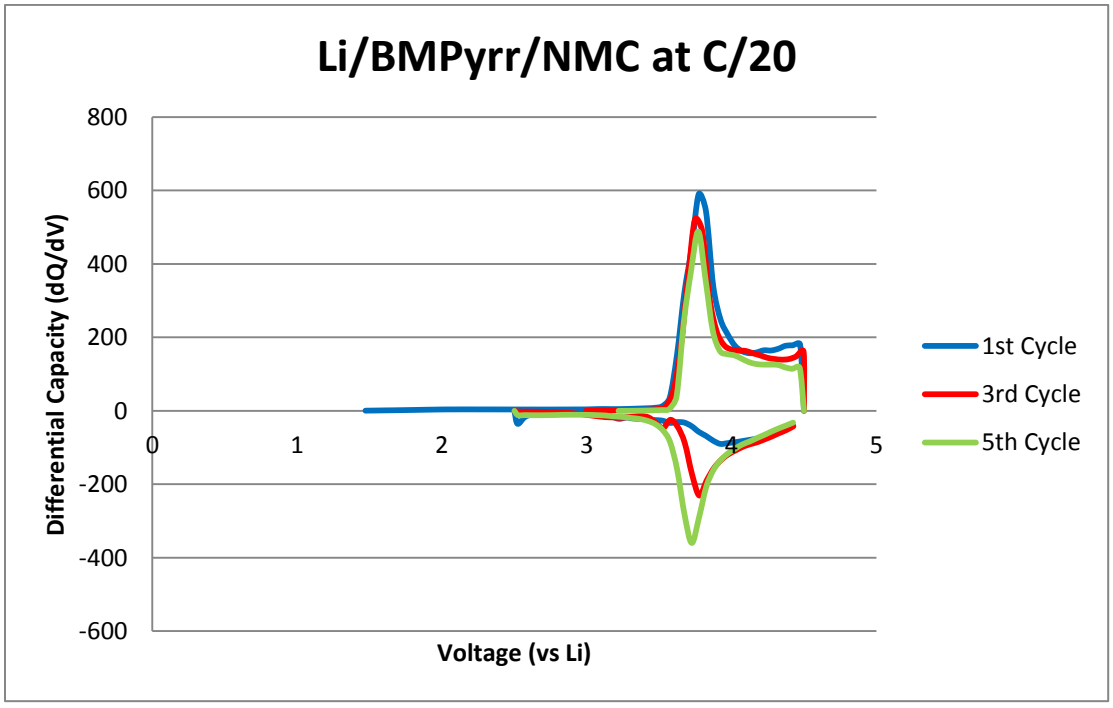

Figure 42: Differential capacity of layered cathode with BMPyrrTFSI electrolyte

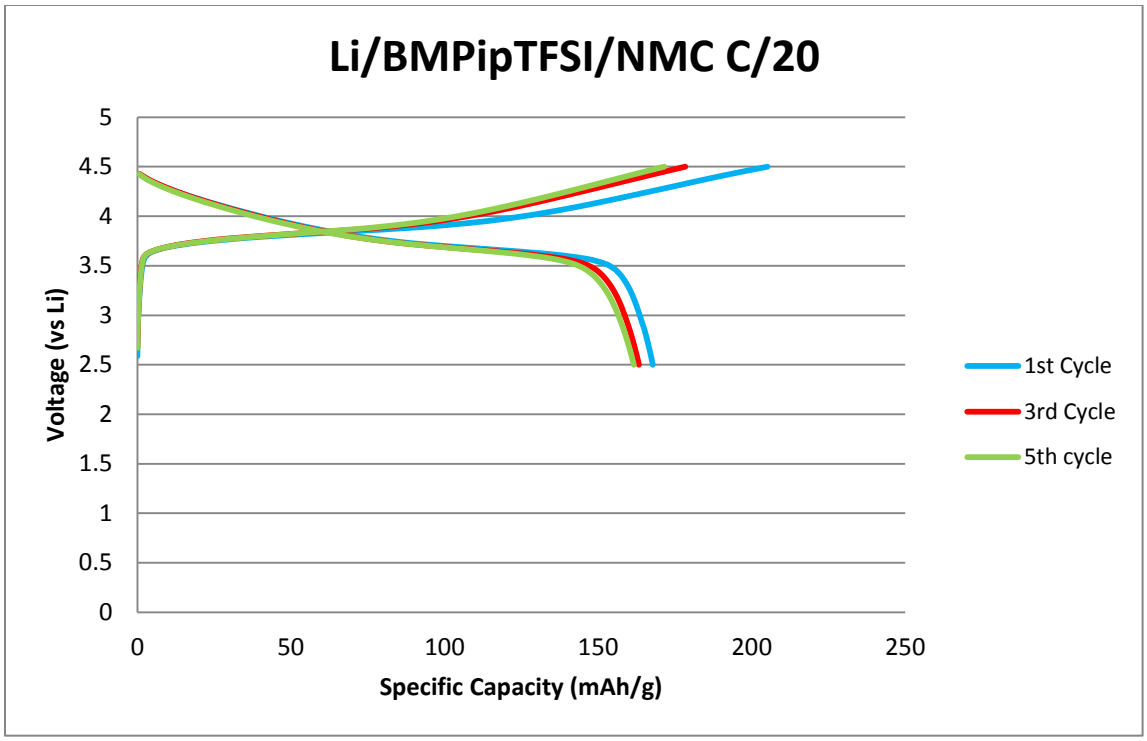

Figure 43: Specific capacity of layered cathode with BMPipTFSI electrolyte

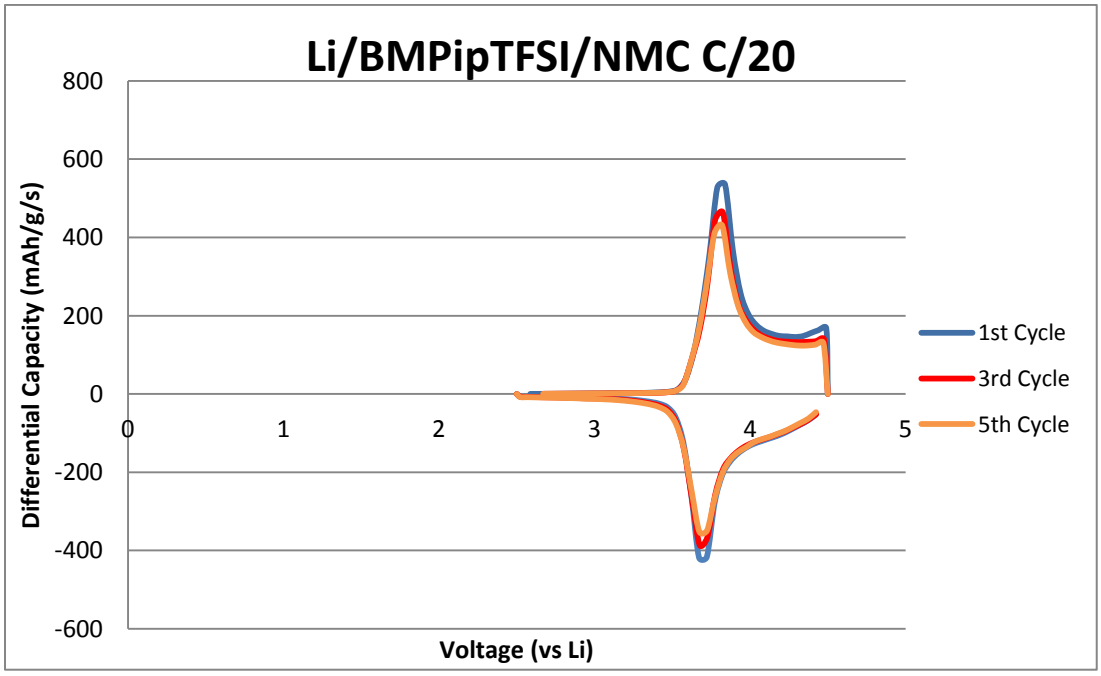

Figure 44: Differential capacity of layered cathode with BMPipTFSI electrolyte

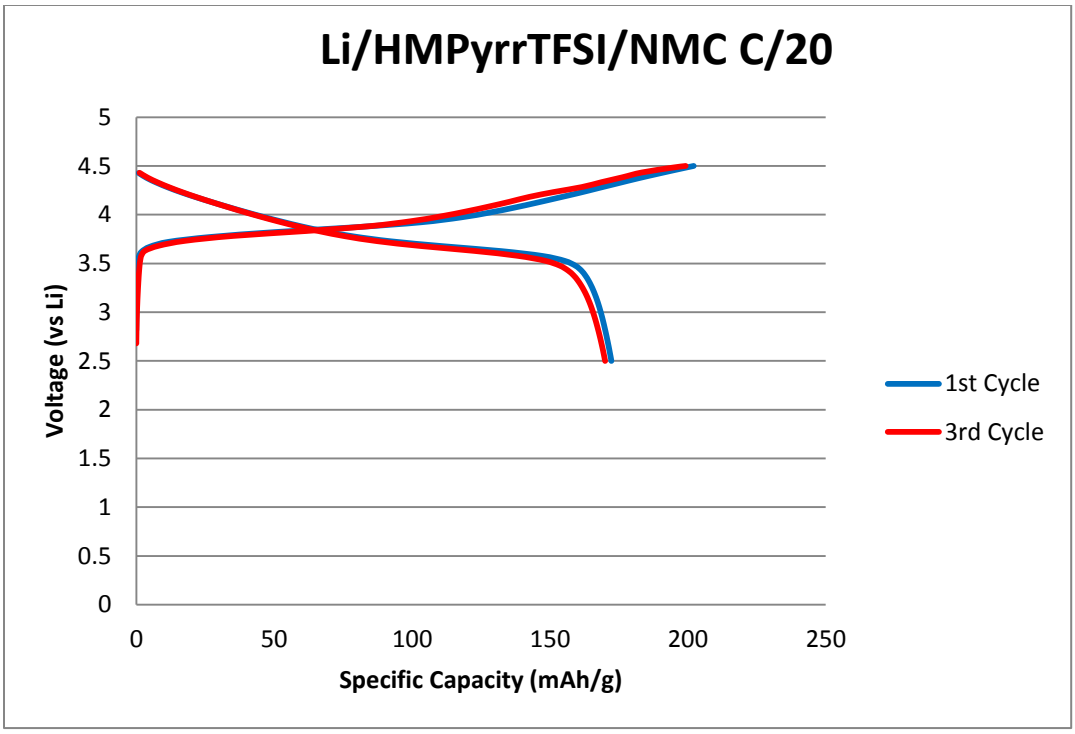

Figure 45: Specific capacity of layered cathode with HMPyrrTFSI electrolyte

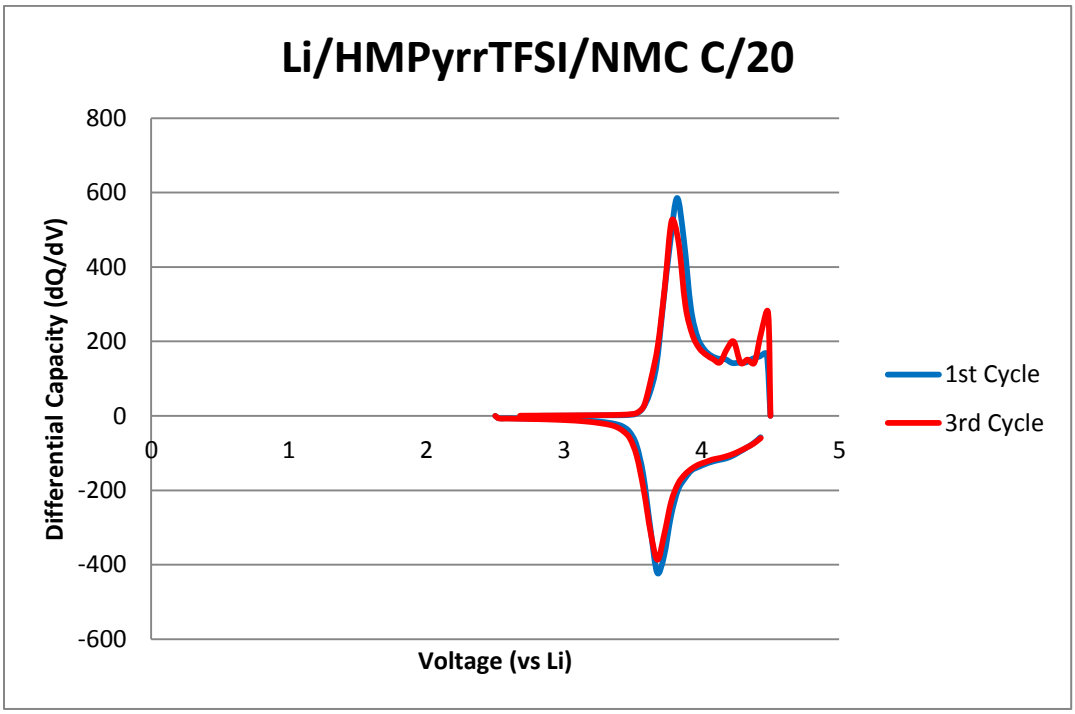

Figure 46: Differential capacity of layered cathode with HMPyrrTFSI electrolyte

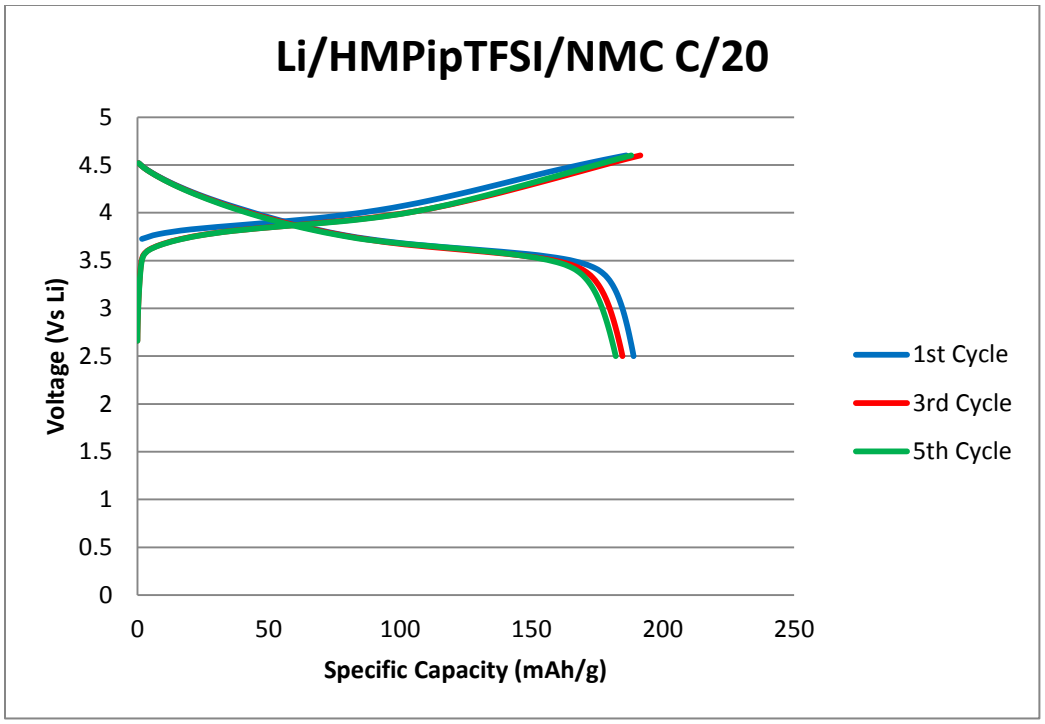

Figure 47: Specific capacity of layered cathode with HMPipTFSI electrolyte

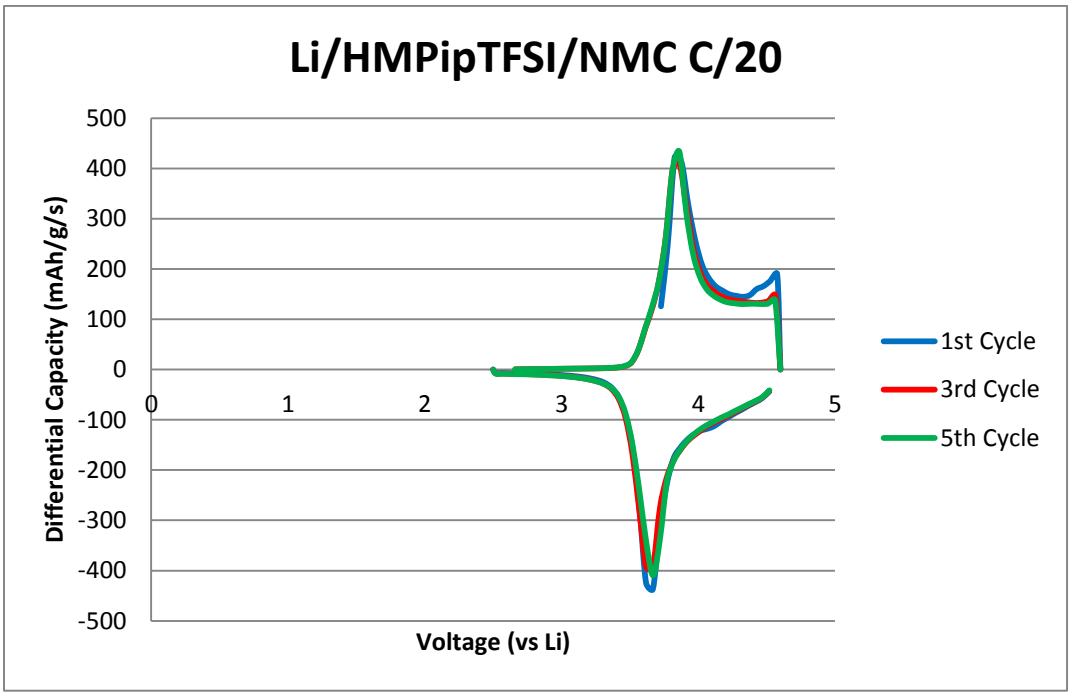

Figure 48: Differential capacity of layered cathode with HMPipTFSI electrolyte

Cells constructed with the BMPyrrTFSI ionic liquid showed a higher failure rate than the cells constructed with other ionic liquids. Out of seven cells constructed with 0.2 mol/kg LiTFSI in BMPyrrTFSI, only one was able to retain a large percentage of its capacity for more than five cycles. The successful cell also showed evidence of impurities but was able to overcome them and cycle effectively. The primary evidence of impurities present in all of the BMPyrrTFSI cells was a much lower open circuit voltage when compared to the other electrolytes. The majority of the cells constructed showed an average open circuit voltage of around 3.0V but the cells constructed with BMPyrrTFSI showed an open circuit voltage of 1.5V. It is unclear why the BMPyrrTFSI cells are more sensitive to impurities. It is most likely due to a problem with the synthesis conditions of the iodide salt since the problems occurred with several different batches of ionic liquid made from the same precursor salt. Passing the ionic liquid through a column of activated carbon (a common method for removing colored impurities) did not have any effect on battery performance. Figure 49 shows the specific capacity at several different rates for the one successful BMPyrrTFSI cell. The differences in specific capacity for different cycles at the same rate are likely due to impurities but the ability to achieve capacities above 100 mAh/g at a C/2 rate indicates a much better rate capability compared to the HMPipTFSI based ionic liquid which was also cycled at different rates.

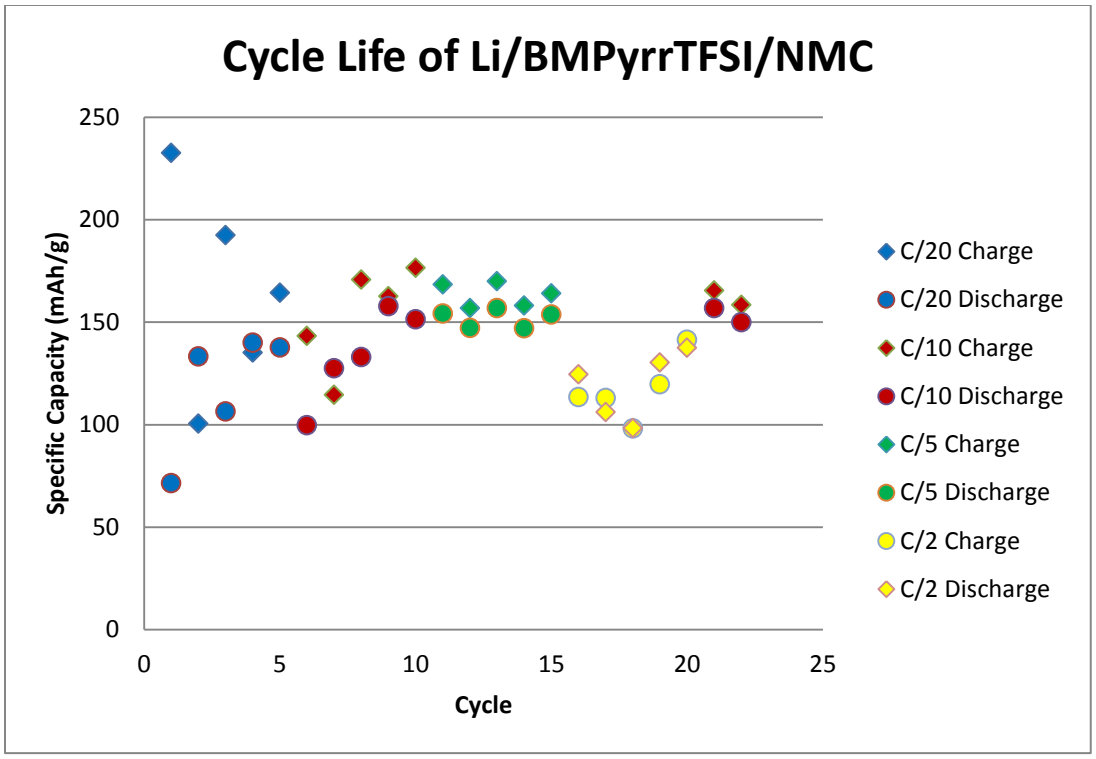

Figure 49: Specific capacities for BMPyrrTFSI electrolyte at different charge rates

The BMPipTFSI electrolyte also showed a greater tendency for failure but did not show the lower open circuit voltage of the BMPyrrTFSI cells. Only one cell was successfully cycled for more than five cycles. It showed very good capacity at C/20 which decreased at C/10 and increased again when the rate returned to C/20.

The HMPyrrTFSI ionic liquid showed overcharging behavior during the fourth through ninth cycles but continued to cycle well. This could indicate the formation of a passivation layer but is impossible to be certain without further investigation.

Figure 50 shows the specific capacities for a HMPipTFSI based ionic liquid cell cycled at several different rates. As expected, the capacity decreases as the rate of charge increases. The low ionic conductivity prevents the lithium ions from diffusing quickly enough to and from the electrode interface. This build-up of charge prevents the

effective intercalation of lithium at the rate required to support the higher currents. The significantly higher discharge capacity (relative to charge capacity) of the final two cycles supports this conclusion because lithium ions that did not diffuse away from the cathode at the higher charge rates are readily available to for intercalation once the rate is lowered. This may also be causing a suppression of the charge capacity of these cycles because it becomes harder to remove all the lithium from the lattice when there is a large amount of lithium ions near the interface. This is likely responsible for the 20 mAh/g increase in charge capacity between cycles 29 and 30.

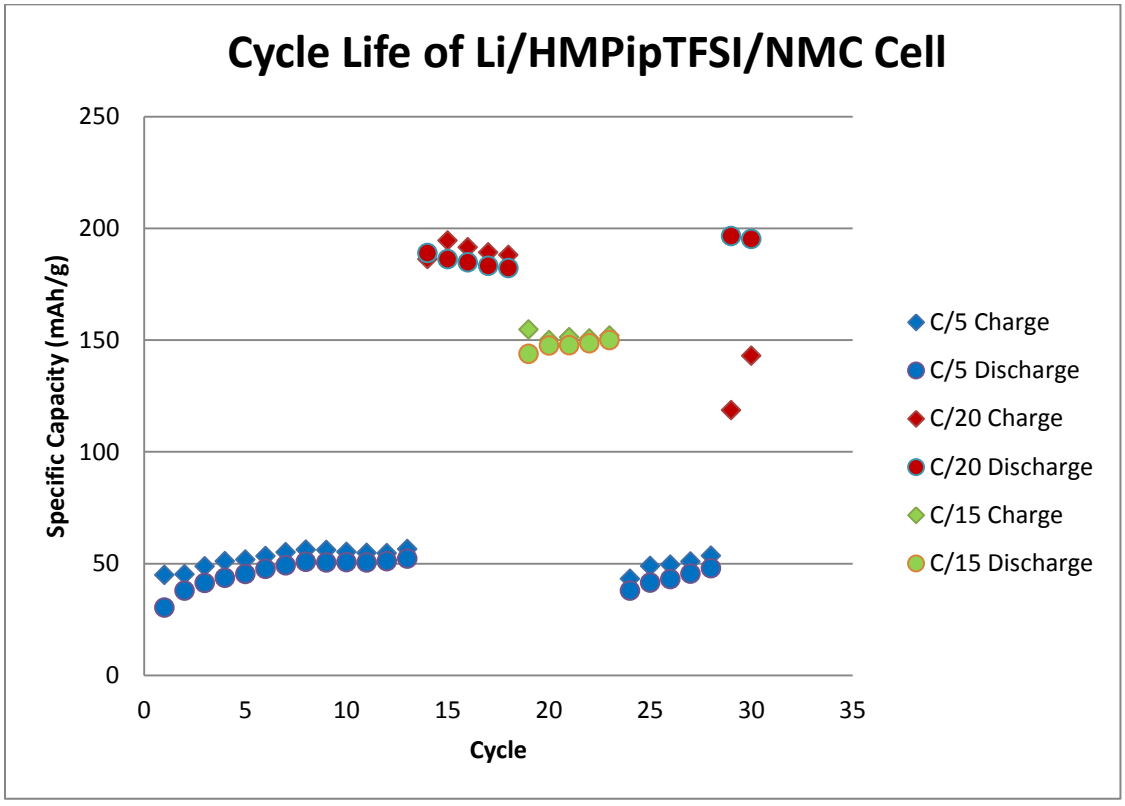

Figure 50: Specific capacities for HMPipTFSI electrolyte at different charge rates

5.8.2.3 Cycling at Elevated Temperature

The high viscosity of ionic liquids is closely related to the low ionic conductivity. Additionally, the viscosity is highly temperature dependent. To test this connection the cell was placed in an oven and cycled at 65°C. Figure 51 shows the capacity of the cell at a rate of C/10. The cell achieved capacities similar to the C/20 rate at room temperature, showing a clear improvement of cell function with increasing temperature.

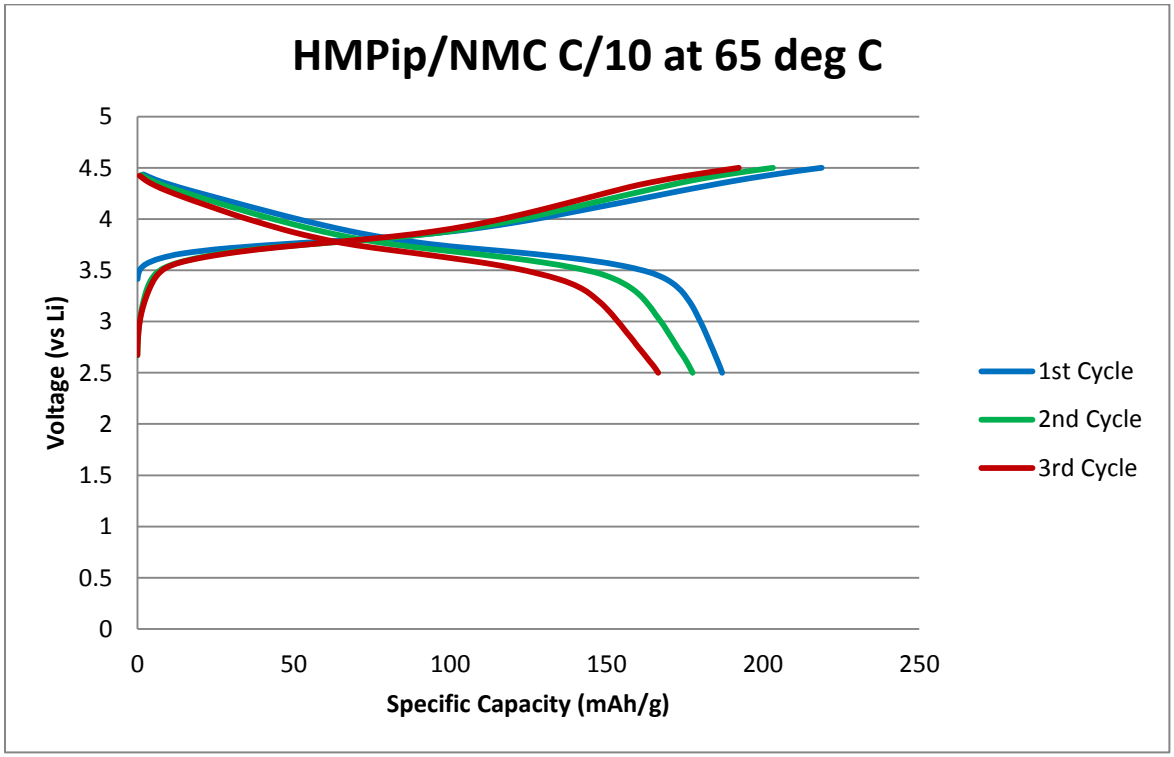

Figure 51: Specific Capacity of Cell cycled at C/10 at 65°C

5.8.3 *$LiNi_{0.5}Mn_{1.5}O_4$ with Carbonate Electrolyte*

Figure 52 shows the specific charge capacity over the first twenty cycles of a cell constructed with the spinel type cathode and the 0.1M $LiPF_6$ in EC:DMC. The first cycle shows a large irreversible capacity likely due to decomposition of the electrolyte which is enhanced by the lower rate of charge. After this first charge the cell cycles very well with a specific capacity of around 120 mAh/g, slightly lower than the theoretical capacity of 147 mAh/g.

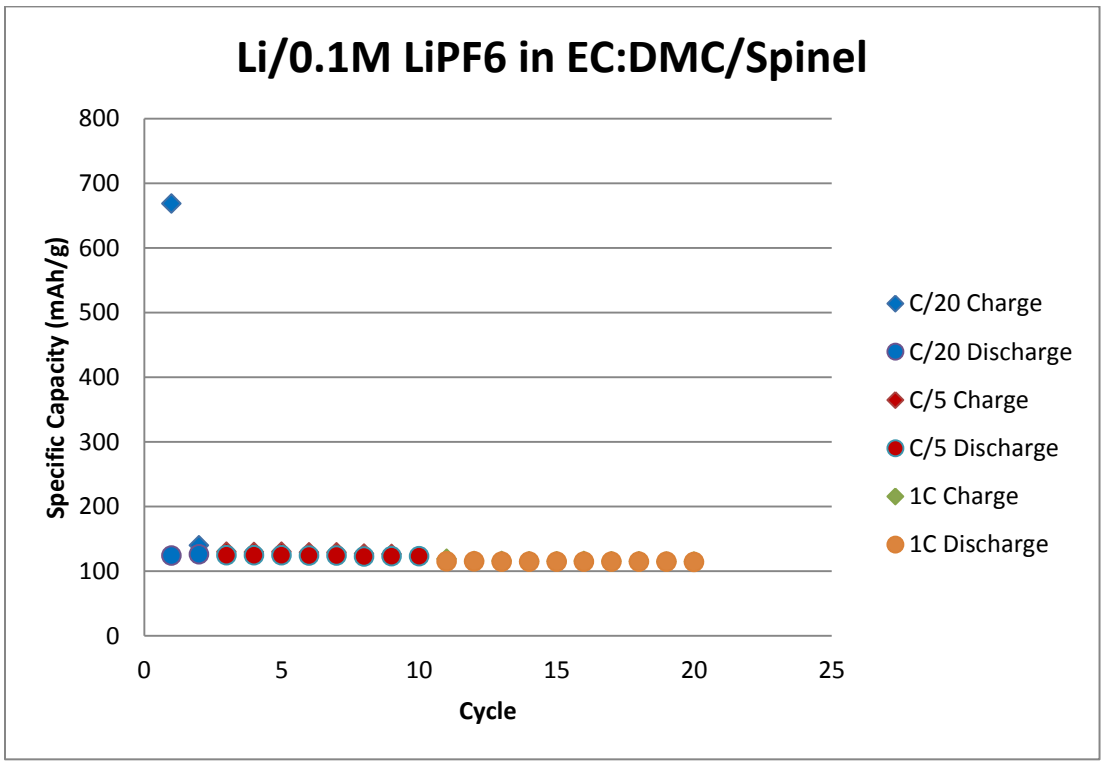

Figure 52: Specific charge capacity for carbonate cell over several cycles

Figures 53 and 54 show the cycling behavior of the cell during the 3rd, 5th, and 7th cycles. The large flat plateau at 4.8 V and smaller plateau around 4.0 V are expected for the spinel cathode and matching this behavior is the goal for the cells with ionic liquid electrolytes.

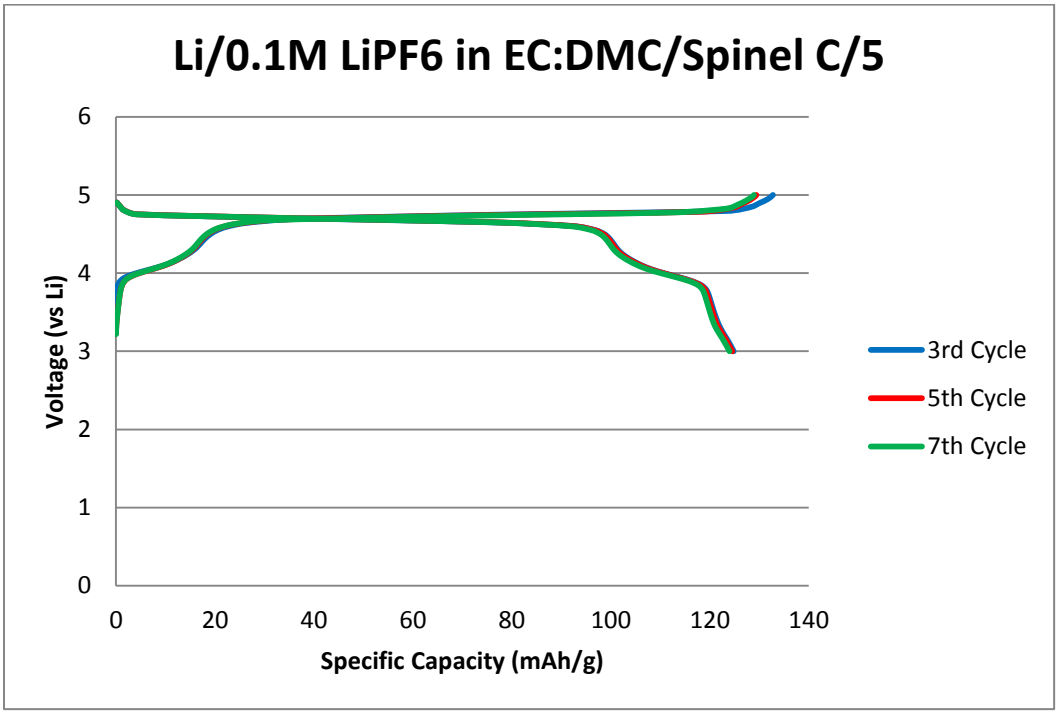

Figure 53: Specific Capacity of $LiNi_{0.5}Mn_{1.5}O_4$ Cell with carbonate electrolyte

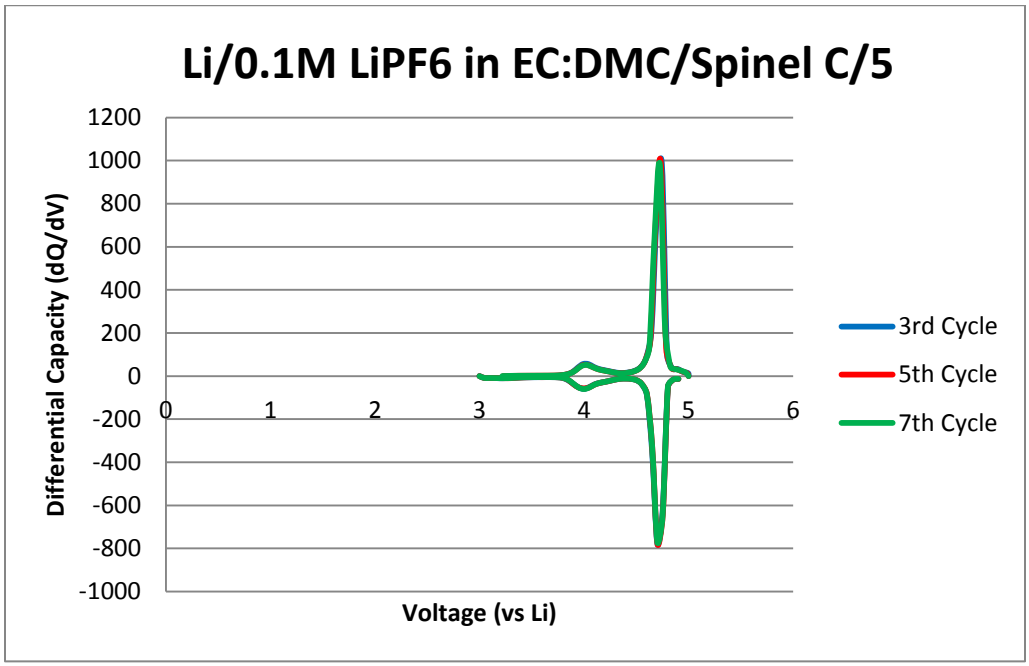

Figure 54: Differential Capacity of $LiNi_{0.5}Mn_{1.5}O_4$ with carbonate electrolyte

5.8.4 $LiNi_{0.5}Mn_{1.5}O_4$ with Ionic Liquid Electrolyte

Since the CV scans showed the anodic limits of BMPyrrTFSI and BMPipTFSI to be close to the redox potential of the spinel cathode, test cells were only created with HMPyrrTFSI and HMPipTFSI. Figures 55 through 58 show the specific and differential capacities of each cell cycled at a rate of C/20.

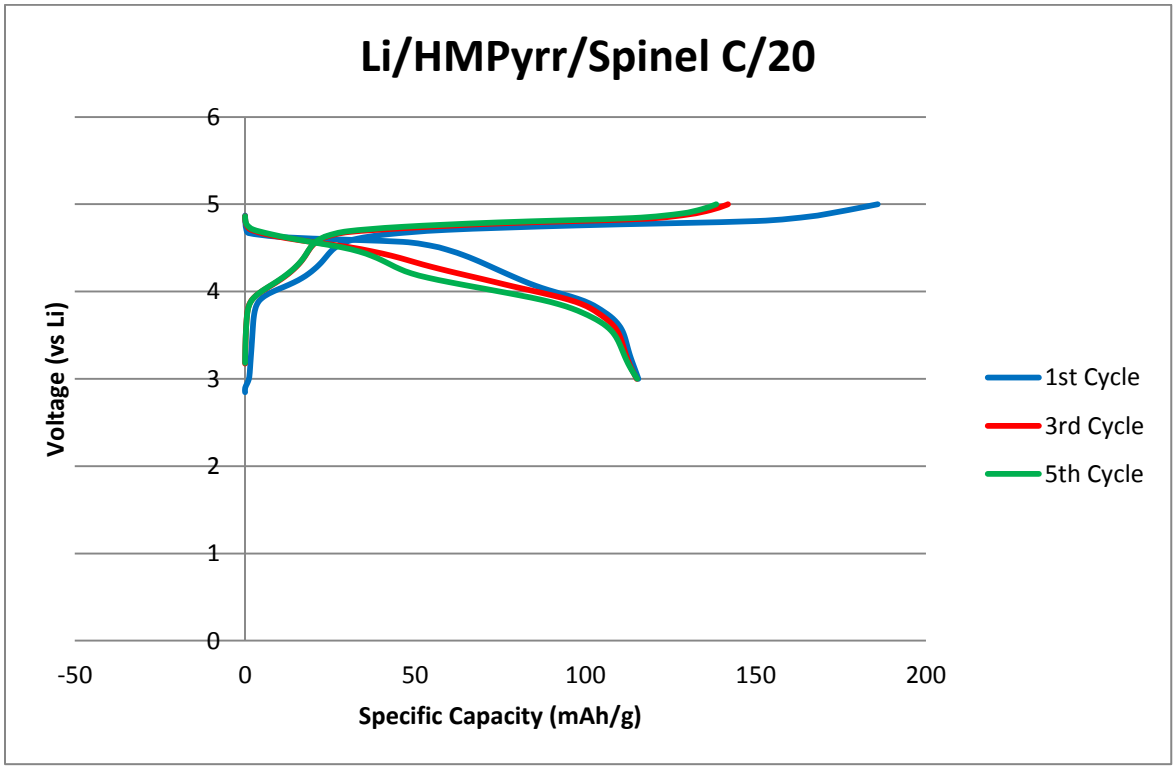

Figure 55: Specific capacity of $LiNi_{0.5}Mn_{1.5}O_4$ with HMPyrrTFSI electrolyte

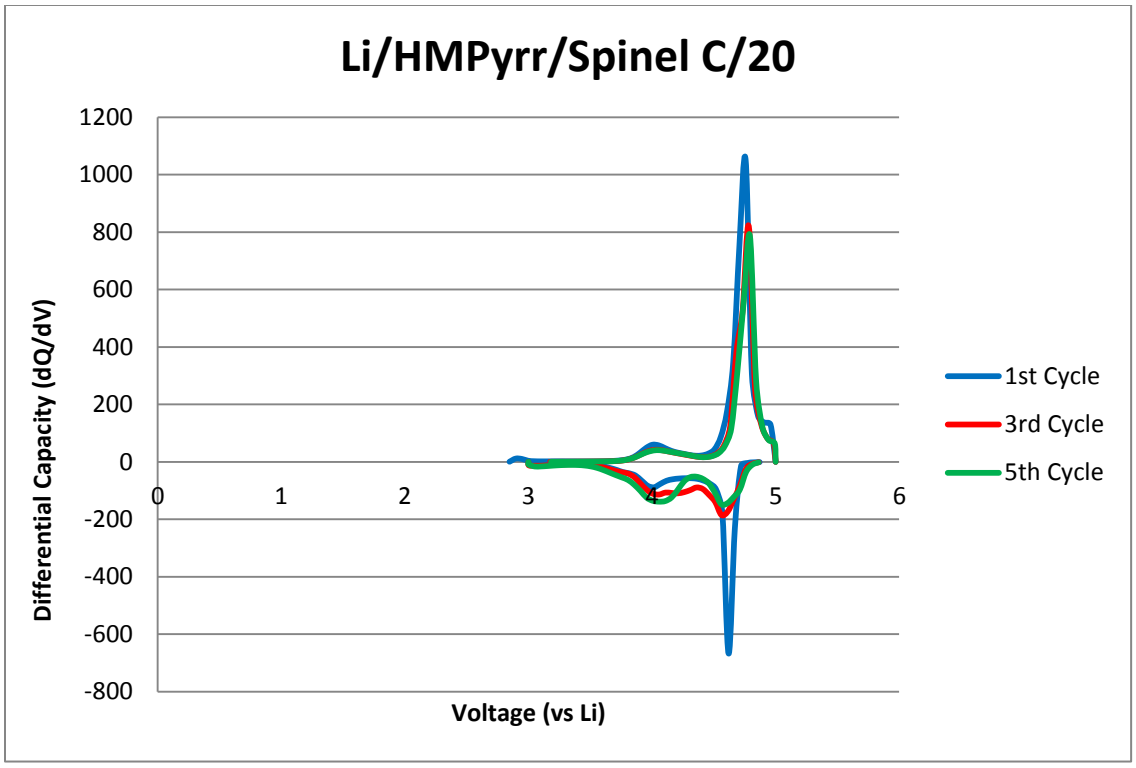

Figure 56: Differential capacity of $LiNi_{0.5}Mn_{1.5}O_4$ with HMPyrrTFSI electrolyte

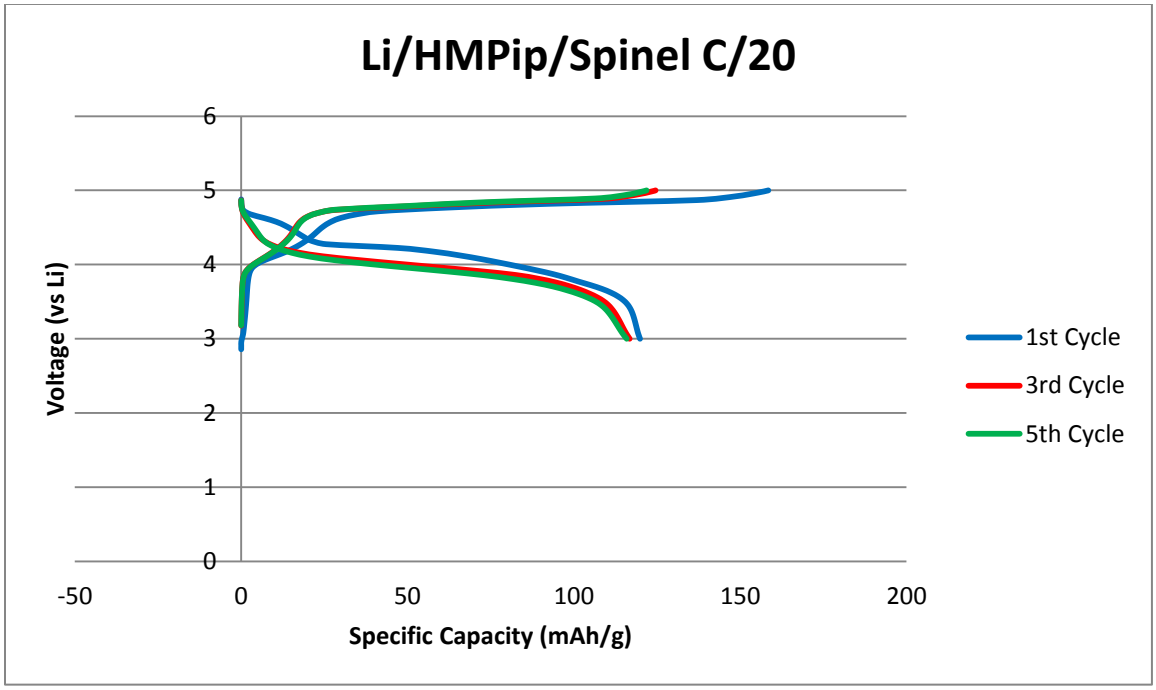

Figure 57: Specific capacity of $LiNi_{0.5}Mn_{1.5}O_4$ with HMPipTFSI electrolyte

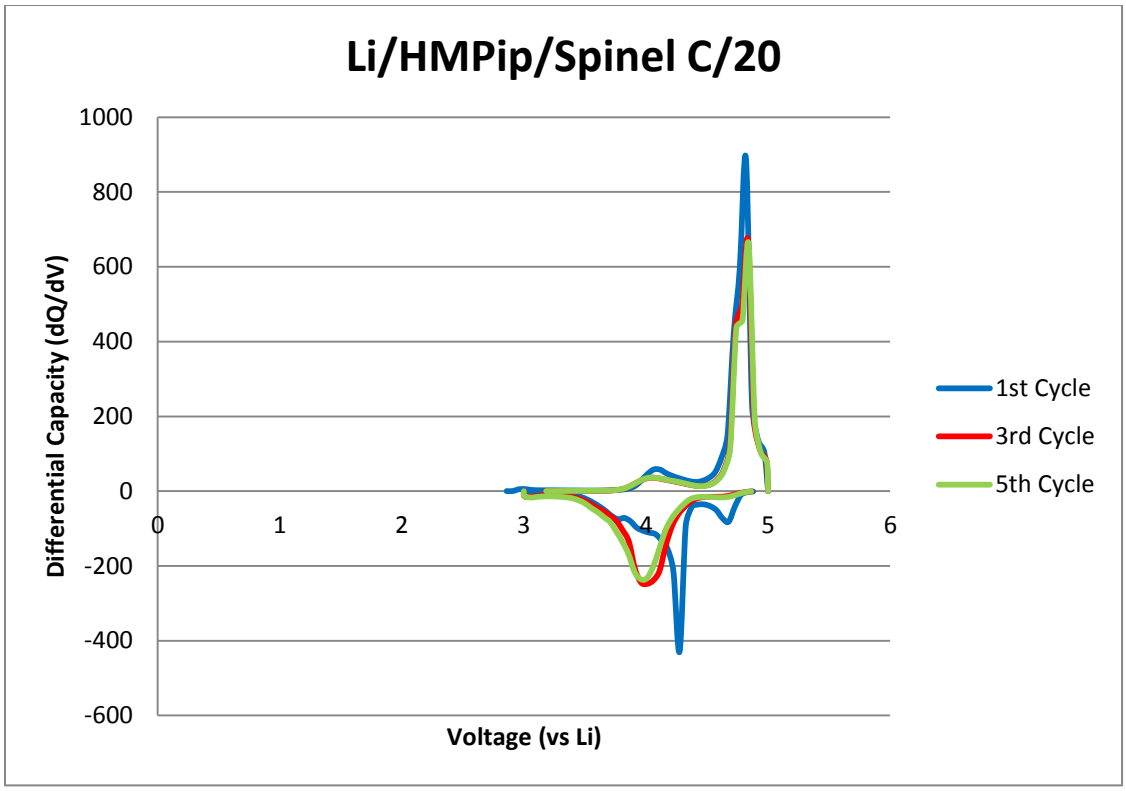

Figure 58: Differential capacity of $LiNi_{0.5}Mn_{1.5}O_4$ with HMPipTFSI electrolyte

The cells show flat charging plateaus similar to the carbonate cell but the discharge behavior is much more slanted indicating that lithium is re-entering the cathode at a range of voltages. This is supported by the differential capacity which shows significant variation in optimal intercalation voltages for different cycles. As with the layered cathode this behavior is due to the low ionic conductivity preventing lithium from diffusing to and from the cathode interface. This is likely a more significant issue for the spinel compared to the layered structure because the redox couple is so close to the voltage limit and is therefore reached more quickly once discharge begins. Both cells show similar discharge capacities to the carbonate cell but the HMPyrrTFSI cell showed slightly higher charging capacities. This leads to lower columbic efficiency (83% for

HMPyrrTFSI vs 95% for HMPipTFSI) which could be a sign of breakdown of the electrolyte.

The spinel cells were also cycled at different rates to show the effect on capacity. Figures 59 and 60 show the specific capacities at different rates for each ionic liquid. Both cells show irreversible capacity in the first cycle but it is much less than the irreversible capacity of the carbonate cell.

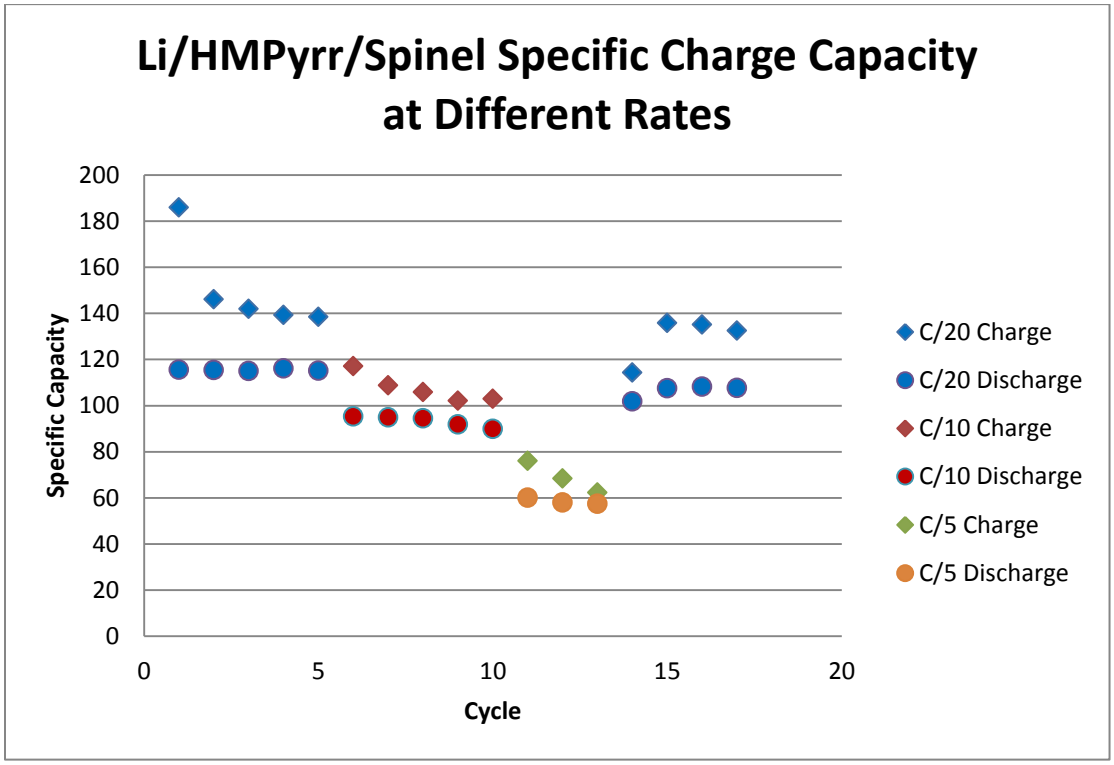

Figure 59: Specific capacity of HMPyrrTFSI at different rates

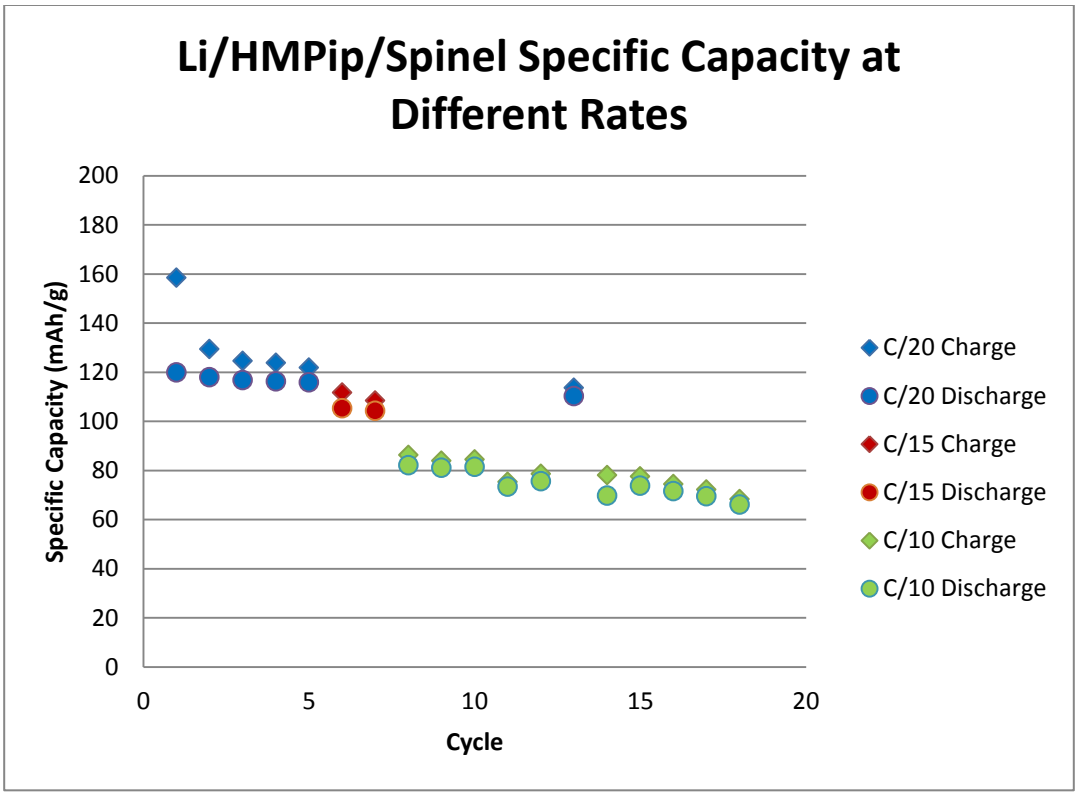

Figure 60: Specific capacity of HMPipTFSI at Different Rates

The decrease in capacity with increasing charge rate is clear for both ionic liquids. The HMPyrrTFSI cell shows better capacity at high rates, which agrees with the conductivity data. The HMPipTFSI cell, however, shows better efficiency as indicated by the nearly identical charge and discharge values. This indicates that while the pyrrolidinium cation provides higher conductivity, the piperidinium cation may increase the stability of the electrolyte.

5.9 Thermal Stability

Figures 61 and 62 show the results of the high temperature DSC scans of each delithiated cathode material with the carbonate electrolyte. Both cathodes show large

endothermic peaks corresponding to oxygen evolution; this is undesirable because the combination of oxygen and the flammable carbonates can cause fires and explosions.

.

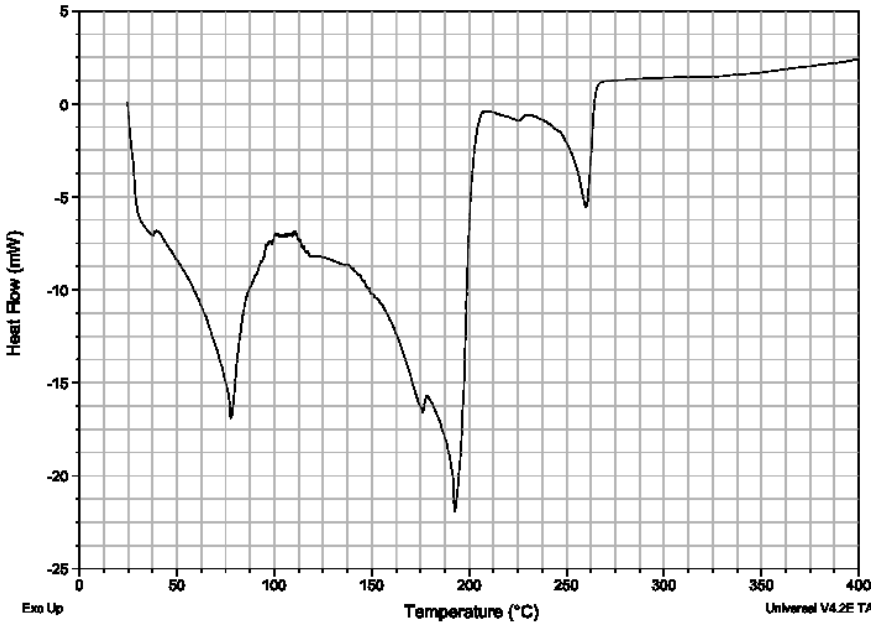

Figure 61: DSC thermogram of delithiated layered cathode and carbonate electrolyte

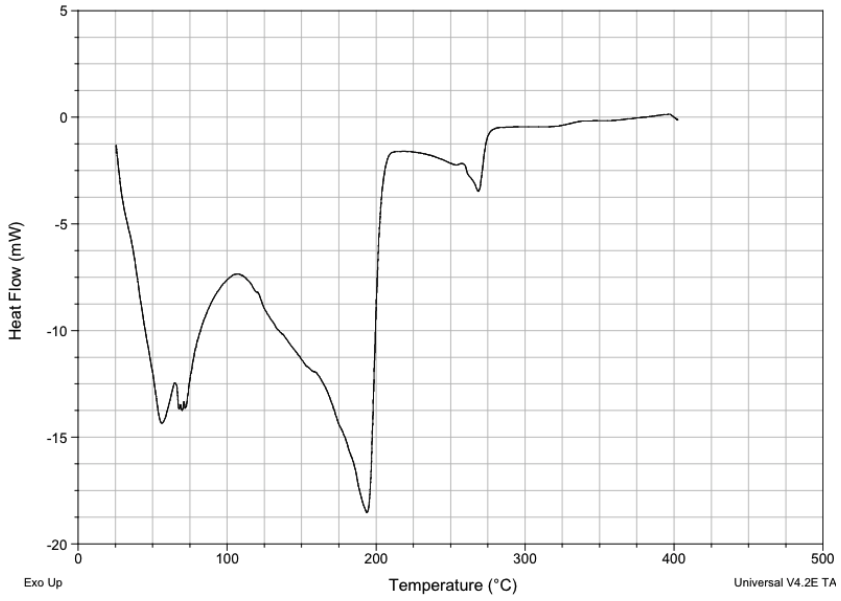

Figure 62: DSC thermogram of delithiated spinel cathode and carbonate electrolyte

Figures 63 and 64 show the results with HMPipTFSI for each cathode. There are no observed peaks, which indicates no reactions between the cathode and electrolyte. This is ideal in terms of safety.

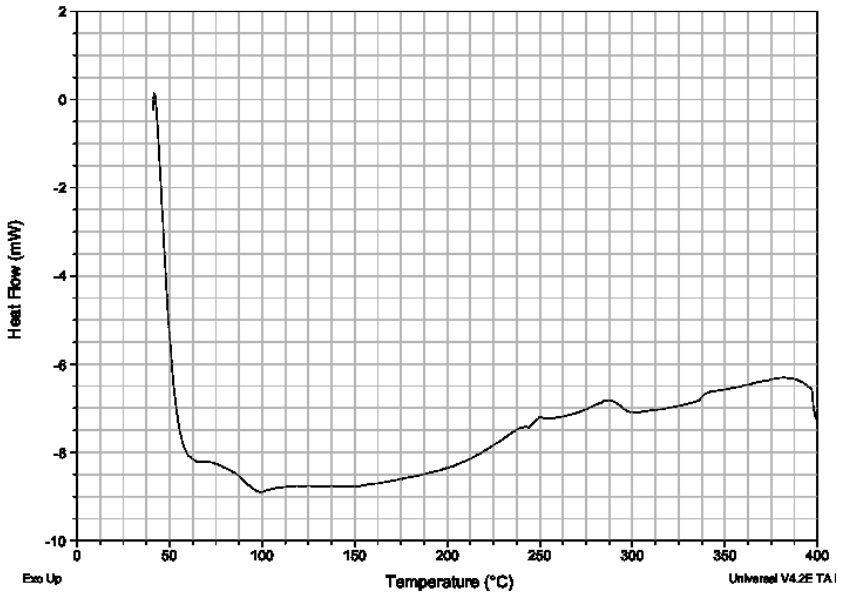

Figure 63: DSC thermogram of delithiated layered cathode and HMPipTFSI

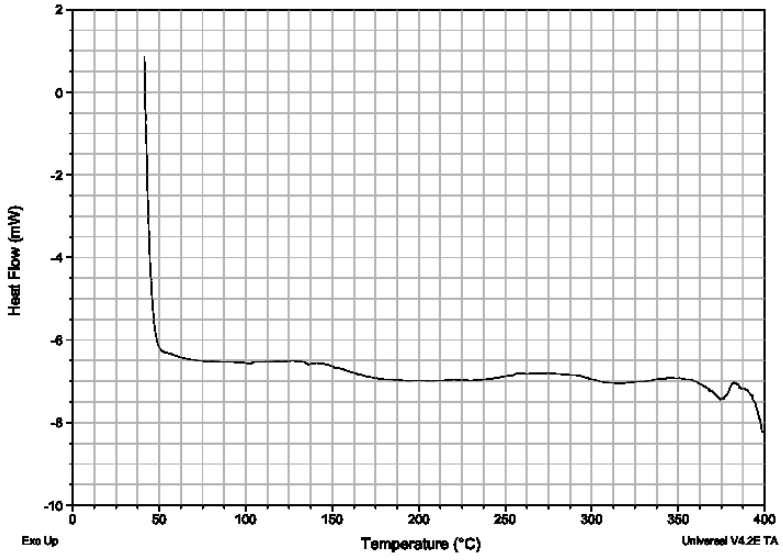

Figure 64: DSC thermogram of delithiated spinel cathode and HMPipTFSI

Chapter 6: Conclusions and Future Work

The four ionic liquids were successfully synthesized using bench top methods and a clear association between cation size and ionic conductivity was shown. The cation size was increased by increasing the number of carbons present in either the ring structure or alkyl side chain. Both changes resulted in a decrease in the ionic conductivity likely due to stronger inter-ionic interactions. This decrease in ionic conductivity was also shown to negatively affect the rate capability of lithium ion batteries constructed with ionic liquids. This is likely because the low ionic conductivity inhibits diffusion of lithium ions to and from the electrode interfaces preventing effective intercalation.

Cyclic voltammetry showed that all of the ionic liquids were electrochemically stable to 4.5 Volts versus lithium indicating compatibility with the $LiNi_{1/3}Mn_{1/3}CO_{1/3}O_2$ layered cathode. The ionic liquids with hexyl chains attached to the cation were stable up to 5 Volts which indicates compatibility with the $LiNi_{0.5}Mn_{1.5}O_4$ spinel cathode. It is unclear why changing the cation has such a pronounced effect on the anodic stability which is predominantly determined by the oxidation potential of the anion. The cations and anions are not completely dissociated in ionic liquids so it is possible that the increased interaction between the ions inhibits the oxidation of the anions. It is more likely, however, that the difference in anodic limits is due to impurities that were not completely removed by simply washing the ionic liquids with deionized water.

The galvanic cycling of electrochemical half-cells confirmed the compatibility of the ionic liquids with the selected high performance cathodes. At least one cell with each

ionic liquid was successfully charged and discharged for more than ten cycles. Unfortunately a high failure rate among cells constructed with the short chain ionic liquids showed evidence of the presence and negative impact of impurities. The longer alkyl chains may minimize the presence or effects of impurities and therefore be better suited to mass production. It is likely, however, that improved control over the synthesis procedure (particularly the formation of the precursor salt) would yield short chain ionic liquids of sufficient purity. This is preferable to using the longer chains due to the significant decrease in ionic conductivity that results in increasing the cation size.

Investigations of the high temperature behavior of HMPipTFSI electrolyte showed further benefits of ionic liquids. A cell cycled at 65°C showed increased capacity at high charge rates. The possible resistance to impurities exhibited by this ionic liquid may therefore be beneficial for constructing batteries designed to operate at higher temperatures where high viscosity is not an issue. The high temperature DSC results also show the decreased reactivity of the ionic liquid compared to a standard electrolyte which is important for safety considerations.

Overall the pyrrolidinium and piperidinium families of cations seem well suited for use as battery electrolytes. The pyrrolidinium cation provides a higher ionic conductivity while the piperidinium cation provides greater stability and higher columbic efficiency. Both are easy to prepare and have reduction potentials very close to that of lithium which may allow for the successful commercialization of rechargeable batteries with lithium anodes. However, control of impurities is essential for proper lithium ion battery behavior and simply washing with deionized water may not be enough to remove impurities once they are introduced. Filtering through a column of activated carbon also

failed to remove the impurities so it is advisable to prevent their introduction through proper control of synthesis procedures. This was achieved with the largest cation studied and is likely possible with smaller cations if extra precautions are taken. The formation of the halide salt is the more sensitive process and care should be taken to minimize the possibility for contamination by purifying the starting reagents by distillation and ensuring that no unreacted reagents remain.

Finally, the identity of the cation seems to have very little effect on the maximum potential of the cell and compatibility with new cathode materials. It is likely that better synthesized samples of the short chain ionic liquids would indeed work with the high voltage spinel cathode since the maximum charge potential is determined by the anion. The delocalized charge of the bis(trifluoromethylsulfonyl)imide anion gives it many qualities desirable for use in ionic liquids but attempts to further increase the maximum charge potential in order to develop even higher voltage cathodes will require the exploration of new anions.

References

[1] D. Linden and T. B. Reddy, Handbook of Batteries, 3rd ed., New York, NY: McGraw-Hill, 2002.

[2] J.-M. Tarascon and M. Armand, "Issues and challenges facing rechargeable lithium batteries," *Nature,* vol. 414, pp. 359-367, 2001.

[3] J. Goodenough and Y. Kim, "Challenges for Rechargeable Li Batteries," *Chemistry of Materials,* pp. 587-603, 2010.

[4] B. Barrow, "Dell recalls 4 million 'exploding' laptops," *The Daily Mail,* 15 August 2006.

[5] J. Henry, "Chevy Volt Battery Fires Threaten All Electric Vehicle Makers, Not Just GM," *Forbes,* 12 December 2011.

[6] B. Scrosati, "History of lithium batteries," *Journal of Solid State Electrochemistry,* vol. 15, pp. 1623-1630, 2011.

[7] S. Whittingham, "Chemistry of Intercalation Compounds: Metal Guests in Chalcogenide Hosts," *Progress in Solid State Chemistry,* vol. 12, pp. 41-99, 1978.

[8] S. M. Wittingham, "Lithium Batteries and Cathode Materials," *Chemical Reviews,* vol. 104, pp. 4271-4301, 2004.

[9] K. Mizushima, P. Jones, P. Wiseman and J. Goodenough, "LixCoO2 (0<x<1): A New Cathode Material for Batteries of High Energy Density," *Materials Research Bullitin,* vol. 15, pp. 783-789, 1980.

[10] B. Scrosati and J. Garche, "Lithium batteries: Status, prospects, and future," *Journal of Power Sources,* vol. 195, pp. 2419-2430, 2009.

[11] K. Xu, "Nonaqueous Liquid Electrolytes for Lithium-Based Rechargable Batteries," *Chemical Reviews,* vol. 104, pp. 4303-4417, 2004.

[12] R. Alcantara, P. Lavela, J. L. Tirado, E. Zhecheva and R. Stoyanova, "Recent advances in the study of layered lithium transition metal oxides and their application as intercalation electrodes," *Journal of Solid State Electrochemistry,* vol. 3, pp. 121-134, 1999.

[13] T. Ohzuku and Y. Makimura, "Layered Lithium Insertion Material of LiNi1/2Mn1/2O2: A Possible Alternative to LiCoO2 for Advanced Lithium-Ion Batteries," *Chemistry Letters,* pp. 744-745, 2001.

[14] T. Ohzuku and Y. Makimura, "Layered Lithium Insertion Material of LiCo1/3Ni1/3Mn1/3O2," *Chemistry Letters,* pp. 642-643, 2001.

[15] G. Amatucci and J. M. Tarascon, "Optimization of Insertion Compounds such as LiMn(2)O(4) for Li-ion Batteries," *Journal of The Electrochemical Society,* vol. 149, no. 12, pp. K31-K46, 2002.

[16] R. Santhanam and B. Rambabu, "Research progress in high voltage spinel LiNi0.5Mn1.5O4 material," *Journal of Power Sources,* vol. 195, pp. 5442-5451, 2010.

[17] D. Liu, J. Han, M. Dontigny, P. Charest, A. Guerfi, K. Zaghib and J. B. Goodenough, "Redox Behaviors of Ni and Cr with Different Counter Cations in Spinel Cathodes for Li-ion Batteries," *Journal of The Electrochemical Society,* vol. 157, no. 7, pp. A770-A775, 2010.

[18] J. S. Wilkes, "Ionic Liquids in Perspective: The Past with an Eye Toward the Industrial Future," *ACS Symposium Series,* pp. 214-229, 2002.

[19] P. Walden, *Bull. Acad. Imper. Sci. (St. Petersburg),* pp. 405-422, 1914.

[20] J. Wilkes, "A short history of ionic liquids-from molten salts to neoteric solvents," *Gree Chemistry,* vol. 4, pp. 73-80, 2002.

[21] J. Wilkes and M. Zaworotko, "Air and Water Stable 1-Ethyl-3-methylimidazolium Based Ionic Liquids," *J. Chem. Soc., Chem. Commun.,* pp. 965-967, 1992.

[22] V. Borgel, E. Markevich, D. Aurbach, G. Semrau and M. Schmidt, "On the application of ionic liquids for rechargeable Li batteries: High voltage systems," *Journal of Power Sources,* vol. 189, pp. 331-336, 2009.

[23] M. Galinski, A. Lewandowski and I. Stepniak, "Ionic Liquids as electrolytes," *Electrochimica Acta,* vol. 51, pp. 5567-5580, 2006.

[24] A. Lewandowski and A. Swiderska-Mocek, "Ionic liquids as electrolytes for Li-ion batteries-An overview of electrochemical studies," *Journal of Power Sources,* pp. 601-609, 2009.

[25] H. Xiang, B. Yin, H. Wang, H. Lin, X. Ge, S. Xie and C. Chen, "Improving electrochemical properties of room temperature ionic liquid (RTIL) based electrolyte for Li-ion batteries," *Electrochimica Acta,* vol. 55, pp. 5204-5209, 2010.

[26] H. Sakaebe, H. Matsumoto and K. Tatsumi, "Discharge-charge properties of Li/LiCoO2 cell using room temperature ionic liquids (RTILs) based on quaternary ammonium cation-Effect of the structure," *Journal of Power Sources,* vol. 146, pp. 693-697, 2005.

[27] D. Macfarlane, , P. Meakin, J. Sun, N. Amini and M. Forsyth, "Pyrrolidnium Imides: A New Family of Molten Salts and Conductive Plastic Crystal Phases," *Journal of Physical Chemistry B,* vol. 103, pp. 4164-4170, 1999.

[28] M. Montanino, M. Carewska, F. Alessandrini, S. Passerini and G. Appetecchi, "The role of the cation aliphatic side chain length in piperidinium bis(trifluoromethansulfonyl)imide ionic liquids," *Electrochimica Acta,* vol. 57, pp. 153-159, 2011.

[29] T. Fromling, M. Kunze, M. Schonhoff, J. Sundermeyer and B. Roling, "Enhanced Lithium Transference Numbers in Ionic Liquid Electrolytes," *Journal of Physical Chemistry B,* vol. 112, pp. 12985-12990, 2008.

[30] H. Kawai, M. Nagata, H. Tukamoto and A. R. West, "High-voltage lithium cathode materials," *Journal of Power Sources,* pp. 67-72, 1999.

[31] H. Kawai, M. Nagata, H. Tukamoto and A. R. West, "High-voltage lithium cathode materials," *Journal of Power Sources,* pp. 67-72, 1999.

[32] E. Antolini, "LiCoO2: formation, structure, lithium and oxygen nonstoichiometry, electrochemical behavior and transport properties," *Solid State Ionics,* vol. 170, pp. 159-171, 2004.

[33] J. W. Fergus, "Recent developments in cathode materials for lithium ion batteries," *Journal of Power Sources,* vol. 195, pp. 939-954, 2010.

[34] H. Xia, H. Wang, W. Xiao, L. Lu and M. O. Lai, "Properties of LiNi1/3Co1/3Mn1/3O2," *Journal of Alloys and Compounds,* vol. 480, pp. 696-701, 2009.

[35] M. M. Thackeray, C. S. Johnson, J. T. Vaughey, N. Li and S. A. Hackney, "Advances in manganese-oxide 'composite' electrodes for lithium-ion batteries,"

Journal of Materials Chemistry, vol. 15, pp. 2257-2267, 2005.

[36] N. K. Karan, J. J. Saavedra-Arias, D. K. Pradhan, R. Melgarejo, A. Kumar, R. Thomas and R. S. Katiyar, "Structural and Electrochemical Characterizations of Solution Derived LiMn0.5Ni0.5O2 as Positive Electrode for Li-Ion Rechargable Batteries," *Electrochemical and Solid-State Letters,* vol. 11, no. 8, pp. A135-A139, 2008.

[37] H. Sclar, D. Kovacheva, E. Zhecheva, R. Stoyanova, R. Lavi, G. Kimmel, J. Grinblat, O. Girshevitz, F. Amalraj, O. Haik, E. Zinigrad, B. Markovsky and D. Aurbach, "On the Performance of LiNi1/3Mn1/3Co1/3O2 Nanoparticles as a Cathode Material for Lithium-Ion Batteries," *Journal of the Electrochemical Society,* vol. 156, no. 11, pp. A938-A948, 2009.

[38] P. Hapiot and C. Lagrost, "Electrochemical Reactivity in Room-Temperature Ionic Liquids," *Chemical Reviews,* vol. 108, no. 7, pp. 2238-2264, 2008.

[39] Gon, P. Gonzolez, J. J. Cornejo, J. Ortiz and J. L. Gautier, "Long Chain 1-Alkyl-3-methlylimidazolium tetrafluoroborates as electrolytes in Li-ion Batteries," *Journal of the Chilean Chemical Society,* vol. 55, no. 2, pp. 274-277, 2010.

[40] H. Sakaebe and H. Matsumoto, "N-Methyl-N-propylpiperidinium bis(trifluoromethanesulfonyl)imide (PP13-TFSI)-novel electrolyte base for Li battery," *Electrochemistry Communications,* vol. 5, pp. 594-598, 2003.

[41] J. Xu, J. Yang, Y. NuLi, J. Wang and Z. Zhang, "Additive-containing ionic liquid electrolytes for secondary lithium battery," *Journal of Power Sources,* vol. 160, pp. 621-626, 2006.

[42] S. Martha, E. Markevich, V. Burgel, G. Salitra, E. Zinigrad, B. Markovsky, H. Sclar, Z. Promovich, O. Heik, D. Aurbach, I. Exnar, H. Buqa, T. Drezen, G. Semrau, M. Schmidt, D. Kovacheva and N. Saliyski, "A short review on surface chemical aspects of Li batteries: A key for a good performance," *Journal of Power Sources,* vol. 189, pp. 288-296, 2009.

[43] E. Markevich, V. Baranchugov and D. Aurbach, "On the possiblity of using ionic liquids as electrolyte solutions for rechargeable 5V Li ion batteries," *Electrochemistry Communications,* vol. 8, pp. 1331-1334, 2006.

[44] P. Wassercheid and T. Welton, Ionic Liquids in Synthesis, vol. 1, Weinheim: Wiley and Sons, 2008.

[45] M. Holzapfel, C. Jost and P. Novak, "Stable cycling of graphite in an ionic liquid based electrolyte," *Chemistry Communications,* pp. 2098-2099, 2004.

[46] J. Wilkes, J. Levisky, M. Druelinger and C. Hussey, "Dialkylimidazolium Chloroaluminate Molten-Salts," *Journal of The Electrochemical Society,* vol. 127, no. 8, pp. C409-C409, 1980.

[47] P. Bonhote, A.-P. Dias, N. Papageorgiou, K. Kalyanasundaram and M. Gratzel, "Hydrophobic, Highly Conductive Ambient-Temperature Molten Salts," *Inorganic Chemistry,* vol. 35, no. 5, pp. 1168-1178, 1995.

[48] B. D. Fitchett, T. N. Knepp and J. C. Conboy, "1-Alkyl-3-methylimidazolium Bis(perfluoroalkylsulfonyl)imide Water-Immiscible Ionic Liquids," *Journal of The Electrochemical Society,* vol. 151, no. 7, pp. E219-225, 2004.

[49] A. B. McEwen, H. L. Ngo, K. LeCompte and J. L. Goldman, "Electrochemical Properties of Imidazolium Salt Electrolytes for Electrochemical Capacitor Applications," *Journal of The Electrochemical Society,* vol. 146, no. 5, pp. 1687-1695, 1999.